Tight Wavelet Frame Construction and its application for Image Processing

by

Kyunglim Nam

(Under the direction of Ming-Jun Lai)

Abstract

As a generalized wavelet function, a wavelet frame gives more rooms for different construction methods. In this dissertation, first we study two constructive methods for the locally supported tight wavelet frame for any given refinable function whose Laurent polynomial satisfies the QMF or the sub-QMF conditions in $\mathbb{R}^d$. Those methods were introduced by Lai and Stöckler. However, to apply the constructive method under the sub-QMF condition we need to factorize a nonnegative Laurent polynomial in the multivariate setting into an expression of a finite square sums of Laurent polynomials. We find an explicit finite square sum of Laurent polynomials that expresses the nonnegative Laurent polynomial associated with a 3-direction or 4-direction box spline for various degrees and smoothness. To facilitate the description of the construction of box spline tight wavelet frames, we start with B-spline tight wavelet frame construction. For B-splines we find the sum of squares form by using Fejér-Riesz factorization theorem and construct tight wavelet frames. We also use the tensor product of B-splines to construct locally supported bivariate tight wavelet frames. Then we explain how to construct box spline tight wavelet frames using Lai and Stöckler's method.

In the second part of dissertation, we apply some of our box spline tight wavelet frames for edge detection and image de-noising. We present a lot of images to compare favorably with other edge detection methods including orthonormal wavelet methods and six engineering methods from MATLAB Image Processing Toolbox. For image de-noising we provide with PSNR numbers for the comparison.

Finally we study the construction of locally supported tight wavelet frame over bounded domains. The situation of the construction of locally supported tight wavelet frames over bounded domains is quite different from the construction we explained above. We introduce a simple approach and obtain B-spline tight wavelet frames and box spline tight wavelet frames over finite intervals and bounded domains.

Index words: B-splines, Box splines,Tight wavelet frames, Refinable function, Laurent polynomial, Edge detection, Image de-noising, MRA, Sub-QMF condition

Tight Wavelet Frame Construction and its application for Image Processing

by

Kyunglim Nam

B.A., The University of Suwon, 1994

M.S., Yonsei University, 1997

A Dissertation Submitted to the Graduate Faculty of The University of Georgia in Partial Fulfillment of the Requirements for the Degree

Doctor of Philosophy

Athens, Georgia

2005

Tight Wavelet Frame Construction and its application for Image Processing

by

Kyunglim Nam

Approved:

Major Professor: Ming-Jun Lai

Committee: Edward A. Azoff
Paul Wenston
Joseph Fu
Akos Magyar

Electronic Version Approved:

Maureen Grasso
Dean of the Graduate School
The University of Georgia
August 2005

Dedication

For my parents

Acknowledgments

It was my advisor professor Lai who introduced me to wavelets by lending me a book called “The world according to wavelets“ written by B. B. Hubbard. After I read this book I wanted to study this field more. I have not regretted my decision since then. I want to thank my advisor for his patience, encouragement and support through all my graduate school years. I also thank professors Azoff and Johnson for their thoughtful mind.

I deeply appreciate my parents and my grandmother. Nothing can be compared to their love. I thank my other family members, my younger brother Chang-ho and his family Ki-sook and Yi-jung and my youngest brother Ik-ho for their love and encouragement.

It was not so easy to come this far and I do not know how much I can go further. But one thing I know is that without all the people in my life I could not have come this far. Especially, I thank Eunja Maria who became a trapist nun and who prays for me and taught me invaluable things from the first year in Athens Georgia. I thank Sr. Agnes who helped me to accept who I am. I thank all the Korean Catholic Community members particularly professor Park's, Doctor Gwak's and choir members Phyllis, Terry, and Mary at the Catholic center who were my family here in Athens. I have never felt lonely because of them. I thank my colleagues Jenice, Steve, Tawanda, Paulo and Peter who inspired me during my graduate student life at UGA. I thank my sincere friends Beaumie, Yeonju, Nisha and Markus for their friendship and love.

Finally, I thank God for His grace and His abundant love. He gave me all the people around me.

Table of Contents

List of Figures

Chapter 1

Introduction

A wavelet frame is a generalized wavelet function whose binary dilations and integer translations span $L^2(\mathbb{R}^d)$, but are not necessarily orthonormal among its translates and dilations. Because of the self duality and the ability of redundant representation, tight wavelet frames have a lot of potential applications. Many results about frames and wavelet frames are available in the literature. The general notion of frames was introduced first by Duffin and Schaeffer in 1952 (see [DS]). In [BL], a multiresolution analysis (MRA) is extended to a frame multiresolution analysis (FMRA). The authors developed the FMRA theory and applied the constructed frames based on FMRA to signal processing. Chui and Shi showed that affine frames can be obtained by oversampling of well-known wavelets in [CS]. In [D1], various aspects of frames and wavelet frames are discussed. In [FGWW] and [HW], authors completely characterized univariate orthonormal wavelet bases. The characterization of tight wavelet frames appears in their work implicitly. Ron and Shen in their paper [RS1] derived the characterization of tight frames and gave sufficient conditions for the construction of tight wavelet frames from the multiresolution analysis. In the paper [DHRS], a general theory of wavelet frames is given via multiresolution analysis over unbounded intervals. In [CH1], Chui and He gave an existence criterion of the locally supported tight wavelet frames for some refinable functions whose associated Laurent polynomial satisfying sub-QMF condition in univariate settings. The maximum vanishing moment for the compactly supported tight wavelet frame construction is introduced in [CHS1]. In this paper sibling frames are also introduced as an extended notion of tight wavelet frames. Recently, by the same authors, a general theory of non-stationary B-spline tight wavelet frame over bounded domains has been developed (see [CHS2]).

In [RS3], authors constructed compactly supported tight affine frames (wavelets) in $L^2(\mathbb{R}^d)$ from 4-directional box splines that are refinable with respect to the special dilation matrix $A = \begin{bmatrix} 1 & 1 \\ 1 & -1 \end{bmatrix}$. The construction method is based on the theory of so-called 'fiberization' which is developed in [RS4]. In [GR], Gröchenig and Ron showed that for any integer dilation matrix A and smoothness, they can construct compactly supported tight wavelet frames in the multivariate setting. In [CH2], a Kronecker product method is introduced for obtaining box spline tight wavelet frames.

In this dissertation, we construct many tight wavelet frames by using bivariate 3-direction, 4-direction and 8-direction meshes box spline functions and apply some of them for edge detection and image de-noising. In [LS], Lai and Stöckler showed how to construct tight wavelet frame for the Laurent polynomial associated with the refinable function satisfying either the QMF(Quadrature Mirror Filter) condition or the sub-QMF condition. These construction methods are simple and can be applied to any dimensional settings. However, we can use the construction method under sub-QMF condition in [LS] only if we can find a finite number of Laurent polynomials $\widetilde{P}_1, \cdots, \widetilde{P}_N$ for the Laurent polynomial P in $e^{-\sqrt{-1}\omega}$ associated with a refinable function satisfying

$$1 - \sum_{\nu \in \{0,\pi\}^d} |P(\omega+\nu)|^2 = \sum_{j=1}^{N} \left|\widetilde{P}_j(2\omega)\right|^2, \ where \omega \in \mathbb{R}^d. \tag{1.1}$$

For the univariate setting, we can find a Laurent polynomial satisfying the condition (1.1) by the Fejér and Riesz in [F] and [Ri]. But in the multivariate setting it is not an easy question. Bivariate box splines are important class of a refinable function whose associated Laurent polynomial satisfies the sub-QMF condition. One of the main contributions of this dissertaion is to find explicit Laurent polynomials satisfying condition (1.1) for the low orders of box splines on 3, 4 and 8-direction meshes. Therefore we can apply the Lai and Stöckler's construction method to construct tight wavelet frames using various order of bivariate box splines on 3, 4, and 8-direction meshes. For the further results on factorizaion of multivariate nonnegative Laurent polynomials, see [GL]. One advantage of our box spline tight wavelet frames in this dissertation is that our method gives smaller numbers of multivariate tight wavelet frame generators than the bivariate tight wavelet framelets using the Kronecker-product method in [CH2].

Similar to wavelets, wavelet frames are efficient basis for separating several high-pass frequency parts from the low-pass frequency part. In addition to this aspect, the redundant property of wavelet frames is know to be useful for recovering information from the corrupted one. Thus it is interesting to replace wavelets in applications by wavelet frames and compare the efficiencies. We first apply our bivariate box spline tight wavelet frames to the edge detection for images. After a lot of experiments we find that the best results among our box spline tight frames. We then compare the edge detected images by our box spline tight frame with many other edge detected images using the tensor product of Haar, Daubechies, biorthogonal 9/7 wavelets. We also provide more experimental data using six different edge detection methods, Sobel, Prewitt, Roberts, Laplacian, Zero-crossing and Canny methods, provided by the MATLAB Image Processing Toolbox. The edge detection method by using wavelets or wavelet frames can be described as follows. First we decompose an image by wavelet filters or wavelet frame filters into several levels of sub-images. Then we have a low-pass sub-image and many high-pass sub-images. When we reconstruct the image, we only use high-pass parts at all levels without the low-pass sub-image. The reconstructed image shows mostly the edge part of the original image. We provide nine images and their edge detected images by using all the above methods. We have much better results of edge detections by our box spline wavelet frame than the edge detections by tensor products of traditional wavelets and as good results as those of engineering edge detection methods from the MATLAB Image Processing Toolbox.

In [DJ], the wavelet method for de-noising is introduced as a near-optimal method among all the linear and nonlinear methods for de-noising. Image de-noising using wavelets or wavelet frames can be described as follows. We first add a Gaussian noise to the image to get a noisy image. We then decompose the noise added image into one low-pass sub-image and many high-pass sub-images by using wavelets or wavelet frames. We apply the soft-thresholding method to all the high-pass sub-images. In this step by shrinking the wavelet coefficients of high-pass parts of images we remove most part of noise in the image. Then we reconstruct the image using the low-pass parts of image and the thresholded high-pass parts of images. The reconstructed image is the image removed noise. For comparison, we report PSNR numbers of different images reconstructed by using the tensor products of traditional univariate wavelets and box spline tight wavelet frames. After de-noising seven images with different levels of noises, we have higher PSNR numbers for the de-noised images by our box spline tight wavelet frame than that of tensor products of traditional wavelets.

In addition to the tight wavelet frame construction over unbounded domains, we introduce a simple construction method for tight wavelet frames over bounded domains. We then construct B-spline tight wavelet frames and box spline tight wavelet frames over bounded domains. Tight wavelet frame construction over bounded domains is quite different than tight wavelet frame construction over unbounded domains. Concrete examples in [CHS2] show that it is impossible to construct tight wavelet frames over bounded domains by modifying tight wavelet frames over unbounded domains. In their paper, Chui, He and Stöckler developed a general theory of non-stationary tight wavelet frame construction over a bounded interval using univariate splines over non-equally spaced knots. Our method for tight wavelet frame construction is an independent work of theirs. One of the advantages of our method is that our method works in the multivariable settings.

This dissertation is organized as follows. In Chapter 2, we first review the concept of tight wavelet frames in the multivariate setting. In Section 2.2, two easy constructive methods are presented to compute tight wavelet frames for any given refinable function whose Laurent polynomial satisfies the QMF or the sub-QMF condition in the multivariate setting. Chapter 3 contains five sections. The first two sections are overviews of B-splines and box splines respectively. We show the construction of B-spine tight wavelet frames, tensor product of B-spline tight wavelet frames in Section 3.3 and in Section 3.4. Our main construction is in Section 3.5. We construct tight wavelet frames for box splines by using Lai and Stöckler's method under the sub-QMF condition in this chapter. The explicit Laurent polynomials satisfying condition (1.1) for various orders of bivariate box splines are given. In Chapter 4, in Section 4.1, we briefly explain the wavelet frame decomposition and reconstruction. In Section 4.2, we present numerical experiments for edge detection using one of the box spline tight wavelet frames we constructed. For effectiveness comparison, we also show edge detected images by the tensor products of traditional wavelets and engineering edge detections. Image de-noising is presented in Section 4.3. We use one of the box spline tight wavelet frame we constructed for image de-noising. The effectiveness of de-noising by using a box spline tight wavelet frame and the tensor product of wavelets will be measured by PSNR numbers. In Chapter 5, in Section 5.1 and Section 5.2 we introduce a simple tight wavelet frame construction. According to the construction scheme, B-spline tight wavelet frames and box spline tight wavelet frames over bounded domains are constructed in Section 5.3 and Section 5.4.

Chapter 2

Tight Wavelet Frames over $\mathbb{R}^d$

2.1 Preliminary

We use the standard inner product and L^2-norm in $L^2(\mathbb{R}^d)$, i.e.,

$$\langle f, g \rangle = \int_{\mathbb{R}^d} f(\mathbf{y})\overline{g(\mathbf{y})}\, d\mathbf{y},$$

$$\|f\|^2 := \langle f, f \rangle.$$

The Fourier transform of f is defined by

$$\widehat{f}(\omega) := \langle f(\cdot), e^{i\omega\cdot} \rangle = \int_{\mathbb{R}^d} f(\mathbf{y})\,\overline{e^{i\omega\mathbf{y}}}\, d\mathbf{y}, \quad i = \sqrt{-1}.$$

Definition 2.1.1 *A family of functions $\{f_j\}_{j\in J}$ in a Hilbert space $\mathcal{H}$ is called a* **frame***, if there exist constants $A, B > 0$ such that*

$$A\|f\|^2 \;\le\; \sum_{j\in J} |\langle f, f_j\rangle|^2 \;\le\; B\|f\|^2 \;,\; \forall f \in \mathcal{H}.$$

If $A = B = 1$ we call $\{f_j\}_{j\in J}$ **a tight frame***. Thus for the tight frame we have*

$$\|f\|^2 = \sum_{j\in\mathbb{Z}} |\, \langle f,\, f_j\rangle \,|^2, \quad \forall f \in \mathcal{H}.$$

The multiresolution analysis(MRA) was introduced by Stéphan Mallar [Ma] and Yves Meyer [Me] for the orthonormal wavelet construction. This definition gave a mathematical properties of multiresolution space that was used to analyze an image from the lower resolution to the higher resolution in the image processing.

Definition 2.1.2 *We call a sequence of subspaces $\{V_j\}_{j\in\mathbb{Z}}$ a multiresolution analysis (MRA) of $L^2(\mathbb{R}^d)$ if it is satisfying*

(1) $0 \subset \cdots \subset V_{-1} \subset V_0 \subset V_1 \subset \cdots \subset L^2$

(2) $\overline{\cup_{j\in\mathbb{Z}} V_j} = L^2$ *and* $\cap_{j\in\mathbb{Z}} V_j = 0$

(3) $f \in V_j \Leftrightarrow f(2\cdot) \in V_{j+1}$

(4) *If* $f \in V_j$ *then* $f(\cdot - 2^j k) \in V_j$ *for all* $k \in \mathbb{Z}$

(5) *There exists* $\phi \in V_0$ *such that* $\{\phi_{0,k} : k \in \mathbb{Z}\}$ *is an orthonormal basis of* V_0

The MRA notion for wavelet frames in this dissertation is following the one in [RS1] which is slightly modified version of Definition 2.1.2. Consider compactly supported function $\phi \in L^2(\mathbb{R}^d)$ satisfying the following conditions :

(i) There exists a Laurent polynomial P such that

$$\widehat{\phi}(\omega) = P(\omega/2)\widehat{\phi}(\omega/2).$$

If we denote $P(\omega) := 2^{-d} \sum p_k e^{i\omega\cdot\mathbf{k}}$, for a sequence $\{p_{\mathbf{k}}\} \in \ell^2(\mathbb{R}^d)$ then

$$\phi(\mathbf{x}) = \sum_{\mathbf{k}\in\mathbb{Z}^d} p_{\mathbf{k}}\, \phi(2\,\mathbf{x} - \mathbf{k}), \ \ \forall \mathbf{x} \in \mathbb{R}^d. \tag{2.1}$$

(ii) $\lim_{\omega\to 0} \widehat{\phi}(\omega) = 1$.

Let us denote

$$V_j := \overline{\text{span}\{2^{\frac{j}{2}}\phi(2^j \cdot -\mathbf{k}) : \mathbf{k} \in \mathbb{Z}^d\}}.$$

Then V_j satisfies all the conditions (1)-(4). We call function ϕ a **refinable function** and $\{V_j\}_{j\in\mathbb{Z}}$ an MRA generated by a refinable function ϕ.

The following condition called Unitary Extension Principle (UEP) was developed by Ron and Shen in [RS1].

$$P(\omega)\overline{P(\omega+\nu)} + \sum_{\ell=1}^{N} Q^{\ell}(\omega)\overline{Q^{\ell}(\omega+\nu)} = \begin{cases} 1 & \text{if } \nu = 0\ , \\ 0 & \text{if } \nu \in \{0,\pi\}^d \backslash \{0\} \end{cases} \tag{2.2}$$

This condition gives sufficient condition to have a tight wavelet frame in $L^2(\mathbb{R}^d)$. For a given Laurent polynomial P associated with a refinable function ϕ such that

$$\widehat{\phi}(\omega) = P(\omega/2)\widehat{\phi}(\omega/2),$$

we define functions $\psi^1, \cdots, \psi^N$ in subspace V_1 by

$$\widehat{\psi^\ell}(\omega) = Q^\ell(\omega/2)\,\widehat{\phi}(\omega/2), \;\; \ell = 1, \ldots, N, \tag{2.3}$$

with Laurent polynomial Q^ℓ's in $e^{i\omega}$ satisfying the Unitary Extension Principle (UEP) condition. If we denote $Q^\ell(\omega) := 2^{-d}\sum q_k^\ell e^{i\omega\cdot\mathbf{k}}$, for some sequence $\{q_{\mathbf{k}}^\ell\} \in \ell^2(\mathbb{R}^d)$ for each $\ell = 1, \cdots, N$, then

$$\psi^\ell(\mathbf{x}) = \sum_{\mathbf{k}\in\mathbb{Z}^d} q_{\mathbf{k}}^\ell\,\phi(2\,\mathbf{x} - \mathbf{k}), \;\; \forall\,\mathbf{x} \in \mathbb{R}^d. \tag{2.4}$$

Let us denote $\psi_{j,\mathbf{k}}^\ell := 2^{\frac{j}{2}}\psi^\ell(2^j\cdot -\mathbf{k})$. Then for all $f \in L^2(\mathbb{R}^d)$,

$$\|f\|^2 \; = \sum_{\ell=1}^{N}\sum_{j\in\mathbb{Z}}\sum_{\mathbf{k}\in\mathbb{Z}^d} |\langle f, \psi_{j,\mathbf{k}}^\ell\rangle|^2. \tag{2.5}$$

We call the collection of functions $\Lambda(\Psi) := \{\psi_{j,\mathbf{k}}^\ell : \ell = 1, \cdots, N, j \in \mathbb{Z}; \mathbf{k} \in \mathbb{Z}^d\}$ constructed in an MRA generated by a refinable function $\phi \in L^2(\mathbb{R}^d)$ an **MRA-tight wavelet frame** and each ψ^ℓ a **tight framelet (or a tight wavelet frame genetrator).**

Let us revisit (2.5). For a fixed f and for all g in $L^2(\mathbb{R}^d)$, we have

$$\|f + g\|^2 = \sum_{\ell=1}^{N}\sum_{j\in\mathbb{Z}}\sum_{\mathbf{k}\in\mathbb{Z}^d} |\langle f + g, \psi_{\mathbf{k},j}\rangle|^2, \tag{2.6}$$

$$\|f - g\|^2 = \sum_{\ell=1}^{N}\sum_{j\in\mathbb{Z}}\sum_{\mathbf{k}\in\mathbb{Z}^d} |\langle f - g, \psi_{\mathbf{k},j}\rangle|^2. \tag{2.7}$$

If we subtract the equation (2.7) from (2.6), by the polarization identity, we have

$$4\langle f, g\rangle = 4\langle \sum_{\ell=1}^{N}\sum_{j\in\mathbb{Z}}\sum_{\mathbf{k}\in\mathbb{Z}^d} \langle f, \psi_{\mathbf{k},j}\rangle\psi_{\mathbf{k},j}\,,\, g\,\rangle.$$

Then

$$f = \sum_{\ell=1}^{N}\sum_{j\in\mathbb{Z}}\sum_{\mathbf{k}\in\mathbb{Z}^d} \langle f,\, \psi_{j,\mathbf{k}}^\ell\rangle\,\psi_{j,\mathbf{k}}^\ell\,, \text{ weakly } \forall f \in L^2(\mathbb{R}^d). \tag{2.8}$$

That is, a tight wavelet frame $\Lambda(\Psi)$ can represent any $f \in L^2(\mathbb{R}^d)$. Compared to the orthonormal wavelet basis representation of a function in $L^2(\mathbb{R}^d)$, the tight frame expression of a function $f \in L^2(\mathbb{R})$ allows redundancy. Also relaxing the orthonormal condition on a family of integer translations of a refinable function $\{\phi_{0,\mathbf{k}} : \mathbf{k} \in \mathbb{Z}^d\}$ and wavelet functions $\{\psi^\ell_{0,\mathbf{k}} : \mathbf{k} \in \mathbb{Z}^d, \ell = 1, \cdots, N\}$ gives room for different possibilities of construction methods.

The following three lemmas are adapted from [LS] and their proofs are different from the ones in [RS1].

Lemma 2.1.1 *Let $\phi \in L^2(\mathbb{R}^d)$. Suppose that $\lim_{\omega\to 0} \widehat{\phi}(\omega) = 1$ and that for some constant $B > 0$*

$$\sum_{m\in 2\pi\mathbb{Z}^d} |\widehat{\phi}(\omega + m)|^2 \le B < +\infty, \quad a.e., \quad \omega \in \mathbb{R}^d$$

Define

$$\beta_j(f,\omega) = 2^{\frac{dj}{2}} \sum_{m\in 2\pi\mathbb{Z}^d} \widehat{f}(2^j(\omega + m))\overline{\widehat{\phi}(\omega + m)}$$

for any fixed $f \in L^2(\mathbb{R}^d)$ and $j \in \mathbb{Z}$. Then

$$\lim_{j\to+\infty} \int_{[0,2\pi]^d} |\beta_j(f,\omega)|^2 \, d\omega = \| f \|^2 \quad and$$

$$\lim_{j\to-\infty} \int_{[0,2\pi]^d} |\beta_j(f,\omega)|^2 \, d\omega = 0$$

Proof By the definition of $\beta_j(f,\omega)$,

$$\begin{aligned}
&\int_{[0,2\pi]^d} |\beta_j(f,\omega)|^2 \, d\omega \\
&= 2^{dj} \sum_{m,n\in 2\pi Z^d} \int_{[0,2\pi]^d} \widehat{f}(2^j(\omega + m))\overline{\widehat{f}(2^j(\omega + n))}\ \overline{\widehat{\phi}(\omega + m)}\widehat{\phi}(\omega + n) \, d\omega \\
&= 2^{dj} \sum_{n\in 2\pi Z^d} \int_{\mathbb{R}^d} \widehat{f}(2^j\omega)\overline{\widehat{f}(2^j(\omega + n))}\ \overline{\widehat{\phi}(\omega)}\widehat{\phi}(\omega + n) \, d\omega \\
&= \int_{\mathbb{R}^d} |\widehat{f}(\omega)|^2 \, |\widehat{\phi}(2^{-j}\omega)|^2 \, d\omega + 2^{dj} \sum_{\substack{n\neq 0 \\ n\in 2\pi\mathbb{Z}^d}} \int_{\mathbb{R}^d} \widehat{f}(2^j\omega)\overline{\widehat{f}(2^j(\omega + n))}\ \overline{\widehat{\phi}(\omega)}\widehat{\phi}(\omega + n) \, d\omega.
\end{aligned} \tag{2.9}$$

We want to show that (2.9) converges to $\| f \|^2$ as $j \to \infty$. Since the first term of the third equality in (2.9)

$$\int_{\mathbb{R}^d} |\widehat{f}(\omega)|^2 \, | \, \widehat{\phi}(2^{-j}\omega) \, |^2 \, d\omega \to \| f \|^2, \text{ as } j \to \infty,$$

we only need to show that the absolute value of the second term in (2.9)

$$|\text{Rest}(f)| := 2^{dj} \left| \sum_{\substack{n\neq 0 \\ n\in 2\pi\mathbb{Z}^d}} \int_{\mathbb{R}^d} \widehat{f}(2^j\omega)\overline{\widehat{f}(2^j(\omega+n))}\ \overline{\widehat{\phi}(\omega)}\widehat{\phi}(\omega+n)d\omega \right| \to 0, \text{ as } j\to\infty. \quad (2.10)$$

Since $|\widehat{\phi}(\omega)|^2 \leq B$, for the function $f \in L^2(\mathbb{R}^d)$ and $\widehat{f} \in C^\infty(\mathbb{R}^d)$,

$$|\text{Rest}(f)| \leq B \sum_{\substack{n\neq 0 \\ n\in 2\pi\mathbb{Z}^d}} \int_{\mathbb{R}^d} \left|\widehat{f}(\omega)\overline{\widehat{f}(\omega+2^jn)}\right|\ d\omega \to 0, \text{ as } j\to\infty,$$

see [D, p.143] for detail. Since these functions f in $L^2(\mathbb{R}^d)$ and whose Fourier Transformation is in $C^\infty(\mathbb{R}^d)$ are dense in $L^2(\mathbb{R}^d)$, we have

$$\lim_{j\to+\infty}\int_{[0,2\pi]^d} |\beta_j(f,\omega)|^2\ d\omega = \| f \|^2 \text{ and}$$

For $j \to -\infty$ we consider characteristic function χ_R of domain $[-R\ R\ ]^d$ and $f_R = f\chi_R$. For any given $\epsilon > 0$, we can find $R_\epsilon > 0$ such that

$$\|f - f_{R_\epsilon}\|_{L^2(\mathbb{R}^d)} \leq \epsilon, \text{ for } f \in L^2(\mathbb{R}^d).$$

Then

$$\begin{aligned}
\int_{[0,2\pi]^d} |\beta_j(f,\omega)|^2\ d\omega &\leq 2^{dj}\int_{[0,2\pi]^d}\left|\sum_{m\in 2\pi\mathbb{Z}^d}\widehat{f_{R_\epsilon}}(2^j(\omega+m))\widehat{\phi}(\omega+m)\right|^2 d\omega \\
&\quad + 2^{dj}\int_{[0,2\pi]^d}\left|\sum_{m\in 2\pi\mathbb{Z}^d}(\widehat{f}-\widehat{f_{R_\epsilon}}(2^j(\omega+m)))\widehat{\phi}(\omega+m)\right|^2 d\omega \\
&\leq \int_{[0,2\pi]^d}|\beta_j(f_{R_\epsilon},\omega)|^2 d\omega \\
&\quad + B2^{dj}\int_{[0,2\pi]^d}\sum_{m\in 2\pi\mathbb{Z}^d}|\widehat{f}-\widehat{f_{R_\epsilon}}(2^j(\omega+m))|^2 d\omega \\
&= \int_{[0,2\pi]^d}|\beta_j(f_{R_\epsilon},\omega)|^2 d\omega + B\int_{\mathbb{R}^d}|\widehat{f}-\widehat{f_{R_\epsilon}}|^2 d\omega \\
&\leq \int_{[0,2\pi]^d}|\beta_j(f_{R_\epsilon},\omega)|^2 d\omega + B\epsilon^2.
\end{aligned}$$

Now we need to show that

$$\int_{[0,2\pi]^d} |\beta_j(f_{R_\epsilon},\omega)|^2\, d\omega \to 0, \quad \text{as} \quad j\to-\infty.$$

By Parseval's equality,

$$\begin{aligned}\int_{[0,2\pi]^d} \left|\beta_j(f_{R_\epsilon},\omega)\right|^2 d\omega &= (2\pi)^{-d} \sum_{\mathbf{k}\in\mathbb{Z}^d} \Big| \int_{[0,2\pi]^d} \beta_j(f_{R_\epsilon},\omega)\, e^{i\mathbf{k}\omega}\, d\omega \Big|^2 \\ &= (2\pi)^{-d} 2^{dj} \sum_{\mathbf{k}\in\mathbb{Z}^d} \Big| \int_{\mathbb{R}^d} \widehat{f}_{R_\epsilon}(2^j\omega)\, \widehat{\phi}(\omega)\, e^{i\mathbf{k}\omega}\, d\omega \Big|^2 \\ &= (2\pi)^{-d} 2^{-dj} \sum_{\mathbf{k}\in\mathbb{Z}^d} \Big| \int_{\mathbb{R}^d} \widehat{f}_{R_\epsilon}(\omega)\, \widehat{\phi}(2^{-j}\omega)\, e^{i2^{-j}\mathbf{k}\omega}\, d\omega \Big|^2 \\ &= (2\pi)^{-d} 2^{dj} \sum_{\mathbf{k}\in\mathbb{Z}^d} \Big| \int_{\mathbb{R}^d} f_{R_\epsilon}(\mathbf{x})\, \phi(2^j\mathbf{x}-\mathbf{k})\, d\mathbf{x} \Big|^2 \\ &\le (2\pi)^{-d} \|f_{R_\epsilon}\|_2^2 \sum_{\mathbf{k}\in\mathbb{Z}^d} \int_{|\mathbf{y}|\le 2^j R_\epsilon} |\phi(\mathbf{y}-\mathbf{k})|^2\, d\mathbf{y} \to 0 \quad \text{as} \quad j \to -\infty,\end{aligned}$$

by the same reason on [D, p. 141]. □

Lemma 2.1.2 *For the refinable function ϕ satisfying the same condition in Lemma 2.1.1 and ψ^ℓ defined in (2.3) in terms of Fourier transform, we have the following equations:*

$$\sum_{\mathbf{k}\in\mathbb{Z}^d} |\langle f, \phi_{j,\mathbf{k}}\rangle|^2 = \int_{[0,2\pi]^d} |\beta_j(f,\omega)|^2 d\omega \tag{2.11}$$

$$\sum_{\mathbf{k}\in\mathbb{Z}^d} |\langle f, \phi_{j-1,\mathbf{k}}\rangle|^2 = \frac{1}{2^d} \int_{[0,2\pi]^d} \left| \sum_{\nu\in\{0,1\}^d\pi} \overline{P\left(\frac{\omega}{2}+\nu\right)}\, \beta_j\left(f, \frac{\omega}{2}+\nu\right) \right|^2 d\omega \tag{2.12}$$

$$\sum_{\mathbf{k}\in\mathbb{Z}^d} |\langle f, \psi^\ell_{j,\mathbf{k}}\rangle|^2 = \frac{1}{2^d} \int_{[0,2\pi]^d} \left| \sum_{\nu\in\{0,1\}^d\pi} \overline{Q^\ell\left(\frac{\omega}{2}+\nu\right)}\, \beta_j\left(f, \frac{\omega}{2}+\nu\right) \right|^2 , d\omega \tag{2.13}$$

where $\phi_{j,\mathbf{k}}(\cdot) = 2^{\frac{dj}{2}}\phi(2^j\cdot-\mathbf{k})$, $\psi^\ell_{j,\mathbf{k}}(\cdot) = 2^{\frac{dj}{2}}\psi^\ell(2^j\cdot-\mathbf{k})$, and β_j is given by the same formula defined in Lemma 2.1.1.

Proof Note that $\widehat{\phi}_{j,\mathbf{k}}(\omega) = 2^{-\frac{dj}{2}}\widehat{\phi}(2^{-j}\omega)e^{-i\frac{\omega\mathbf{k}}{2^j}}$. The equation in (2.11) can be proved by the Parseval Identity.

$$\begin{aligned}
\sum_{\mathbf{k}\in\mathbb{Z}^d} |\langle f, \phi_{j,\mathbf{k}}\rangle|^2 &= \frac{1}{(2\pi)^d}\sum_{\mathbf{k}\in\mathbb{Z}^d}\left|\int_{\mathbb{R}^d}\widehat{f}(\omega)\overline{\widehat{\phi}_{j\mathbf{k}}(\omega)}\,d\omega\right|^2 \\
&= \frac{2^{-dj}}{(2\pi)^d}\sum_{\mathbf{k}\in\mathbb{Z}^d}\left|\int_{\mathbb{R}^d}\widehat{f}(\omega)\overline{e^{-i\frac{\mathbf{k}\cdot\omega}{2^j}}\widehat{\phi}(2^{-j}\omega)}\,d\omega\right|^2 \\
&= \frac{2^{-dj}}{(2\pi)^d}\sum_{\mathbf{k}\in\mathbb{Z}^d}\left|\int_{\mathbb{R}^d}\widehat{f}(\omega)\overline{\widehat{\phi}(2^{-j}\omega)}\,e^{i\frac{\mathbf{k}\cdot\omega}{2^j}}\,d\omega\right|^2 \\
&= \frac{2^{dj}}{(2\pi)^d}\sum_{\mathbf{k}\in\mathbb{Z}^d}\left|\int_{\mathbb{R}^d}\widehat{f}(2^j\omega)\overline{\widehat{\phi}(\omega)}\,e^{i\mathbf{k}\cdot\omega}\,d\omega\right|^2 \\
&= \frac{1}{(2\pi)^d}\sum_{\mathbf{k}\in\mathbb{Z}^d}\left|\int_{[0,\,2\pi]^d}\sum_{n\in 2\pi\mathbb{Z}}2^{\frac{dj}{2}}\widehat{f}(2^j(\omega+n))\overline{\widehat{\phi}(\omega+n)}\,e^{i\mathbf{k}\cdot\omega}\,d\omega\right|^2 \\
&= \frac{1}{(2\pi)^d}\sum_{\mathbf{k}\in\mathbb{Z}^d}\left|\int_{[0,\,2\pi]^d}\beta_j(f,\omega)\,e^{i\mathbf{k}\cdot\omega}\,d\omega\right|^2 \\
&= \int_{[0,\,2\pi]^d}|\beta_j(f,\omega)|^2\,d\omega
\end{aligned}$$

From the previous argument,

$$\begin{aligned}
&\sum_{\mathbf{k}\in\mathbb{Z}^d} |\langle f, \phi_{j-1,\mathbf{k}}\rangle|^2 \\
&= \int_{[0,\,2\pi]^d}|\beta_{j-1}(f,\omega)|^2\,d\omega \\
&= 2^{(j-1)d}\int_{[0,2\pi]^d}\left|\sum_{m\in 2\pi\mathbb{Z}^d}\widehat{f}(2^{j-1}(\omega+m))\,\overline{P\left(\frac{\omega}{2}+\frac{m}{2}\right)\widehat{\phi}\left(\frac{\omega}{2}+\frac{m}{2}\right)}\right|^2 d\omega \\
&= 2^{(j-1)d}\int_{[0,2\pi]^d}\left|\sum_{m\in 2\pi\mathbb{Z}^d}\overline{P\left(\frac{\omega+m}{2}\right)}\widehat{f}\left(2^j\left(\frac{\omega+m}{2}\right)\right)\overline{\widehat{\phi}\left(\frac{\omega+m}{2}\right)}\right|^2 d\omega \\
&= 2^{-d}\int_{[0,2\pi]^d}\left|\sum_{\nu\in\{0,\pi\}^d}\overline{P\left(\frac{\omega}{2}+\nu\right)}\beta_j\left(f,\frac{\omega}{2}+\nu\right)\right|^2 d\omega
\end{aligned}$$

Similarly, we can prove the equation (2.13). □

The following Lemma 2.1.3 says that if we find Laurent polynomial Q^ℓ's satisfying the Unitary Extension Principle (UEP) in (2.2) for the Laurent polynomial P associated with the refinable function ϕ, then the ψ^ℓ's defined in (2.3) in terms of Fourier transform are tight wavelet frame generators (cf. [DHRS]).

Lemma 2.1.3 *Suppose that we can find Q^ℓ, $\ell = 1, \ldots, N$ satisfying (2.2). Let ψ^ℓ be the function defined by its Fourier transform in (2.3). Then the collection of functions $\Lambda(\Psi) = \{\psi^\ell_{j,\mathbf{k}} \,:\, \ell = 1, \ldots, N, j \in \mathbb{Z}$ and $\mathbf{k} \in \mathbb{Z}^d\}$ is a tight wavelet frame.*

Proof We need to show that

$$\sum_{\ell=1}^{N}\sum_{j\in\mathbb{Z}}\sum_{\mathbf{k}\in\mathbb{Z}^d} |\,\langle f, \psi^\ell_{j,\mathbf{k}}\,\rangle\,|^2 = \|f\|_2^2, \qquad \forall f \in L^2(\mathbb{R}^d).$$

By (2.11) and (2.13), for fixed j

$$\begin{aligned}
\sum_{\ell=1}^{N}\sum_{\mathbf{k}} |\,\langle f, \psi^\ell_{j,\mathbf{k}}\rangle\,|^2 &= \frac{1}{2^d}\int_{[0,2\pi]^d} \sum_{\ell=1}^{N}\Big|\sum_{\nu\in\{0,\pi\}^d} \overline{Q^\ell\left(\frac{\omega}{2}+\nu\right)}\,\beta_j\left(f, \frac{\omega}{2}+\nu\right)\,\Big|^2 d\omega \\
&= \frac{1}{2^d}\int_{[0,2\pi]^d} \sum_{\nu,m\in\{0,\pi\}^d} \beta_j\left(f, \frac{\omega}{2}+\nu\right)\,\overline{\beta_j\left(f, \frac{\omega}{2}+m\right)} \\
&\qquad \sum_{\ell=1}^{N} \overline{Q^\ell\left(\frac{\omega}{2}+\nu\right)}\,Q^\ell\left(\frac{\omega}{2}+m\right) d\omega \\
&= \frac{1}{2^d}\int_{[0,2\pi]^d} \sum_{\nu\in\{0,\pi\}^d} |\beta_j\left(f, \frac{\omega}{2}+\nu\right)|^2\, \sum_{\ell=1}^{N} |Q^\ell\left(\frac{\omega}{2}+\nu\right)|^2\, d\omega \\
&\qquad - \sum_{\nu\neq m} \beta_j\left(f, \frac{\omega}{2}+\nu\right)\,\overline{\beta_j\left(f, \frac{\omega}{2}+m\right)}\,\overline{P\left(\frac{\omega}{2}+\nu\right)}\,P\left(\frac{\omega}{2}+m\right)\,]\, d\omega \\
&= \frac{1}{2^d}\int_{[0,2\pi]^d} \sum_{\nu\in\{0,\pi\}^d} |\beta_j\left(f, \frac{\omega}{2}+\nu\right)|^2\,\left(1 - |P\left(\frac{\omega}{2}+\nu\right)|^2\right) \\
&\qquad - \frac{1}{2^d}\sum_{\nu\neq m} \beta_j\left(f, \frac{\omega}{2}+\nu\right)\,\overline{\beta_j\left(f, \frac{\omega}{2}+m\right)}\,\overline{P\left(\frac{\omega}{2}+\nu\right)}\,P\left(\frac{\omega}{2}+m\right) d\omega \\
&= \frac{1}{2^d}\int_{[0,\pi]^d} \sum_{\nu\in\{0,\pi\}^d} |\beta_j\left(f, \omega+\nu\right)|^2\, d\omega \\
&\qquad - \frac{1}{2^d}\int_{[0,2\pi]^d} \sum_{\nu\in\{0,\pi\}^d} \left|\beta_j\left(f, \frac{\omega}{2}+\nu\right)\right|^2 d\omega \\
&= \int_{[0,2\pi]^d} |\beta_j(f,\omega)\,|^2\, d\omega - \int_{[0,2\pi]^d} |\beta_{j-1}(f,\omega)|^2\, d\omega.
\end{aligned}$$

If we sum for j from 1 to ∞, by Lemma 2.1.1,

$$\begin{aligned}
\sum_{\ell=1}^{N}\sum_{j\in\mathbb{Z}}\sum_{\mathbf{k}\in\mathbb{Z}^d} |\,\langle f, \psi_{i;\,j,\mathbf{k}}\rangle\,|^2 &= \lim_{j\to+\infty}\int_{[0,2\pi]^d} |\beta_j(f,\omega)\,|^2\, d\omega - \lim_{j\to-\infty}\int_{[0,2\pi]^d} |\beta_{j-1}(f,\omega)|^2\, d\omega \\
&= \|f\|_2^2
\end{aligned}$$

□

2.2 Construction Scheme

In this section we consider the tight wavelet frame construction on MRA generated by a refinable function whose Laurent polynomial satisfies either the QMF condition or the sub-QMF condition. By Lemma 2.1.3, if we find Laurent polynomials Q^ℓ satisfying the UEP condition for the given Laurent polynomial P, we can construct a tight wavelet frame. First we consider the following equivalent condition (2.14) to the UEP condition as a construction tool.

Lemma 2.2.1 *Let $\mathcal{P} = (P(\omega+\nu))_{\nu\in\{0,\pi\}^d}$ a vector of size $2^d \times 1$ and $\mathcal{Q} = (Q^\ell(\omega+\nu))_{\substack{\ell=1,\ldots,N \\ \nu\in\{0,\pi\}^d}}$ be a matrix of size $N \times 2^d$. Then the UEP condition in (2.2) is equivalent to*

$$\mathcal{Q}^*\mathcal{Q} = I - \overline{\mathcal{P}}\mathcal{P}^T. \tag{2.14}$$

Proof This can be verified by direct calculation. □

2.2.1 Under the QMF Condition

In signal and image processing, engineers call the Laurent polynomial P associated with a refinable function ϕ a low-pass filter and each Q^ℓ associated with ψ^ℓ a high-pass filter. The *Quadrature Mirror Filter* was constructed coefficients of a high-pass filter by alternating signs of the low-pass filter coefficients by Croisier-Estaban-Galand in 1976. Since then the following condition for a low-pass filter P

$$\sum_{\nu\in\{0,\pi\}^d} |P(\omega+\nu)|^2 = 1 \tag{2.15}$$

is called the QMF condition. Let

$$\mathcal{M} := \frac{1}{2^{d/2}} (e^{im\cdot(\omega+\nu)})_{\substack{m\in\{0,1\}^d \\ \nu\in\{0,\pi\}^d}}. \tag{2.16}$$

Where let m be the row index and ν be the column index. Note that $\mathcal{M}^*\mathcal{M} = I$.

Theorem 2.2.1 (Lai& Stöckler'04) *Suppose that Laurent polynomial P satisfies the QMF condition (2.15). Define $Q^1, \ldots, Q^{2^d}$ by*

$$\mathcal{Q} := (Q^\ell(\omega+\nu))_{\substack{\ell=1,\ldots,2^d \\ \nu\in\{0,\pi\}^d}} = \mathcal{M}(I_{2^d\times 2^d} - \overline{\mathcal{P}}\mathcal{P}^T), \tag{2.17}$$

where $\mathcal{P} = (P(\omega+\nu))_{\nu\in\{0,\pi\}^d}$ is a vector of size $2^d \times 1$ and $\mathcal{M}$ is the matrix in (2.16). Then P and $Q^\ell, \ell = 1, \cdots, 2^d$ satisfy (2.2) .

Proof It is trivial to verify that

$$\mathcal{Q}^*\mathcal{Q} = I_{2^d\times 2^d} - \overline{\mathcal{P}}\mathcal{P}^T$$

which is (2.14). Thus Q^ℓ's in the first column of the matrix $\mathcal{Q}$ are the desired Laurent polynomials. □

Using the Laurent polynomials Q^ℓ given in Theorem 2.2.1, we construct tight framelets ψ^ℓ corresponding to a refinable function ϕ whose Laurent polynomial P satisfying the QMF condition. There are many construction methods for a refinable function whose Laurent polynomial satisfies the QMF condition (cf. [L2]).

2.2.2 Under The Sub-QMF Condition

In general the filter P of a refinable function does not satisfy the QMF condition. Instead, it may satisfy the following condition (2.18) which is called sub-QMF condition :

$$\sum_{\nu\in\{0,\pi\}^d} |P(\omega+\nu)|^2 \le 1. \tag{2.18}$$

We now explain how to construct tight wavelet frames associated with the standard dilation matrix $2I_{d\times d}$ using the refinable function ϕ whose Laurent polynomial P satisfies (2.18). Let

$$\widehat{\mathcal{P}} := (\widehat{P}_n(2\omega))_{n\in\{0,1\}^d} := \mathcal{M}(\overline{P(\omega+\nu)})_{\nu\in\{0,\pi\}^d}, \tag{2.19}$$

where $\mathcal{M}$ is the polyphase matrix given in (2.16). That is, the $\widehat{P}_n$'s are polyphase components of $\overline{P}$. Then (2.18) implies that

$$\sum_{n\in\{0,1\}^d} |\widehat{P}_n(2\omega)|^2 \le 1.$$

Theorem 2.2.2 (Lai& Stöckler'04) *Suppose that the Laurent polynomial P satisfies the sub-QMF condition (2.18). Suppose that there exist Laurent polynomials $\widetilde{P}_1, \ldots, \widetilde{P}_N$ such that*

$$\sum_{m\in\{0,1\}^d} |\widehat{P}_n(2\omega)|^2 + \sum_{i=1}^{N} |\widetilde{P}_i(2\omega)|^2 = 1, \tag{2.20}$$

where $\widehat{P}_n$'s are defined in (2.19). Then there exist $2^d + N$ locally supported tight framelets with Laurent polynomials $Q^\ell, \ell = 1, \ldots, 2^d + N$ such that P and Q^ℓ, $\ell = 1, \ldots, 2^d + N$ satisfy UEP condition in (2.2).

Proof Let $\widetilde{\mathcal{P}} = (\widehat{P}_n(2\omega), \widetilde{P}_1(2\omega), \ldots \widetilde{P}_N(2\omega))^T_{n\in\{0,1\}^d}$ be a vector of size $(2^d + N) \times 1$. Define

$$\widetilde{\mathcal{Q}} := I_{(2^d+N)\times(2^d+N)} - \widetilde{\mathcal{P}}\widetilde{\mathcal{P}}^*.$$

Clearly $\widetilde{\mathcal{Q}}^*\widetilde{\mathcal{Q}} = \widetilde{\mathcal{Q}}$. In particular, we have

$$\widetilde{\mathcal{P}}\widetilde{\mathcal{P}}^* + \widetilde{\mathcal{Q}}^*\widetilde{\mathcal{Q}} = I_{(2^d+N)\times(2^d+N)}.$$

Restricting to the principle $2^d \times 2^d$ blocks in the above matrices, we have

$$\widehat{\mathcal{P}}\widehat{\mathcal{P}}^* + \widehat{\mathcal{Q}}^*\widehat{\mathcal{Q}} = I_{2^d\times 2^d}, \tag{2.21}$$

where $\widehat{\mathcal{P}} = (\widehat{P}_n(2\omega))^T_{n\in\{0,1\}^d}$ and

$$\widehat{\mathcal{Q}} = (\widetilde{Q}_{n,\ell})_{\substack{1\le\ell\le 2^d+N \\ n\in\{0,1\}^d}}$$

with the $\widetilde{Q}_{n,\mathbf{k}}$'s being entries of $\widetilde{\mathcal{Q}}$.

Multiplying a polyphase matrix $\mathcal{M}$ and $\mathcal{M}^*$ defined in (2.16) to both sides of the above equation, we have

$$\mathcal{M}^*\widehat{\mathcal{P}}(\mathcal{M}^*\widehat{\mathcal{P}})^* + (\widehat{\mathcal{Q}}\mathcal{M})^*\widehat{\mathcal{Q}}\mathcal{M} = I_{2^d\times 2^d}.$$

Then $\overline{\mathcal{P}} = \mathcal{M}^*\widehat{\mathcal{P}}$ and

$$(\widehat{\mathcal{Q}}\mathcal{M})^*\widehat{\mathcal{Q}}\mathcal{M} = I_{2^d\times 2^d} - \overline{\mathcal{P}}\mathcal{P}^T$$

If we let $\mathcal{Q} = \widehat{\mathcal{Q}}\mathcal{M}$ then $\mathcal{Q}$ satisfies condition (2.14). Thus the first column $(Q^1, \ldots, Q^{2^d+N})^T$ of $\mathcal{Q}$ gives the desirable Laurent polynomials for locally supported tight framelets. $\square$

We shall use the constructive scheme in Theorem 2.2.2 to find locally supported tight wavelet frames based on multivariate box splines, in particular, bivariate box splines on three, four and eight direction meshes in Section 3.5 and univariate cardinal B-splines in Section 3.3.

Chapter 3

Classes of B-spline and Box Spline Tight Wavelet Frames

3.1 B-splines

The name spline function was introduced by Schönberg in 1946. A spline function is a piecewise polynomial with a certain degree of smoothness. Because of easy computer implementation and some flexibility, spline functions are used in many applications such as interpolation, data fitting, numerical solution of ordinary and partial differential equations (finite element method), and in curve and surface fitting.

A (cardinal) B-spline function of order m is a spline function with equally spaced simple knot sequence $\mathbb{Z}$. We define the B-spline of order ϕ_m for an integer $m \geq 2$, inductively by

$$\phi_m(x) := \phi_{m-1} * \phi_1(x) = \int_0^1 \phi_{m-1}(x-t)\,dt, \tag{3.1}$$

where ϕ_1 is the characteristic function of the interval $[0, 1)$.

Let $\{V_j^m\}_{j\in\mathbb{Z}}$ be the subspace generated by B-spline $\phi_m(2^j\cdot)$ and its translations, i.e.,

$$V_j^m := \overline{\text{span}\,\{\phi_m(2^j\cdot - k) : k \in \mathbb{Z}\}}. \tag{3.2}$$

Then $\{V_j^m\}_{j\in\mathbb{Z}}$ is nested subspace sequence, (see[C2, p. 85]) , i.e. ,

$$\leftarrow \cdots \subset V_{-1}^m \subset V_0^m \subset V_1^m \subset \cdots \rightarrow . \tag{3.3}$$

Moreover, it satisfies for some constants $A, B > 0$

$$A \leq \sum_{k\in\mathbb{Z}} \left|\widehat{\phi}_m(\omega + 2\pi k)\right|^2 \leq B < \infty$$

which is equivalent to saying that $\{\phi_m(2^j \cdot -k) : k \in \mathbb{Z}\}$ is a Riesz basis (or unconditional) of V_j^m in the sense that for each m, there exist constants $A_m, B_m > 0$ for any $\{c_k\} \in \ell^2$,

$$A_m \|\{c_k\}\|^2 \leq \left\| \sum_{k=-\infty}^{\infty} c_k \phi_m(\cdot - k) \right\|^2 \leq B_m \|\{c_k\}\|^2 \tag{3.4}$$

(see [C2, p. 90]). Then $\{V_j^m\}$ satisfies the following conditions (see [D, p. 141- p. 143]) :

$$\begin{aligned} &\overline{\cup_{j\in\mathbb{Z}} V_j^m} = L^2(\mathbb{R}), \\ &\cap_{j\in\mathbb{Z}} V_j^m = \{0\}. \end{aligned} \tag{3.5}$$

We state the basic and important properties of B-splines in the following Theorem. These properties are useful to evaluate B-spline function values, derivatives and integrals of B-splines. Theorem can be proved mostly by induction and definition of B-splines. We prove only condition (10) which will be used later. See other proofs in [C2, p. 92].

Theorem 3.1.1 *(1) For every $f \in C(\mathbb{R})$,*

$$\int_{-\infty}^{\infty} f(x)\phi_m \, dx = \int_0^1 \cdots \int_0^1 f(x_1 + \cdots + x_m) \, dx_1 \cdots dx_m.$$

(2) For every $g \in C^m(\mathbb{R})$,

$$\int_{-\infty}^{\infty} g^{(m)}(x)\phi_m(x) \, dx = (-1)^{m-k} \sum_{k=0}^{m} \binom{m}{k} g(k).$$

(3) $\phi_m(x) = \frac{1}{(m-1)!} \sum_{k=0}^{m} (-1)^k \binom{m}{k} (x-k)_+^{m-1}$, *where* $x_+ := max\,(0, m)$ *and* $x_+^{m-1} = (x_+)^{m-1}$.

(4) *supp* $\phi_m = [0, m]$.

(5) $\phi_m(x) \geq 0, \quad$ *for* $0 < x < m$.

(6) $\sum_{k=-\infty}^{\infty} \phi_m(x-k) = 1, \quad$ *for all* x.

(7) The derivative of B-spline ϕ_m *is*

$$\phi_m'(x) = \phi_{m-1}(x) + \phi_{m-1}(x-1).$$

(8) The B-spline ϕ_m and ϕ_{m-1} are related as follows

$$\phi_m(x) = \frac{x}{m-1}\phi_{m-1}(x) + \frac{m-x}{m-1}\phi_{m-1}(x-1).$$

(9) The B-spline ϕ_m is symmetric with respect to the center of its support .

$$\phi_m\left(\frac{m}{2}+x\right) = \phi_m\left(\frac{m}{2}-x\right), \quad x \in \mathbb{R}.$$

(10) ϕ_m has the following dyadic dilation relation

$$\phi_m(x) = \sum_{k=0}^{m} 2^{-m+1}\binom{m}{k}\phi_m(2x-k).$$

Proof of (10) Since $V_0 \subset V_1$, for some sequence $\{p_{m,k}\} \in \ell^2$,

$$\phi_m(x) = \sum_{k=-\infty}^{\infty} p_{m,k}\phi_m(2x-k) \tag{3.6}$$

We take the Fourier transform on both sides of (3.6),

$$\widehat{\phi_m}(\omega) = \frac{1}{2}\sum_{k=-\infty}^{\infty} p_{m,k}e^{-ik\omega/2}\widehat{\phi_m}\left(\frac{\omega}{2}\right), \quad i = \sqrt{-1}.$$

Denote $P_m(\omega)$ by the trigonometric function of the form $\frac{1}{2}\sum_{k=-\infty}^{\infty} p_{m,k}e^{-ik\omega}$. By using $\widehat{\phi_m}(\omega) = \widehat{\phi}_1(\omega)^m = \left(\frac{1-e^{-i\omega}}{i\omega}\right)^m$, we have

$$\widehat{\phi_m}(2\omega) = P_m(\omega)\widehat{\phi_m}(\omega) \tag{3.7}$$

where

$$P_m(\omega) = \frac{1}{2}\sum_{k=-\infty}^{\infty} p_{m,k}e^{-ik\omega} = \left(\frac{1+e^{-i\omega}}{2}\right)^m = \frac{1}{2^m}\sum_{k=0}^{m}\binom{m}{k}e^{-ik\omega}. \tag{3.8}$$

This gives the explicit form

$$p_{m,k} = \frac{1}{2^{m-1}}\binom{m}{k},$$

where $0 \le k \le m$ and $p_{m,k}$ is zero otherwise. □

Lemma 3.1.1 *For any $m \ge 1$, the trigonometric polynomial P_m associated with B-spline ϕ_m in (3.7) satisfies sub-QMF condition in (2.18).*

Proof From the second equality of the equations in (3.8), we have

$$|P_m(\omega)|^2 + |P_m(\omega+\pi)|^2 = |\cos^2(\omega/2)|^m + |\sin^2(\omega/2)|^m \le 1.$$

□

3.2 Box Splines

Multivariate box splines can be interpreted as a multivariate extension of univariate B-splines. Because of their useful geometric interpolation, multivariate box splines have been used for surface design. Thus multivariate box splines are very important class of refinable functions .

Let us assume that $s \geq d$ and that $\mathbf{v}_1, \cdots, \mathbf{v}_d$ are linearly independent vectors in $\mathbb{R}^d$. We define multivariate box spline $\phi_Y(\mathbf{x})$ determined by a directional set $Y := \{\mathbf{v}_1, \cdots, \mathbf{v}_s\}$ as follows inductively (cf. [BHR] and [C1]).

$$\phi_Y(\mathbf{x}) := \begin{cases} \begin{cases} 1/\det[\mathbf{v}_1 \cdots \mathbf{v}_d] & \text{if } \mathbf{x} \in [\mathbf{v}_1 \cdots \mathbf{v}_d][0,1)^d \\ 0 & \text{otherwise} , \end{cases} & \text{for } Y = \{\mathbf{v}_1, \cdots, \mathbf{v}_d\} \\ \int_0^1 \phi(\mathbf{x} - t\mathbf{v}_s | Y^*)\, dt, & \text{for } Y^* = \{\mathbf{v}_1, \cdots, \mathbf{v}_{d+1}, \cdots, \mathbf{v}_{s-1}\} \end{cases}$$

Then multivariate box spline $\phi_Y(\mathbf{x})$ is a piecewise polynomial of degree $\leq s-d$. Let $\{V_j^Y\}_{j\in\mathbb{Z}}$ be a subspace generated by box spline $\phi_Y(2^j\cdot)$ and its translations, i.e.,

$$V_j^Y := \overline{\text{ span } \{\phi_Y(2^j \cdot - \eta) : \eta \in \mathbb{Z}^d\}}. \tag{3.9}$$

Then $\{V_j^Y\}_{j\in\mathbb{Z}}$ satisfies the following conditions (see[BHR, p. 125]) .

$$\begin{aligned} &\leftarrow \cdots \subset V_{-1}^Y \subset V_0^Y \subset V_1^Y \subset \cdots \rightarrow, \\ &\overline{\cup_{j\in\mathbb{Z}} V_j^Y} = L^2(\mathbb{R}^d), \\ &\cap_{j\in\mathbb{Z}} V_j^Y = \{0\}. \end{aligned} \tag{3.10}$$

We recall the directional derivative with respect to $\mathbf{u}$ as

$$D_{\mathbf{u}} := \sum_{j=1}^{d} u_j \frac{\partial}{\partial x_j}, \qquad \text{where } (x_1, \cdots, x_d) \in \mathbb{R}^d$$

Similar to B-splines, we summarize some properties of multivariable box splines $\phi_Y(\mathbf{x})$(see [C1] for proof). For more properties of multivariate box splines, see [C1] and [BHR].

Theorem 3.2.1 *(1)* $\int_{\mathbb{R}^d} \phi_Y(\mathbf{x})\ d\mathbf{x} = 1.$

(2) *For all* $f \in C(\mathbb{R}^d)$

$$\int_{\mathbb{R}^d} \phi_Y(\mathbf{x}) f(\mathbf{x})\ d\mathbf{x} = \int_{[0,1)^s} f([\mathbf{v}_1 \cdots \mathbf{v}_s]t)\ dt.$$

(3) $\phi_Y(\mathbf{x}) > 0, \quad$ *for* $\mathbf{x} \in [\mathbf{v}_1 \cdots \mathbf{v}_s][0,1)^s$,

(4) *supp* $\phi_Y(\cdot) = [\mathbf{v}_1 \cdots \mathbf{v}_s][0,1]^s$.

(5) *The Fourier transform of* $\phi_Y(\cdot)$ *is*

$$\widehat{\phi}_Y(\omega) = \prod_{\mathbf{v}_j \in Y} \frac{1 - e^{-i\omega \cdot \mathbf{v}_j}}{i\omega \cdot \mathbf{v}_j}, \quad i = \sqrt{-1}$$

(6) $D_{\mathbf{v}_j} \phi_Y(\cdot) = -\phi_{Y \setminus \{\mathbf{v}_j\}}(\cdot - \mathbf{v}_j) + \phi_{Y \setminus \{\mathbf{v}_j\}}(\cdot)$

(7) *For* $s > d$, *and* $f \in C^1(\mathbb{R}^d)$,

$$\int_{\mathbb{R}^d} \phi_Y(\mathbf{x}) D_{\mathbf{v}_j} f(\mathbf{x})\ d\mathbf{x} = -\int_{[0,1)^s} D_{\mathbf{v}_j} \phi_Y(\mathbf{x}) f(\mathbf{x})\ d\mathbf{x}.$$

(8) *There exists a finite sequence* $\{c_\eta\}_{\eta \in \mathbb{Z}^d}$ *such that*

$$\phi_Y(\mathbf{x}) = \sum_{\eta \in \mathbb{Z}^d} c_\eta \phi_Y(2\mathbf{x} - \eta).$$

From (5) and (8) in Theorem 3.2.1 we have

$$\widehat{\phi}_Y(\omega) = \prod_{\xi \in Y} \frac{1 + e^{-i\xi \cdot \omega}}{2} \widehat{\phi}_Y(\omega/2) \tag{3.11}$$

for a directional set Y. We denote

$$P_Y(\omega) := \prod_{\xi \in Y} \frac{1 + e^{-i\xi \cdot \omega}}{2}, \quad i = \sqrt{-1}.$$

Then we have the equivalent form of (8) in terms of Fourier transform.

$$\widehat{\phi}_Y(2\omega) = P_Y(\omega) \widehat{\phi}_Y(\omega) \tag{3.12}$$

We have the following Lemma for the property of the trigonometric polynomial P_Y.

Lemma 3.2.1 *Suppose that a given direction set* Y *contains standard unit vectors* e_j *in* $\mathbb{R}^d$*,* $j = 1, \ldots, d$*. Then* P_Y *associated with the multivariate box spline* $\phi_Y(\cdot)$ *satisfies sub-QMF condition in (2.18).*

Proof Since $|P_Y(\omega)|^2 \le \prod_{j=1}^d \cos^2 \frac{\omega_j}{2}$ with $\omega = (\omega_1, \ldots, \omega_d)^T \in \mathbb{R}^d$, we have

$$\sum_{\nu \in \{0,\pi\}^d} |P_Y(\omega + \nu)|^2 \le \prod_{j=1}^d (\cos^2 \frac{\omega_j}{2} + \sin^2 \frac{\omega_j}{2}) = 1.$$

□

3.3 B-spline Tight Wavelet Frames

In this section, we construct a tight wavelet frame based on MRA generated by a B-spline. By Lemma 3.1.1, we know that a B-spline ϕ_m is a refinable function whose associated Laurent polynomial P_m satisfying the sub-QMF condition. Therefore, if we find Laurent polynomials $\widetilde{P}_j$ satisfying

$$1 - |P_m(\omega)|^2 - |P_m(\omega + \pi)|^2 = \sum_j |\widetilde{P}_j(2\omega)|^2, \quad \omega \in \mathbb{R} \tag{3.13}$$

then we can construct a tight wavelet frame for a B-spline by using the constructive method in the proof of Theorem 2.2.2.

Lemma 3.3.1 *Let* A *be a nonnegative trigonometric polynomial invariant under the substitution* $\xi \to -\xi$*.* A *is the form*

$$A(\xi) = \sum_{m=0}^{M} a_m \cos(m\xi), \quad a_m \in \mathbb{R}.$$

Then there exists a trigonometric polynomial B *of order* M*, i.e,,*

$$B(\xi) = \sum_{m=0}^{M} b_m e^{im\xi}, \quad b_m \in \mathbb{R},$$

such that $|B(\xi)|^2 = A(\xi)$*.*

Proof See in [D]. □

The above lemma by Fejér and Riesz provides the existence of a Laurent polynomial satisfying the condition in (3.13) for the Laurent polynomial P_m associated with B-spline ϕ_m. Let $\widetilde{P}_m$ be the trigonometric polynomial satisfying

$$|P_m(\omega)|^2 + |P_m(\omega+\pi)|^2 + |\widetilde{P}_m(2\omega)|^2 = 1 \tag{3.14}$$

for the Laurnet polynomial P_m associated with B-spline ϕ_m. We now follow each step from the constructive method in the proof of Theorem 2.2.2 for the B-spline tight wavelet frame construction.

Let $\mathcal{P} := [P_m(\omega)\ P_m(\omega+\pi)]^T$. We multiply the matrix $\mathcal{M}$ in (2.16) on the left side of the matrix $\mathcal{P}$. That is,

$$\mathcal{M}\overline{\mathcal{P}} = \frac{1}{\sqrt{2}}\begin{bmatrix} 1 & 1 \\ e^{i\omega} & -e^{i\omega} \end{bmatrix}\begin{bmatrix} \overline{P_m(\omega)} \\ \overline{P_m(\omega+\pi)} \end{bmatrix} = \frac{1}{\sqrt{2}}\begin{bmatrix} \overline{P_m(\omega)} + \overline{P_m(\omega+\pi)} \\ e^{i\omega}(\overline{P_m(\omega)} - \overline{P_m(\omega+\pi)}) \end{bmatrix}$$

Then the Laurent polynomial $\overline{P_m(\omega)} + \overline{P_m(\omega+\pi)}$ has only odd powers of $P_m(\omega)$ and the Laurent polynomial $\overline{P_m(\omega)} - \overline{P_m(\omega+\pi)}$ has all even powers of $P_m(\omega)$. We denote this odd polynomial be $P_{1,m}(2\omega)$ and the even polynomial be $P_{2,m}(2\omega)$. We call this process polyphase decomposition(see [D p. 318]) . It is easy to check

$$|P_{1,m}(2\omega)|^2 + |P_{2,m}(2\omega)|^2 + |\widetilde{P}_m(2\omega)|^2 = 1.$$

Thus we do not need to deal with translated versions in ω of the Laurent polynomial $P_m(\omega)$.

Let $\widetilde{\mathcal{P}}$ be a column vector $[P_{1,m}(2\omega)\ P_{2,m}(2\omega)\ \widetilde{P}_m(2\omega)]^T$. Define

$$\widetilde{\mathcal{Q}} := I - \widetilde{\mathcal{P}}\widetilde{\mathcal{P}}^* = \begin{bmatrix} 1-|P_{1,m}(2\omega)|^2 & -P_{1,m}(2\omega)\overline{P_{2,m}(2\omega)} & -P_{1,m}(2\omega)\overline{\widetilde{P}_m(2\omega)} \\ -P_{2,m}(2\omega)\overline{P_{1,m}(2\omega)} & 1-|P_{2,m}(2\omega)|^2 & -P_{2,m}(2\omega)\overline{\widetilde{P}_m(2\omega)} \\ -\widetilde{P}_m(2\omega)\overline{P_{1,m}(2\omega)} & -\widetilde{P}_m(2\omega)\overline{P_{2,m}(2\omega)} & 1-|\widetilde{P}_m(2\omega)|^2 \end{bmatrix}. \tag{3.15}$$

Straight forward calculation verifies $\widetilde{\mathcal{Q}}^*\widetilde{\mathcal{Q}} = I - \widetilde{\mathcal{P}}\widetilde{\mathcal{P}}^*$. Let $\widehat{\mathcal{Q}}$ be the first 3×2 block matrix in $\widetilde{\mathcal{Q}}$

$$\widehat{\mathcal{Q}} := \begin{bmatrix} 1-|P_{1,m}(2\omega)|^2 & -P_{1,m}(2\omega)\overline{P_{2,m}(2\omega)} \\ -P_{2,m}(2\omega)\overline{P_{1,m}(2\omega)} & 1-|P_{2,m}(2\omega)|^2 \\ -\widetilde{P}_m(2\omega)\overline{P_{1,m}(2\omega)} & -\widetilde{P}_m(2\omega)\overline{P_{2,m}(2\omega)} \end{bmatrix} \tag{3.16}$$

and multiply $\mathcal{M}$ in (2.16) on the right side of matrix $\widehat{\mathcal{Q}}$

$$\mathcal{Q} := \widehat{\mathcal{Q}}\mathcal{M} = \frac{1}{\sqrt{2}} \begin{bmatrix} 1-|P_{1,m}(2\omega)|^2 & -P_{1,m}(2\omega)\overline{P_{2,m}(2\omega)} \\ -P_{2,m}(2\omega)\overline{P_{1,m}(2\omega)} & 1-|P_{2,m}(2\omega)|^2 \\ -\widetilde{P}_m(2\omega)\overline{P_{1,m}(2\omega)} & -\widetilde{P}_m(2\omega)\overline{P_{2,m}(2\omega)} \end{bmatrix} \begin{bmatrix} 1 & 1 \\ e^{i\omega} & -e^{i\omega} \end{bmatrix} \tag{3.17}$$

Then by straight forward calculation we have $\mathcal{Q}^*\mathcal{Q} = I - \overline{\mathcal{P}}\mathcal{P}^{\mathcal{T}}$. That is, $\mathcal{Q}$ satisfies the matrix form of UEP condition. The second column of matrix $\mathcal{Q}$ is the shift of the first column of matrix $\mathcal{Q}$. We denote each component of the first column of matrix $\mathcal{Q}$ by $Q_m^1(\omega), Q_m^2(\omega)$, and $Q_m^3(\omega)$ respectively. They are the desirable Laurent polynomials associated with the tight framelets ψ_m^1, ψ_m^2 and ψ_m^3 based on B-spline ϕ_m. That is, with these Q_m^1, Q_m^2 and Q_m^2 we define ψ_m^1, ψ_m^2, and ψ_m^3 in terms of the Fourier transform such as

$$\widehat{\psi}_m^\ell(\omega) = Q_m^\ell(\omega/2)\widehat{\phi}_m^\ell(\omega/2), \text{ for } \ell = 1, 2, 3.$$

The following examples give the extra Laurent polynomial $\widetilde{P}_m$ satisfying the condition in (3.14) and Laurent polynomial Q_m^1, Q_m^2, and Q_m^3 associated with tight wavelet frame generators for mth order B-spline, where $m = 2, 3$ and 4. For any B-splines of order m we have three tight wavelet frame generators.

Example 3.3.1 *For the Laurent polynomial* $P_2(\omega) = \left(\frac{1+e^{i\omega}}{2}\right)^2$ *associated with the linear B-spline* ϕ_2 *we have*

$$\widetilde{P}_2(2\omega) = \frac{\sqrt{2}}{4}\left(1 - e^{2i\omega}\right), \quad i = \sqrt{-1}$$

satisfying

$$1 - |P_2(\omega)|^2 - |P_2(\omega+\pi)|^2 = |\widetilde{P}_2(2\omega)|^2.$$

Then with the polyphase forms $P_{1,2}$ *and* $P_{2,2}$ *of Laurent polynomial* P_2

$$P_{1,2}(2\omega) = \frac{\sqrt{2}}{4}(e^{-2i\omega} + 1), \text{ and } P_{2,2}(2\omega) = \frac{\sqrt{2}}{4}$$

we set the column vector $\widetilde{\mathcal{P}} := [P_{1,2}(2\omega)\ P_{1,2}(2\omega)\ \widetilde{P}_2(2\omega)]^T$. *First we calculate*

$$\widetilde{\mathcal{Q}} = I - \widetilde{\mathcal{P}}\widetilde{\mathcal{P}}^* = -\frac{1}{8}\begin{bmatrix} e^{2\omega} - 6 + e^{-2\omega} & 2(1+e^{-2\omega}) & 1 + e^{-4\omega} \\ 2(1+e^{-2\omega}) & \frac{1}{2} & -4(1-e^{-2\omega}) \\ -(e^{4\omega}-1) & -2(e^{2\omega}-1) & -(e^{2\omega}+6+e^{-2\omega}) \end{bmatrix}.$$

Then we restrict $\widetilde{\mathcal{Q}}$ *to the first* 3×2 *block matrix*

$$\widehat{\mathcal{Q}} = -\frac{1}{8}\begin{bmatrix} e^{2\omega} - 6 + e^{-2\omega} & 2(1+e^{-2\omega}) \\ 2(1+e^{-2\omega}) & \frac{1}{2} \\ -(e^{4\omega}-1) & -2(e^{2\omega}-1) \end{bmatrix}.$$

By multiplying $\mathcal{M}$ *in (2.16), we have*

$$\mathcal{Q} =$$

$$\begin{bmatrix} -\frac{\sqrt{2}}{16}e^{-2i\omega} - \frac{\sqrt{2}}{8}e^{-i\omega} + \frac{3\sqrt{2}}{8} - \frac{\sqrt{2}}{8}e^{i\omega} - \frac{\sqrt{2}}{16}e^{2i\omega} & -\frac{\sqrt{2}}{16}e^{-2i\omega} + \frac{\sqrt{2}}{8}e^{-i\omega} + \frac{3\sqrt{2}}{8} + \frac{\sqrt{2}}{8}e^{i\omega} - \frac{\sqrt{2}}{16}e^{2i\omega} \\ -\frac{\sqrt{2}}{8} + \frac{\sqrt{2}}{4}e^{i\omega} - \frac{\sqrt{2}}{8}e^{2i\omega} & -\frac{\sqrt{2}}{8} - \frac{\sqrt{2}}{4}e^{i\omega} - \frac{\sqrt{2}}{8}e^{2i\omega} \\ -\frac{\sqrt{2}}{16} - \frac{\sqrt{2}}{8}e^{i\omega} + \frac{\sqrt{2}}{8}e^{3i\omega} + \frac{\sqrt{2}}{16}e^{4i\omega} & -\frac{\sqrt{2}}{16} + \frac{\sqrt{2}}{8}e^{i\omega} - \frac{\sqrt{2}}{8}e^{3i\omega} + \frac{\sqrt{2}}{16}e^{4i\omega} \end{bmatrix}.$$

We obtained three Laurent polynomials associated with B-spline tight framelets from the first column of the matrix $\mathcal{Q}$.

$$\begin{aligned} Q_2^1(\omega) &= -\frac{\sqrt{2}}{16}e^{-2i\omega} - \frac{\sqrt{2}}{8}e^{-i\omega} + \frac{3\sqrt{2}}{8} - \frac{\sqrt{2}}{8}e^{i\omega} - \frac{\sqrt{2}}{16}e^{2i\omega}, \\ Q_2^2(\omega) &= -\frac{\sqrt{2}}{8} + \frac{\sqrt{2}}{4}e^{i\omega} - \frac{\sqrt{2}}{8}e^{2i\omega}, \\ Q_2^3(\omega) &= -\frac{\sqrt{2}}{16} - \frac{\sqrt{2}}{8}e^{i\omega} + \frac{\sqrt{2}}{8}e^{3i\omega} + \frac{\sqrt{2}}{16}e^{4i\omega}. \end{aligned}$$

The each element of the second column of the matrix $\mathcal{Q}$ *is* $Q_2^1(\omega+\pi), Q_2^2(\omega+\pi)$ *and* $Q_2^3(\omega+\pi)$. *Therefore we have the following B-spline tight framelets* $\{\psi_2^1, \psi_2^2, \psi_2^3\}$ *for linear B-spline* ϕ_2

$$\begin{aligned} \psi_2^1(x) &= -\frac{\sqrt{2}}{8}\phi_2(2x+2) - \frac{\sqrt{2}}{4}\phi_2(2x+1) + \frac{3\sqrt{2}}{4}\phi_2(2x) - \frac{\sqrt{2}}{4}\phi_2(2x-1) - \frac{\sqrt{2}}{8}\phi_2(2x-2), \\ \psi_2^2(x) &= -\frac{\sqrt{2}}{4} - \frac{\sqrt{2}}{2}\phi_2(2x-1) + \frac{\sqrt{2}}{4}\phi_2(2x-2), \\ \psi_2^3(x) &= -\frac{\sqrt{2}}{8} - \frac{\sqrt{2}}{4}\phi_2(2x-1) + \frac{\sqrt{2}}{4}\phi_2(2x-3) + \frac{\sqrt{2}}{8}\phi_2(2x-4). \end{aligned}$$

We illustrate the linear B-spline ϕ_2 *and its tight wavelet frameletes* ψ_2^1, ψ_2^2, *and* ψ_2^3 *in Figure 3.3.* $\square$

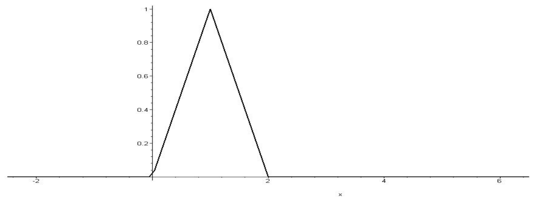

Linear B-spline ϕ_2

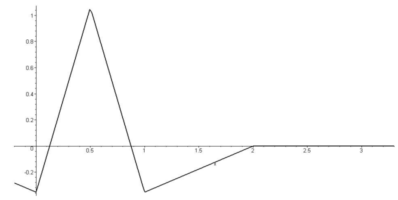

Tight Framelet ψ_2^1

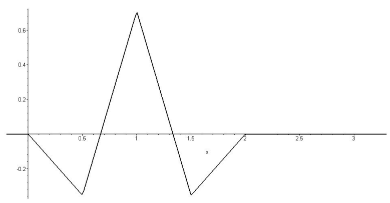

Tight Framelet ψ_2^2

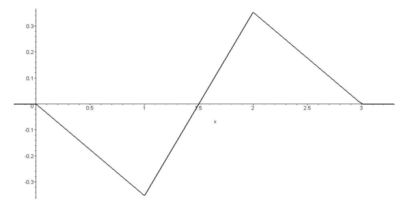

Tight Framelet ψ_2^3

Figure 3.1: Linear B-spline and its Tight Framelets in Example 3.3.1

Example 3.3.2 *For the Laurent polynomial* $P_3(\omega) = \left(\frac{1+e^{i\omega}}{2}\right)^3$ *associated with the quadratic B-spline* ϕ_3 *we have*

$$\widetilde{P}_3(2\omega) = \frac{\sqrt{3}}{4}\left(1 - e^{2i\omega}\right), \quad i = \sqrt{-1}$$

satisfying

$$1 - |P_3(\omega)|^2 - |P_3(\omega + \pi)|^2 = |\widetilde{P}_3(2\omega)|^2.$$

Then with the polyphase forms $P_{1,3}$ *and* $P_{2,3}$ *of Laurent polynomial* P_3

$$P_{1,3}(2\omega) = \frac{3\sqrt{2}}{8}(e^{-2i\omega} + 1) \quad \text{and } P_{2,3}(2\omega) = \frac{\sqrt{2}}{8}(e^{-2i\omega} + 3)$$

we set the column vector $\widetilde{\mathcal{P}} := [P_{1,3}(2\omega)\ P_{1,3}(2\omega)\ \widetilde{P}_3(2\omega)]^T$. *Following the construction steps (3.15)-(3.17) we obtained three Laurent polynomials associated with B-spline tight framelets.*

Since the detail steps are similar to Example 3.3.1, we omit the detail steps.

$$Q_3^1(\omega) = -\frac{3\sqrt{2}}{64}e^{-2i\omega} - \frac{9\sqrt{2}}{64}e^{-i\omega} + \frac{11\sqrt{2}}{32} - \frac{3\sqrt{2}}{32}e^{i\omega} - \frac{3\sqrt{2}}{64}e^{2i\omega} - \frac{\sqrt{2}}{64}e^{3i\omega}$$
$$Q_3^2(\omega) = -\frac{\sqrt{2}}{64}e^{-2i\omega} - \frac{3\sqrt{2}}{64}e^{-i\omega} - \frac{3\sqrt{2}}{32} + \frac{11\sqrt{2}}{32}e^{i\omega} - \frac{9\sqrt{2}}{64}e^{2i\omega} - \frac{3\sqrt{2}}{64}e^{3i\omega}$$
$$Q_3^3(\omega) = -\frac{\sqrt{3}}{32} - \frac{3\sqrt{3}}{32}e^{i\omega} - \frac{\sqrt{3}}{16}e^{2i\omega} + \frac{\sqrt{3}}{16}e^{3i\omega} + \frac{3\sqrt{3}}{32}e^{4i\omega} + \frac{\sqrt{3}}{32}e^{5i\omega}$$

Therefore we have the following B-spline tight framelets $\{\psi_3^1, \psi_3^2, \psi_3^3\}$ *for quadratic B-spline* ϕ_3

$$\begin{aligned}
\psi_3^1(x) = &-\frac{3\sqrt{2}}{32}\phi_3(2x+2) - \frac{9\sqrt{2}}{32}\phi_3(2x+1) + \frac{11\sqrt{2}}{16}\phi_3(2x) \\
&- \frac{3\sqrt{2}}{16}\phi_3(2x-1) - \frac{3\sqrt{2}}{32}\phi_3(2x-2) - \frac{\sqrt{2}}{32}\phi_3(2x-3) \\
\psi_3^2(x) = &-\frac{\sqrt{2}}{32}\phi_3(2x+2) - \frac{3\sqrt{2}}{32}\phi_3(2x+1) - \frac{3\sqrt{2}}{16}\phi_3(2x) \\
&+ \frac{11\sqrt{2}}{16}\phi_3(2x-1) - \frac{9\sqrt{2}}{32}\phi_3(2x-2) - \frac{3\sqrt{2}}{32}\phi_3(2x-3) \\
\psi_3^3(x) = &-\frac{\sqrt{3}}{16}\phi_3(2x) - \frac{3\sqrt{3}}{16}\phi_3(2x-1) - \frac{\sqrt{3}}{8}\phi_3(2x-2) \\
&+ \frac{\sqrt{3}}{8}\phi_3(2x-3) + \frac{3\sqrt{3}}{16}\phi_3(2x-4) + \frac{\sqrt{3}}{16}\phi_3(2x-5)
\end{aligned}$$

We illustrate the quadratic B-spline ϕ_3 *and its tight wavelet frameletes* $\psi_3^1, \psi_3^2,$ *and* ψ_3^3 *in Figure 3.3.* □

Example 3.3.3 *For the Laurent polynomial* $P_4(\omega) = \left(\frac{1+e^{i\omega}}{2}\right)^4$ *associated with the cubic B-spline* ϕ_4 *we have*

$$\widetilde{P}_4(2\omega) = -\left(\frac{1}{4} + \frac{\sqrt{14}}{16}\right) + \frac{\sqrt{14}}{8}e^{2i\omega} + \left(\frac{1}{4} - \frac{\sqrt{14}}{16}\right)e^{8i\omega}, \quad i = \sqrt{-1}$$

satisfying

$$1 - |P_4(\omega)|^2 - |P_4(\omega+\pi)|^2 = |\widetilde{P}_4(2\omega)|^2.$$

Then with the polyphase forms $P_{1,4}$ *and* $P_{2,4}$ *of Laurent polynomial* P_4

$$P_{1,4}(2\omega) = \frac{\sqrt{2}}{16}(e^{-8i\omega} + 6e^{-4i\omega} + 1) \quad \text{and } P_{2,4}(2\omega) = \frac{\sqrt{2}}{4}(e^{-4i\omega} + 1)$$

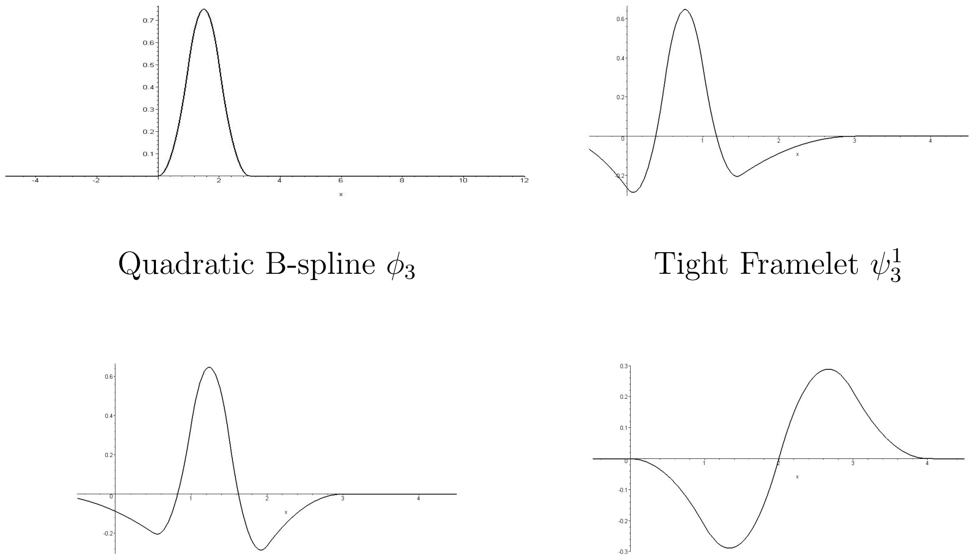

Quadratic B-spline ϕ_3 Tight Framelet ψ_3^1

Tight Framelet ψ_3^2 Tight Framelet ψ_3^3

Figure 3.2: Quadratic B-spline and its Tight Framelets in Example 3.3.2

we set the column vector $\widetilde{\mathcal{P}} := [P_{1,4}(2\omega)\ P_{1,4}(2\omega)\ \widetilde{P}_4(2\omega)]^T$. *Following the construction steps (3.15)-(3.17) we obtained three Laurent polynomials associated with B-spline tight framelets:*

$$
\begin{aligned}
Q_4^1(\omega) = &-\frac{\sqrt{2}}{256}e^{-4i\omega} - \frac{\sqrt{2}}{64}e^{-3i\omega} - \frac{3\sqrt{2}}{64}e^{-2i\omega} - \frac{7\sqrt{2}}{64}e^{-i\omega} + \frac{45\sqrt{2}}{128} \\
&- \frac{7\sqrt{2}}{64}e^{i\omega} - \frac{3\sqrt{2}}{64}e^{2i\omega} - \frac{\sqrt{2}}{64}e^{3i\omega} - \frac{\sqrt{2}}{256}e^{4i\omega}, \\
Q_4^2(\omega) = &-\frac{\sqrt{2}}{64}e^{-2i\omega} - \frac{\sqrt{2}}{16}e^{-i\omega} - \frac{7\sqrt{2}}{64} - \frac{3\sqrt{2}}{8}e^{i\omega} - \frac{7\sqrt{2}}{64}e^{2i\omega} - \frac{\sqrt{2}}{16}e^{3i\omega} - \frac{\sqrt{2}}{64}e^{4i\omega}, \\
Q_4^3(\omega) = &\left(\frac{1}{64} + \frac{\sqrt{14}}{256}\right) + \left(\frac{1}{16} + \frac{\sqrt{14}}{64}\right)e^{i\omega} + \left(\frac{3}{32} + \frac{\sqrt{14}}{64}\right)e^{2i\omega} \\
&+ \left(\frac{1}{16} - \frac{\sqrt{14}}{64}\right)e^{3i\omega} - \frac{5\sqrt{14}}{128}e^{4i\omega} - \left(\frac{1}{16} + \frac{\sqrt{14}}{64}\right)e^{5i\omega} \\
&- \left(\frac{3}{32} - \frac{\sqrt{14}}{64}\right)e^{6i\omega} - \left(\frac{1}{16} - \frac{\sqrt{14}}{64}\right)e^{7i\omega} - \left(\frac{1}{64} - \frac{\sqrt{14}}{256}\right)e^{8i\omega}.
\end{aligned}
$$

Therefore we have the following B-spline tight framelets $\{\psi_4^1, \psi_4^2, \psi_4^3\}$ *for cubic B-spline* ϕ_4

$$
\begin{aligned}
\psi_4^1(x) =& -\frac{\sqrt{2}}{128}\phi_4(2x+4) - \frac{\sqrt{2}}{32}\phi_4(2x+3) - \frac{3\sqrt{2}}{32}\phi_4(2x+2) - \frac{7\sqrt{2}}{32}\phi_4(2x+1) + \frac{45\sqrt{2}}{64}\phi_4(2x) \\
& - \frac{7\sqrt{2}}{32}\phi_4(2x-1) - \frac{3\sqrt{2}}{32}\phi_4(2x-2) - \frac{\sqrt{2}}{32}\phi_4(2x-3) - \frac{\sqrt{2}}{128}\phi_4(2x-4), \\
\psi_4^2(x) =& -\frac{\sqrt{2}}{32}\phi_4(2x+2) - \frac{\sqrt{2}}{8}\phi_4(2x+1) - \frac{7\sqrt{2}}{32}\phi_4(2x) - \frac{3\sqrt{2}}{4}\phi_4(2x-1) \\
& - \frac{7\sqrt{2}}{32}\phi_4(2x-2) - \frac{\sqrt{2}}{8}\phi_4(2x-3) - \frac{\sqrt{2}}{32}\phi_4(2x-4), \\
\psi_4^3(x) =& \left(\frac{1}{32} + \frac{\sqrt{14}}{128}\right)\phi_4(2x) + \left(\frac{1}{8} + \frac{\sqrt{14}}{32}\right)\phi_4(2x-1) + \left(\frac{3}{16} + \frac{\sqrt{14}}{32}\right)\phi_4(2x-2) \\
& + \left(\frac{1}{8} - \frac{\sqrt{14}}{32}\right)\phi_4(2x-3) - \frac{5\sqrt{14}}{64}\phi_4(2x-4) - \left(\frac{1}{8} + \frac{\sqrt{14}}{32}\right)\phi_4(2x-5) \\
& - \left(\frac{3}{16} - \frac{\sqrt{14}}{32}\right)\phi_4(2x-6) - \left(\frac{1}{8} - \frac{\sqrt{14}}{32}\right)\phi_4(2x-7) - \left(\frac{1}{32} - \frac{\sqrt{14}}{128}\right)\phi_4(2x-8).
\end{aligned}
$$

We illustrate the Quadratic B-spline ϕ_4 *and its tight wavelet frameletes* ψ_4^1, ψ_4^2, *and* ψ_4^3 *in Figure 3.3.* $\square$

It is interesting to know how to construct locally supported tight frames based on multivariate box splines. We first study two dimensional tensor product in the following section. The tensor product is a simple extension tool of univariate functions to multivariate functions.

3.4 Tensor Products of Univariate Tight Wavelet Frames

In this section we consider the multivariate tight wavelet frame construction using a tensor product. We only consider the bivariate tight wavelet frame construction using tensor product of two univariate multiresolution analyses. Higher variable settings are similar to the bivariate setting.

We consider the tensor product of two Multiresolution analyses $\{V_j^m\}_{j\in\mathbb{Z}}$ generated by mth order B-spline functions. Denote $\mathbf{V}_j^m$, for $j \in \mathbb{Z}$, by

$$
\mathbf{V}_j^m := V_j^m \otimes V_j^m = \overline{\text{span}\{\phi(2^j x - k)\phi(2^j y - \ell) : \phi(2^j\cdot) \in V_j^m\}} \tag{3.18}
$$

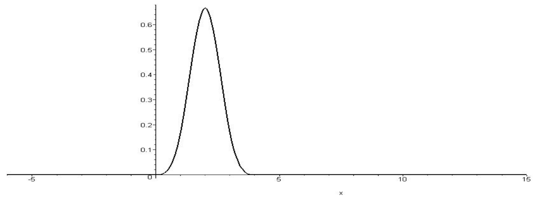

Cubic B-spline ϕ_4

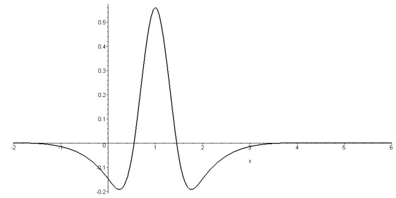

Tight Framelet ψ_4^1

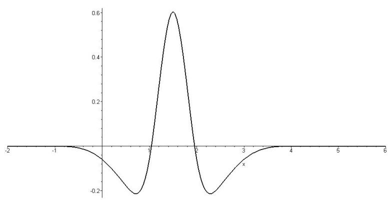

Tight Framelet ψ_4^2

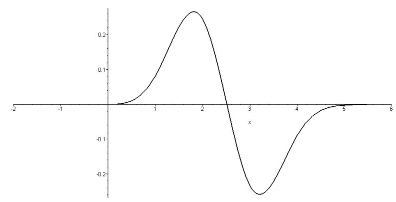

Tight Framelet ψ_4^3

Figure 3.3: Cubic B-spline and its Tight Framelets in Example 3.3.3

The same level of MRA is used when we do tensor product. Then $\{\mathbf{V}_j^m\}$ satisfies the following conditions by (3.2)-(3.5) and (3.18) ,

$$\begin{aligned} \leftarrow \cdots \subset \mathbf{V}_{-1}^m \subset \mathbf{V}_0^m \subset \mathbf{V}_1^m \subset \cdots \rightarrow \\ \overline{\cup_{j\in\mathbb{Z}}\mathbf{V}_j^m} = L^2(\mathbb{R}^2) \\ \cap_{j\in\mathbb{Z}}\mathbf{V}_j^m = \{0\}. \end{aligned} \tag{3.19}$$

We denote $\mathbf{W}_j^m$ be a subset of V_{j+1}^m such that $\mathbf{V}_{j+1}^m := \mathbf{V}_j^m + \mathbf{W}_j^m$. Since we consider the subspace $\mathbf{V}_{j+1}^m = V_{j+1}^m \otimes V_{j+1}^m$ where $V_{j+1}^m = V_j^m + W_j^m$,

$$\begin{aligned} \mathbf{V}_{j+1}^m =&(V_j^m + W_j^m) \otimes (V_j^m + W_j^m) \\ =&\mathbf{V}_j^m + \mathbf{W}_j^m. \end{aligned} \tag{3.20}$$

We notice that $\mathbf{W}_j^m$ can be expressed by the generators of $(V_j^m \otimes W_j^m)$, $(W_j^m \otimes V_j^m)$, and $(W_j^m \otimes W_j^m)$. Let us define bivariate functions using B-spline ϕ_m and three tight wavelet frame generators $\{\psi_m^1, \psi_m^2, \psi_m^3\}$ as follows. For $k, \ell = 1, 2$, and 3,

$$\begin{aligned} \Phi_m^{0,0}(x,y) &= \phi_m(x)\phi_m(y), \quad \text{for } V_0^m \otimes W_0^m, \\ \Psi_m^{0,\ell}(x,y) &= \phi_m(x)\psi_m^\ell(y), \quad \text{for } V_0^m \otimes W_0^m, \\ \Psi_m^{k,0}(x,y) &= \psi_m^k(x)\phi_m(y), \quad \text{for } W_0^m \otimes V_0^m, \\ \Psi_m^{k,\ell}(x,y) &= \psi_m^k(x)\psi_m^\ell(y), \quad \text{for } W_0^m \otimes W_0^m. \end{aligned} \tag{3.21}$$

Then

$$\{\Psi_m^{0,\ell}(2^j x - n_1, 2^j y - n_2), \Psi_m^{k,0}(2^j x - n_1, 2^j y - n_2), \Psi_m^{k,\ell}(2^j x - n_1, 2^j y - n_2) : \\ n_1, n_2 \in \mathbb{Z} \textit{ and } k, \ell = 1, 2 \textit{ or } 3\}$$

generates $\mathbf{W}_j^m$ and there are fifteen generators in $\mathbf{W}_j^m$.

We show the tensor product of quadratic B-spline tight wavelet frame genertators in the following example. For the linear and cubic B-spline tight wavelet frames are similar to the quadratic B-splines tight wavelet frames.

Example 3.4.1 *In Exampe 3.3.2, we have the quadratic B-spline ϕ_2 and the following three tight wavelet framelets*

$$\begin{aligned} \psi_3^1(x) &= -\frac{3\sqrt{2}}{64}\phi_3(2x+2) - \frac{9\sqrt{2}}{64}\phi_3(2x+1) + \frac{11\sqrt{2}}{32}\phi_3(2x) \\ &\quad - \frac{3\sqrt{2}}{32}\phi_3(2x-1) - \frac{3\sqrt{2}}{64}\phi_3(2x-2) - \frac{\sqrt{2}}{64}\phi_3(2x-3), \\ \psi_3^2(x) &= -\frac{\sqrt{2}}{32}\phi_3(2x+2) - \frac{3\sqrt{2}}{32}\phi_3(2x+1) - \frac{3\sqrt{2}}{16}\phi_3(2x) \\ &\quad + \frac{11\sqrt{2}}{16}\phi_3(2x-1) - \frac{9\sqrt{2}}{32}\phi_3(2x-2) - \frac{3\sqrt{2}}{32}\phi_3(2x-3), \\ \psi_3^3(x) &= -\frac{\sqrt{3}}{16}\phi_3(2x) - \frac{3\sqrt{3}}{16}\phi_3(2x-1) - \frac{\sqrt{3}}{8}\phi_3(2x-2) \\ &\quad + \frac{\sqrt{3}}{8}\phi_3(2x-3) + \frac{3\sqrt{3}}{16}\phi_3(2x-4) + \frac{\sqrt{3}}{16}\phi_3(2x-5). \end{aligned}$$

Thus we have a refinable function $\Phi_2^{0,0}(x,y) = 4\sum_{j=0}^{3}\sum_{k=0}^{3} p_{jk}\Phi_2^{0,0}(2x-j,2y-k)$ *with*

$$(p_{j+1k+1})_{\substack{0\le j\le 3\\ 0\le k\le 3}} = \frac{1}{64}\begin{bmatrix} 1 & 3 & 3 & 1 \\ 3 & 9 & 9 & 3 \\ 3 & 9 & 9 & 3 \\ 1 & 3 & 3 & 1 \end{bmatrix}.$$

The following fifteen tight wavelet frame generators of the form $\Psi_2^{0,\ell}, \Psi_2^{n,0}$, *and* $\Psi_2^{n,\ell}$ *where* $n, \ell = 1, 2,$ *and* 3 :

$\Psi_2^{0,1}(x,y) = 4\sum_{j=0}^{3}\sum_{k=-2}^{3} q_{jk}\Psi_2^{0,1}(2x-j,2y-k)$ *with*

$$(q_{jk})_{\substack{0\le j\le 3\\ -2\le k\le 3}} = \frac{\sqrt{2}}{128}\begin{bmatrix} -1 & -2 & 6 & -2 & -1 \\ -3 & -6 & 18 & -6 & -3 \\ -3 & -6 & 18 & -6 & -3 \\ -1 & -2 & 6 & -2 & -1 \end{bmatrix},$$

$\Psi_2^{0,2}(x,y) = 4\sum_{j=0}^{3}\sum_{k=0}^{2} q_{jk}\Psi_2^{0,2}(2x-j,2y-k)$ *with*

$$(q_{jk})_{\substack{0\le j\le 3\\ 0\le k\le 2}} = \frac{\sqrt{2}}{64}\begin{bmatrix} -1 & 2 & -1 \\ -3 & 6 & -3 \\ -3 & 6 & -3 \\ -1 & 2 & -1 \end{bmatrix},$$

$\Psi_2^{0,3}(x,y) = 4\sum_{j=0}^{3}\sum_{k=0}^{4} q_{jk}\Psi_2^{0,3}(2x-j,2y-k)$ *with*

$$(q_{jk})_{\substack{0\le j\le 3\\ 0\le k\le 4}} = \frac{\sqrt{2}}{128}\begin{bmatrix} 1 & 2 & 0 & -2 & -1 \\ 3 & 6 & 0 & -6 & -3 \\ 3 & 6 & 0 & -6 & -3 \\ 1 & 2 & 0 & -2 & -1 \end{bmatrix},$$

$$\Psi_2^{1,0}(x,y) = 4\sum_{j=0}^{4}\sum_{k=0}^{3} q_{jk}\Psi_2^{0,3}(2x-j, 2y-k) \ \textit{with}$$

$$(q_{jk})_{\substack{0\le j\le 4\\ 0\le k\le 3}} = \frac{\sqrt{2}}{128}\begin{bmatrix} -1 & -3 & -3 & -1 \\ -2 & -6 & -6 & -2 \\ 6 & 18 & 18 & 6 \\ -2 & -6 & -6 & -2 \\ -1 & -3 & -3 & -1 \end{bmatrix},$$

$$\Psi_2^{1,1}(x,y) = 4\sum_{j=0}^{4}\sum_{k=0}^{4} q_{jk}\Psi_2^{1,1}(2x-j, 2y-k) \ \textit{with}$$

$$(q_{jk})_{\substack{0\le j\le 4\\ 0\le k\le 4}} = \frac{1}{128}\begin{bmatrix} 1 & 2 & -6 & 2 & 1 \\ 2 & 4 & -12 & 4 & 2 \\ -6 & -12 & 36 & -12 & -6 \\ 2 & 4 & -12 & 4 & 2 \\ 1 & 2 & -6 & 2 & 1 \end{bmatrix},$$

$$\Psi_2^{1,2}(x,y) = 4\sum_{j=0}^{4}\sum_{k=0}^{2} q_{jk}\Psi_2^{1,2}(2x-j, 2y-k) \ \textit{with}$$

$$(q_{jk})_{\substack{0\le j\le 4\\ 0\le k\le 2}} = \frac{1}{64}\begin{bmatrix} 1 & -2 & 1 \\ 2 & -4 & 2 \\ -6 & 12 & -6 \\ 2 & -4 & 2 \\ 1 & -2 & 1 \end{bmatrix},$$

$$\Psi_2^{1,3}(x,y) = 4\sum_{j=-2}^{3}\sum_{k=0}^{5} q_{jk}\Psi_2^{1,3}(2x-j,2y-k) \ \textit{with}$$

$$(q_{jk})_{\substack{-2\le j\le 3\\ 0\le k\le 5}} = \frac{1}{128}\begin{bmatrix} -1 & -2 & 0 & 2 & 1 \\ -2 & -4 & 0 & 4 & 2 \\ 6 & 12 & 0 & -12 & -6 \\ -2 & -4 & 0 & 4 & 2 \\ -1 & -2 & 0 & 2 & 1 \end{bmatrix},$$

$$\Psi_2^{2,0}(x,y) = 4\sum_{j=-2}^{3}\sum_{k=0}^{3} q_{jk}\Psi_2^{2,0}(2x-j,2y-k) \ \textit{with}$$

$$(q_{jk})_{\substack{-2\le j\le 3\\ 0\le k\le 3}} = \frac{\sqrt{2}}{64}\begin{bmatrix} -1 & -3 & -3 & -1 \\ 2 & 6 & 6 & 2 \\ -1 & -3 & -3 & -1 \end{bmatrix},$$

$$\Psi_2^{2,1}(x,y) = 4\sum_{j=-2}^{3}\sum_{k=-2}^{3} q_{jk}\Psi_2^{2,1}(2x-j,2y-k) \ \textit{with}$$

$$(q_{jk})_{\substack{-2\le j\le 3\\ -2\le k\le 3}} = \frac{1}{64}\begin{bmatrix} 1 & 2 & -6 & 2 & 1 \\ -2 & -4 & 12 & -4 & -2 \\ 1 & 2 & -6 & 2 & 1 \end{bmatrix},$$

$$\Psi_2^{2,2}(x,y) = 4\sum_{j=0}^{2}\sum_{k=0}^{2} q_{jk}\Psi_2^{2,2}(2x-j,2y-k) \ \textit{with}$$

$$(q_{jk})_{\substack{0\le j\le 4\\ 0\le k\le 4}} = \frac{1}{32}\begin{bmatrix} 1 & -2 & 1 \\ -2 & 4 & -2 \\ 1 & -2 & 1 \end{bmatrix},$$

$$\Psi_2^{2,3}(x,y) = 4\sum_{j=-2}^{3}\sum_{k=0}^{5} q_{jk}\Psi_2^{2,3}(x-j,2y-k) \ \textit{with}$$

$$(q_{jk})_{\substack{-2\le j\le 3\\ 0\le k\le 5}} = \frac{1}{64}\begin{bmatrix} -1 & -2 & 0 & 2 & 1 \\ 2 & 4 & 0 & -4 & -2 \\ -1 & -2 & 0 & 2 & 1 \end{bmatrix},$$

$$\Psi_2^{3,0}(x,y) = 4\sum_{j=0}^{4}\sum_{k=0}^{3} q_{jk}\Psi_2^{3,0}(2x-j,2y-k) \ \textit{with}$$

$$(q_{jk})_{\substack{0\le j\le 4\\ 0\le k\le 3}} = \frac{\sqrt{2}}{128}\begin{bmatrix} -1 & -3 & -3 & -1 \\ -2 & -6 & -6 & -2 \\ 0 & 0 & 0 & 0 \\ 2 & 6 & 6 & 2 \\ 1 & 3 & 3 & 1 \end{bmatrix},$$

$$\Psi_2^{3,1}(x,y) = 4\sum_{j=0}^{5}\sum_{k=-2}^{3} q_{jk}\Psi_2^{3,1}(2x-j,2y-k) \ \textit{with}$$

$$(q_{jk})_{\substack{0\le j\le 5\\ -2\le k\le 3}} = \frac{1}{128}\begin{bmatrix} 1 & 2 & -6 & 2 & 1 \\ 2 & 4 & -12 & 4 & 2 \\ 0 & 0 & 0 & 0 & 0 \\ -2 & -4 & 12 & -4 & -2 \\ -1 & -2 & 6 & -2 & -1 \end{bmatrix},$$

$$\Psi_2^{3,2}(x,y) = 4\sum_{j=0}^{5}\sum_{k=-2}^{3} q_{jk}\Psi_2^{3,2}(2x-j,2y-k) \ \textit{with}$$

$$(q_{jk})_{\substack{0\le j\le 5\\ -2\le k\le 3}} = \frac{1}{64}\begin{bmatrix} 1 & -2 & 1 \\ 2 & -4 & 2 \\ 0 & 0 & 0 \\ -2 & 4 & -2 \\ -1 & 2 & -1 \end{bmatrix},$$

$$\Psi_2^{3,3}(x,y) = 4\sum_{j=0}^{5}\sum_{k=0}^{5} q_{jk}\Psi_2^{3,3}(2x-j, 2y-k) \ \textit{with}$$

$$(q_{jk})_{\substack{0\le j\le 5\\ 0\le k\le 5}} = \frac{1}{128}\begin{bmatrix} -1 & -2 & 0 & 2 & 1 \\ -2 & -4 & 0 & 4 & 2 \\ 0 & 0 & 0 & 0 & 0 \\ 2 & 4 & 0 & -4 & -2 \\ 1 & 2 & 0 & -2 & -1 \end{bmatrix}.$$

□

3.5 Box spline tight wavelet frames

In this section, we consider tight wavelet construction for the bivariate box spline over 3-direction, 4-direction and 8-direction meshes. By using standard unit vectors $e_1 = (1,0)^T, e_2 = (0,1)^T$ in $\mathbb{R}^2$, we define a 3-direction mesh bivariate box spline $\phi_{\ell mn}(x,y)$ in terms of Fourier transform as follows :

$$\widehat{\phi}_{\ell mn}(\xi,\eta) = \left(\frac{1-e^{-i\xi}}{i\xi}\right)^{\ell}\left(\frac{1-e^{-i\eta}}{i\eta}\right)^{m}\left(\frac{1-e^{-i(\xi+\eta)}}{i(\xi+\eta)}\right)^{n}, \quad i=\sqrt{-1}$$

on the set of direction Y such that

$$Y = \{\underbrace{e_1,\ldots,e_1}_{\ell}, \underbrace{e_2,\ldots,e_2}_{m}, \underbrace{e_1+e_2,\ldots,e_1+e_2}_{n}\}.$$

Similarly, a bivariate box spline $\phi_{\ell mnk}(x,y)$ based on a 4-direction mesh is defined in terms of Fourier transform by

$$\widehat{\phi}_{\ell mnk}(\xi,\eta) = \widehat{\phi}_{\ell mn}(\xi,\eta)\left(\frac{1-e^{-i(\xi-\eta)}}{i(\xi-\eta)}\right)^{k}, \quad i=\sqrt{-1}.$$

on the direction set

$$Y = \{\underbrace{e_1,\ldots,e_1}_{\ell}, \underbrace{e_2,\ldots,e_2}_{m}, \underbrace{e_1+e_2,\ldots,e_1+e_2}_{n}, \underbrace{e_1-e_2,\ldots,e_1-e_2}_{k}\}.$$

(For computation of 3-direction and 4-direction meshes box splines, see [L].)

If we consider four more directions such as $e_1+2e_2, 2e_1+e_2, e_1-2e_2$ and $-2e_1+e_2$ in addition to the four directions e_1, e_2, e_1+e_2 and e_1-e_2 of 4-direction mesh box spline , we have 8-direction mesh box spline. To avoid complicated indexes, we give the formula for the smallest order of 8-direction mesh box spline ${}_8\phi$, i.e. ,

$$\widehat{{}_8\phi}(\xi,\eta) = \left(\frac{1-e^{-i\xi}}{i\xi}\right)\left(\frac{1-e^{-i\eta}}{i\eta}\right)\left(\frac{1-e^{-i(\xi+\eta)}}{i(\xi+\eta)}\right)\left(\frac{1-e^{-i(\xi-\eta)}}{i(\xi-\eta)}\right) \times \left(\frac{1-e^{-i(\xi+2\eta)}}{i(\xi+2\eta)}\right)\left(\frac{1-e^{-i(2\xi+\eta)}}{i(2\xi+\eta)}\right)\left(\frac{1-e^{-i(\xi-2\eta)}}{i(\xi-2\eta)}\right)\left(\frac{1-e^{-i(-2\xi+\eta)}}{i(-2\xi+\eta)}\right), \quad i=\sqrt{-1}. \tag{3.22}$$

on the direction set $Y = \{e_1, e_2, e_1+e_2, e_1-e_2, e_1+2e_2, 2e_1+e_2, e_1-2e_2, -2e_1+e_2\}$.

Lemma 3.2.1 says that a Laurent polynomial P_Y associated with a box spline ϕ_Y on any direction set Y containing standard unit vectors $e_1=(1,0)$ and $e_2=(0,1)$ in $\mathbb{R}^2$ satisfies sub-QMF condition. Therefore, to use the constructive method in Theorem 2.2.2 for a box spline tight wavelet frame construction, we need to find a finite number of Laurent polynomials $\widetilde{P}_j$ for a given Laurent polynomial P_Y such that

$$1-\sum_{\nu\in\{0,\pi\}^2}|P_Y(\omega+\nu)|^2 = \sum_j |\widetilde{P}_j(2\omega)|^2 \text{ } where \omega=(\xi,\eta). \tag{3.23}$$

For a univariate setting, a nonnegative Laurent polynomial can be factored by a square root of a Laurent polynomial by Fejér and Riesz Lemma. However, it is not easy to generalize Fejér and Riesz Lemma to multivariate settings. We do not know the answer for the question whether any nonnegative Laurent polynomial can be expressed by a finite sum of squares of Laurent polynimials for multivariate settings. It is related to the 17th of Hilbert's 23 problems : Find a representation of definite form by squares. Further results on factorization of a multivariate nonnegative Laurent polynomial, see [LS] and [GL]. We found $\widetilde{P}_j$'s for specific box splines such as 3-direction mesh box splines ϕ_{111}, ϕ_{221} and ϕ_{222}, 4-direction mesh box splines ϕ_{1111} and ϕ_{2211} and a 8-direction mesh box spline ${}_8\phi$ by solving corresponding systems of non linear equations with a help by using MAPLE software. We will give the explicit Laurent polynomials satisfying (3.23) for each box spline we mentioned above at the end of this section. Unfortunately, so far we do not have an algorithm to find the Laurent polynomial $\widetilde{P}_j$'s systematically.

Now we are ready to describe the tight wavelet frame construction step by step. We take a bivariate 3-direction mesh box spline ϕ_{111} as an example. There are two Laurent polynomials

$$\widetilde{P}_1(\xi,\eta) = \frac{\sqrt{6}}{8}(1-e^{i\xi}),$$
$$\widetilde{P}_2(\xi,\eta) = \frac{\sqrt{2}}{8}(2-e^{i\xi}-e^{i(\xi+\eta)}),\ i=\sqrt{-1}.$$

such that

$$1-\sum_{\nu\in\{0,\pi\}^2}|P_{111}(\omega+\nu)|^2 = \sum_{j=1}^{2}|\widetilde{P}_j(2\omega)|^2, \quad \omega=(\xi,\eta). \tag{3.24}$$

for the Laurent polynomial P_{111} associated with box spline of order ϕ_{111}. Thus 3-direction mesh box spline ϕ_{111} satisfies the hypothesis of Theorem 2.2.2.

We first multiply the matrix $\mathcal{M}$ in (2.16) on the left side of the matrix $\overline{\mathcal{P}}$. That is,

$$\mathcal{M}\overline{\mathcal{P}} = \frac{1}{\sqrt{2}}\begin{bmatrix} 1 & 1 & 1 & 1 \\ e^{i\xi} & e^{i\xi} & -e^{i\xi} & -e^{i\xi} \\ e^{i\eta} & -e^{i\eta} & e^{i\eta} & -e^{i\eta} \\ e^{i(\xi+\eta)} & -e^{i(\xi+\eta)} & -e^{i(\xi+\eta)} & e^{i(\xi+\eta)} \end{bmatrix}\begin{bmatrix} \overline{P_{111}(\xi,\eta)} \\ \overline{P_{111}(\xi+\pi,\eta)} \\ \overline{P_{111}(\xi,\eta+\pi)} \\ \overline{P_{111}(\xi+\pi,\eta+\pi)} \end{bmatrix},\ i=\sqrt{-1}. \tag{3.25}$$

We denote the first polynomial of the column vector $\mathcal{M}\overline{\mathcal{P}}$ to be $\widehat{P}_1(2\xi,2\eta)$, the second one to be $\widehat{P}_2(2\xi,2\eta))$, the third one $\widehat{P}_3(2\xi,2\eta)$, and $\widehat{P}_4(2\xi,2\eta)$. It is easy to check

$$\sum_{n=1}^{4}|\widehat{P}_n(2\xi,2\eta)|^2 + \sum_{j=1}^{2}|\widetilde{P}_j(2\xi,2\eta)|^2 = 1.$$

Thus we do not need to deal with translated versions in ξ or η of the Laurent polynomial $P_{111}(2\xi,2\eta)$.

Let $\widetilde{\mathcal{P}}$ be a column vector

$$\left[\widehat{P}_1(2\xi,2\eta)\ \widehat{P}_2(2\xi,2\eta)\ \widehat{P}_3(2\xi 2\eta)\ \widehat{P}_4(2\xi,2\eta)\ \widetilde{P}_1(2\xi,2\eta)\ \widetilde{P}_2(2\xi,2\eta)\right]^T. \tag{3.26}$$

Define

$$\widetilde{\mathcal{Q}} := I - \widetilde{\mathcal{P}}\widetilde{\mathcal{P}}^* \tag{3.27}$$

Straight forward calculation verifies $\widetilde{\mathcal{Q}}^*\widetilde{\mathcal{Q}} = I - \widetilde{\mathcal{P}}\widetilde{\mathcal{P}}^*$.

Let $\widehat{\mathcal{Q}}$ be the first 6×4 block matrix in $\widetilde{\mathcal{Q}}$ and multiply $\mathcal{M}$ in (2.16) on the right side of matrix $\widehat{\mathcal{Q}}$

$$\mathcal{Q} := \widehat{\mathcal{Q}}\mathcal{M} = \frac{1}{\sqrt{2}}\,\widehat{\mathcal{Q}} \begin{bmatrix} 1 & 1 & 1 & 1 \\ e^{i\xi} & e^{i\xi} & -e^{i\xi} & -e^{i\xi} \\ e^{i\eta} & -e^{i\eta} & e^{i\eta} & -e^{i\eta} \\ e^{i(\xi+\eta)} & -e^{i(\xi+\eta)} & -e^{i(\xi+\eta)} & e^{i(\xi+\eta)} \end{bmatrix},\ i = \sqrt{-1}. \tag{3.28}$$

Then by straight forward calculation we have $\mathcal{Q}^*\mathcal{Q} = I - \overline{\mathcal{P}}\mathcal{P}^T$. That is, $\mathcal{Q}$ satisfies the matrix form of UEP condition. We denote each component of the first column of matrix $\mathcal{Q}$ by $Q^1_{111}(\xi,\eta), \cdots, Q^6_{111}(\xi,\eta)$, respectively. They are the desirable Laurent polynomials associated with the tight framelets $\psi^1_{111}, \cdots, \psi^6_{111}$ based on B-spline ϕ_{111}. That is, with these $Q^1_{111}, \cdots, Q^6_{111}$, we define $\psi^1_{111}, \cdots, \psi^6_{111}$ in terms of the Fourier transform such as

$$\widehat{\psi}^j_{111}(\xi,\eta) = Q^j_{111}(\xi/2,\eta/2)\widehat{\phi}_{111}(\xi/2,\eta/2),\ \text{for } j = 1, \cdots, 6.$$

In the following examples, we show the extra Laurent polynomials satisfying the condition in (3.23) for the Laurent polynomial P_{111}, P_{221}, P_{222}, P_{1111} ,P_{2211} and ${}_8P$. associated with box splines ϕ_{111}, ϕ_{221}, ϕ_{222}, ϕ_{1111} ,ϕ_{2211} and ${}_8\phi$, respectively.

Example 3.5.1 *Consider box spline ϕ_{111} on a three direction mesh. The Laurent polynomial associated with ϕ_{111} is*

$$P_{111}(\xi,\eta) = \left(\frac{1+e^{i\xi}}{2}\right)\left(\frac{1+e^{i\eta}}{2}\right)\left(\frac{1+e^{i(\xi+\eta)}}{2}\right),\ i = \sqrt{-1}.$$

It is easy to see that

$$1 - \sum_{\nu\in\{0,\pi\}^2} |P_{111}(\omega+\nu)|^2 = \frac{3}{8} - \frac{1}{8}\cos(\xi) - \frac{1}{8}\cos(\eta) - \frac{1}{8}\cos(\xi+\eta), \quad \textit{where } \omega = (\xi,\eta).$$

Thus, we let

$$\widetilde{P}_1(\xi,\eta) = \frac{\sqrt{6}}{8}(1 - e^{i\xi}),$$
$$\widetilde{P}_2(\xi,\eta) = \frac{\sqrt{2}}{8}(2 - e^{i\xi} - e^{i(\xi+\eta)}),\ i = \sqrt{-1}.$$

Then we can check

$$|P_{111}(\xi,\nu)|^2 + |P_{111}(\xi+\pi,\nu)|^2 + |P_{111}(\xi,\nu+\pi)|^2 + |P_{111}(\xi+\pi,\nu+\pi)|^2 + |\widetilde{P}_2(2\xi,2\nu)|^2 + |\widetilde{P}_2(2\xi,2\nu)|^2 = 1.$$

Thus, we can apply the constructive steps (3.25) - (3.28) to get 6 tight frame high-pass filters $Q^\ell, \ell = 1, \cdots, 6$. *We write the constructive steps in MAPLE code and found these* Q^ℓ*'s. We note that the constructive procedure in [CH2] yields 7 tight frame generators.*

$Q^1(\xi,\eta) = \sum_{j=-2}^{2}\sum_{k=-2}^{2} c^1_{jk} e^{-\sqrt{-1}j\xi} e^{-\sqrt{-1}k\eta}$ *with*

$$(c^1_{jk})_{\substack{-2\le j\le 2\\ -2\le k\le 2}} = \frac{1}{32}\begin{bmatrix} -1 & -1 & 0 & 0 & 0\\ -1 & -2 & -1 & 0 & 0\\ 0 & -1 & 14 & -1 & 0\\ 0 & 0 & -1 & -2 & -1\\ 0 & 0 & 0 & -1 & -1 \end{bmatrix},$$

$Q^2(\xi,\eta) = \sum_{j=0}^{2}\sum_{k=-2}^{2} c^2_{jk} e^{-\sqrt{-1}j\xi} e^{-\sqrt{-1}k\eta}$ *with*

$$(c^2_{jk})_{\substack{0\le j\le 2\\ -2\le k\le 2}} = \frac{1}{32}\begin{bmatrix} -1 & -1 & -1 & -1 & 0\\ -1 & -2 & 14 & -2 & -1\\ 0 & -1 & -1 & -1 & -1 \end{bmatrix},$$

$Q^3(\xi,\eta) = \sum_{j=-2}^{2}\sum_{k=0}^{2} c^3_{jk} e^{-\sqrt{-1}j\xi} e^{-\sqrt{-1}k\eta}$ *with*

$$(c^3_{jk})_{\substack{-2\le j\le 2\\ 0\le k\le 2}} = \frac{1}{32}\begin{bmatrix} -1 & -1 & 0\\ -1 & -2 & -1\\ -1 & 14 & -1\\ -1 & -2 & -1\\ 0 & -1 & -1 \end{bmatrix},$$

$$Q^4(\xi,\eta)=\sum_{j=0}^{2}\sum_{k=0}^{2}c^4_{jk}e^{-\sqrt{-1}j\xi}e^{-\sqrt{-1}k\eta}\ \textit{with}$$

$$(c^4_{jk})_{\substack{0\le j\le 2\\0\le k\le 2}}=\frac{1}{16}\begin{bmatrix}-1&-1&0\\-1&6&-1\\0&-1&-1\end{bmatrix},$$

$$Q^5(\xi,\eta)=\sum_{j=0}^{2}\sum_{k=0}^{4}c^5_{jk}e^{-\sqrt{-1}j\xi}e^{-\sqrt{-1}k\eta}\ \textit{with}$$

$$(c^5_{jk})_{\substack{0\le j\le 2\\0\le k\le 4}}=\frac{\sqrt{6}}{64}\begin{bmatrix}-1&-1&1&1&0\\-1&-2&0&2&1\\0&-1&-1&1&1\end{bmatrix},$$

$$Q^6(\xi,\eta)=\sum_{j=0}^{4}\sum_{k=0}^{4}c^6_{jk}e^{-\sqrt{-1}j\xi}e^{-\sqrt{-1}k\eta}\ \textit{with}$$

$$(c^6_{jk})_{\substack{0\le j\le 4\\0\le k\le 4}}=\frac{\sqrt{6}}{64}\begin{bmatrix}2&2&0&0&0\\2&4&2&0&0\\-1&1&1&-1&0\\-1&-2&-2&-2&-1\\0&-1&-1&-1&-1\end{bmatrix}.$$

Then our box spline tight wavelet framelets $\psi^1_{111},\cdots,\psi^6_{111}$ *on 3-direction mesh are defined as follows :*

$$\psi^1_{111}(x,y)=4\sum_{j=-2}^{2}\sum_{k=-2}^{2}c^1_{j,k}\phi^1_{111}(2x-j,2y-k),$$

$$\psi^2_{111}(x,y)=4\sum_{j=0}^{2}\sum_{k=-2}^{2}c^2_{j,k}\phi^2_{111}(2x-j,2y-k),$$

$$\psi^3_{111}(x,y)=4\sum_{j=-2}^{2}\sum_{k=0}^{2}c^3_{j,k}\phi^3_{111}(2x-j,2y-k),$$

$$\psi^4_{111}(x,y)=4\sum_{j=0}^{2}\sum_{k=0}^{2}c^4_{j,k}\phi^4_{111}(2x-j,2y-k),$$

$$\psi_{111}^5(x,y) = 4\sum_{j=0}^{2}\sum_{k=0}^{4} c_{j,k}^5 \phi_{111}^5(2x-j, 2y-k),$$

$$\psi_{111}^6(x,y) = 4\sum_{j=0}^{4}\sum_{k=0}^{4} c_{j,k}^6 \phi_{111}^6(2x-j, 2y-k).$$

$\square$

Example 3.5.2 *Consider box spline ϕ_{221}. The Laurent polynomial associated with ϕ_{221} is*

$$P_{221}(\xi,\eta) = \left(\frac{1+e^{i\xi}}{2}\right)^2 \left(\frac{1+e^{i\eta}}{2}\right)^2 \left(\frac{1+e^{i(\xi+\eta)}}{2}\right), \ i = \sqrt{-1}.$$

We find that

$$1 - \sum_{\nu\in\{0,\pi\}^2} |P_{221}(\omega+\nu)|^2 =$$
$$\frac{19}{32} - \frac{7}{32}\cos(\xi) - \frac{7}{32}\cos(\eta) - \frac{1}{64}\cos(\xi-\eta) - \frac{9}{64}\cos(\xi+\eta), \quad \textit{where } \omega = (\xi,\eta).$$

Let

$$\widetilde{P}_1(\xi,\eta) = \frac{\sqrt{21}}{12} - \frac{\sqrt{102}+2\sqrt{21}}{48}e^{i\xi} + \frac{\sqrt{102}-2\sqrt{21}}{48}e^{i\eta}$$
$$\widetilde{P}_2(\xi,\eta) = -\frac{\sqrt{42}+2\sqrt{51}}{48} + \frac{\sqrt{42}}{24}e^{i\eta} - \frac{\sqrt{42}-2\sqrt{51}}{48}e^{i(\xi+\eta)}$$

It is easy to check that

$$|P_{221}(\xi,\nu)|^2 + |P_{221}(\xi+\pi,\nu)|^2 + |P_{221}(\xi,\nu+\pi)|^2 + |P_{221}(\xi+\pi,\nu+\pi)|^2$$
$$+ |\widetilde{P}_2(2\xi,2\nu)|^2 + |\widetilde{P}_2(2\xi,2\nu)|^2 = 1.$$

Hence, the constructive steps (3.25) - (3.28) yield 6 tight wavelet frame high-pass filters and thus, 6 tight wavelet frame generators. We note that using the constructive procedure in [CH2], one will get 7 tight wavelet frame generators. generators.

$$Q^1(\xi,\eta) = \sum_{j=-2}^{3}\sum_{k=-2}^{3} c^1_{jk} e^{-\sqrt{-1}j\xi} e^{-\sqrt{-1}k\eta} \textit{ with}$$

$$(c^1_{jk})_{\substack{-2\le j\le 3\\ -2\le k\le 3}} = \frac{1}{512}\begin{bmatrix} -5 & -10 & -6 & -2 & -1 & 0 \\ -10 & -25 & -22 & -10 & -4 & -1 \\ -6 & -22 & 228 & -16 & -6 & -2 \\ -2 & -10 & -16 & -12 & -6 & -2 \\ -1 & -4 & -6 & -6 & -5 & -2 \\ 0 & -1 & -2 & -2 & -2 & -1 \end{bmatrix},$$

$$Q^2(\xi,\eta) = \sum_{j=-2}^{3}\sum_{k=-2}^{3} c^2_{jk} e^{-\sqrt{-1}j\xi} e^{-\sqrt{-1}k\eta} \textit{ with}$$

$$(c^2_{jk})_{\substack{-2\le j\le 3\\ -2\le k\le 3}} = \frac{1}{256}\begin{bmatrix} -1 & -2 & -1 & 0 & 0 & 0 \\ -2 & -5 & -4 & -1 & 0 & 0 \\ -3 & -8 & -8 & -4 & -1 & 0 \\ -4 & -11 & 116 & -8 & -4 & -1 \\ -2 & -8 & -11 & -8 & -5 & -2 \\ 0 & -2 & -4 & -3 & -2 & -1 \end{bmatrix},$$

$$Q^3(\xi,\eta) = \sum_{j=-2}^{3}\sum_{k=-2}^{3} c^3_{jk} e^{-\sqrt{-1}j\xi} e^{-\sqrt{-1}k\eta} \textit{ with}$$

$$(c^3_{jk})_{\substack{0\le j\le 5\\ 0\le k\le 5}} = \frac{1}{256}\begin{bmatrix} -1 & -2 & -3 & -4 & -2 & 0 \\ -2 & -5 & -8 & -11 & -8 & -2 \\ -1 & -4 & -8 & 116 & -11 & -4 \\ 0 & -1 & -4 & -8 & -8 & -3 \\ 0 & 0 & -1 & -4 & -5 & -2 \\ 0 & 0 & 0 & -1 & -2 & -1 \end{bmatrix},$$

$Q^4(\xi,\eta) = \sum_{j=0}^{5}\sum_{k=0}^{5} c_{jk}^4 e^{-\sqrt{-1}j\xi} e^{-\sqrt{-1}k\eta}$ *with*

$$(c_{jk}^4)_{\substack{0\le j\le 5\\ 0\le k\le 5}} = \frac{1}{512}\begin{bmatrix} -1 & -2 & -2 & -2 & -1 & 0 \\ -2 & -5 & -6 & -6 & -4 & -1 \\ -2 & -6 & -12 & -16 & -10 & -2 \\ -2 & -6 & -16 & 228 & -22 & -6 \\ -1 & -4 & -10 & -22 & -25 & -10 \\ 0 & -1 & -2 & -6 & -10 & -5 \end{bmatrix},$$

We provide decimal expression of Q^5 *and* Q^6 *because of its complicated expression. (We are willing to provide its exact values upon request.)*

$Q^5(\xi,\eta) = \sum_{j=0}^{5}\sum_{k=0}^{5} c_{jk}^5 e^{-\sqrt{-1}j\xi} e^{-\sqrt{-1}k\eta}$ *with*

$$(c_{jk}^5)_{\substack{0\le j\le 5\\ 0\le k\le 5}} = \begin{bmatrix} -0.01193 & -0.02387 & -0.01254 & -0.00122 & -0.000608 & 0.0 \\ -0.02387 & -0.05967 & -0.04895 & -0.01498 & -0.00243 & -0.000608 \\ 0.000608 & -0.02265 & -0.04775 & -0.02630 & -0.00304 & -0.00122 \\ 0.02508 & 0.05078 & 0.02630 & 0.0 & -0.00122 & -0.000608 \\ 0.01254 & 0.05017 & 0.06272 & 0.02508 & 0.0 & 0.0 \\ 0.0 & 0.01254 & 0.02508 & 0.01254 & 0.0 & 0.0 \end{bmatrix},$$

$Q^6(\xi,\eta) = \sum_{j=0}^{5}\sum_{k=0}^{5} c_{jk}^6 e^{-\sqrt{-1}j\xi} e^{-\sqrt{-1}k\eta}$ *with*

$$(c_{jk}^6)_{\substack{0\le j\le 5\\ 0\le k\le 5}} = \begin{bmatrix} 0.01352 & 0.02704 & 0.005079 & -0.01688 & -0.008438 & 0.0 \\ 0.02704 & 0.06759 & 0.03719 & -0.02867 & -0.03375 & -0.008438 \\ 0.01352 & 0.05407 & 0.05407 & -0.01688 & -0.04727 & -0.01688 \\ 0.0 & 0.01352 & 0.01688 & -0.02031 & -0.03719 & -0.01352 \\ 0.0 & 0.0 & -0.005079 & -0.02031 & -0.02539 & -0.01016 \\ 0.0 & 0.0 & 0.0 & -0.005079 & -0.01016 & -0.005079 \end{bmatrix}.$$

Then our box spline tight wavelet framelets $\psi^1_{221}, \cdots, \psi^6_{221}$ *on 3-direction mesh are defined as follows :*

$$\psi^1_{221}(x,y) = 4\sum_{j=-2}^{3}\sum_{k=-2}^{3} c^1_{j,k}\phi^1_{221}(2x-j, 2y-k),$$

$$\psi^2_{221}(x,y) = 4\sum_{j=-2}^{3}\sum_{k=-2}^{3} c^2_{j,k}\phi^2_{221}(2x-j, 2y-k),$$

$$\psi^3_{221}(x,y) = 4\sum_{j=-2}^{3}\sum_{k=-2}^{3} c^3_{j,k}\phi^3_{221}(2x-j, 2y-k),$$

$$\psi^4_{221}(x,y) = 4\sum_{j=-2}^{3}\sum_{k=-2}^{3} c^4_{j,k}\phi^4_{221}(2x-j, 2y-k),$$

$$\psi^5_{221}(x,y) = 4\sum_{j=0}^{5}\sum_{k=0}^{5} c^5_{j,k}\phi^5_{221}(2x-j, 2y-k),$$

$$\psi^6_{221}(x,y) = 4\sum_{j=0}^{5}\sum_{k=0}^{5} c^6_{j,k}\phi^6_{221}(2x-j, 2y-k).$$

□

Example 3.5.3 *For box spline* ϕ_{222}*, the Laurent polynomial associated with* ϕ_{222} *is*

$$P_{222}(\xi,\eta) = \left(\frac{1+e^{i\xi}}{2}\right)^2\left(\frac{1+e^{i\eta}}{2}\right)^2\left(\frac{1+e^{i(\xi+\eta)}}{2}\right)^2, \ i=\sqrt{-1}.$$

Then we have

$$\begin{aligned}
&1-\sum_{\nu\in\{0,\pi\}^2}|P_{222}(\omega+\nu)|^2\\
=&\frac{1}{512}(339-106(\cos(\xi)+\cos(\eta)+\cos(\xi+\eta))\\
&-(\cos(2\xi)+\cos(2\eta)+\cos(2(\xi+\eta))\\
&-6(\cos(2\xi+\eta)+\cos(\xi+2\eta)+\cos(\xi-\eta))\\
=&\sum_{j=1}^{3}|\widetilde{P}_j(2\omega)|^2, \quad \textit{where } \omega=(\xi,\eta).
\end{aligned}$$

where

$$
\begin{aligned}
\widetilde{P}_1(\xi,\eta) &= \frac{\sqrt{14}}{96} + \frac{\sqrt{14}}{16}\ e^{i\xi} + \frac{\sqrt{14}}{16}\ e^{i\eta} - \frac{173}{1344}\sqrt{14}\ e^{i(\xi+\eta)} - \frac{3}{448}\sqrt{14}\ e^{2i(\xi+\eta)},\\
\widetilde{P}_2(\xi,\eta) &= \frac{1}{5376}\left(\sqrt{713608+42\sqrt{178402}}+\sqrt{713608-42\sqrt{178402}}\right)\\
&\quad - \frac{\sqrt{178402}}{2854432}\left(\sqrt{713608+42\sqrt{178402}}-\sqrt{713608-42\sqrt{178402}}\right)\ e^{2i\eta}\\
&\quad - \frac{\sqrt{178402}}{40281744384}\Bigg(14112\left(\sqrt{713608-42\sqrt{178402}}-\sqrt{713608+42\sqrt{178402}}\right)\\
&\quad + 42\sqrt{178402}\left(\sqrt{713608-42\sqrt{178402}}+\sqrt{713608+42\sqrt{178402}}\right)\Bigg)\ e^{i(\xi+\eta)}\\
\widetilde{P}_3(\xi,\eta) &= \frac{1}{5376}\left(\sqrt{713608+42\sqrt{178402}}-\sqrt{713608-42\sqrt{178402}}\right)\\
&\quad - \frac{\sqrt{178402}}{2854432}\left(\sqrt{713608+42\sqrt{178402}}+\sqrt{713608-42\sqrt{178402}}\right)\ e^{2i\xi}\\
&\quad + \frac{\sqrt{178402}}{40281744384}\Bigg(14112\left(\sqrt{713608-42\sqrt{178402}}+\sqrt{713608+42\sqrt{178402}}\right)\\
&\quad + 42\sqrt{178402}\left(\sqrt{713608-42\sqrt{178402}}-\sqrt{713608+42\sqrt{178402}}\right)\Bigg)e^{i(\xi+\eta)}.
\end{aligned}
$$

Thus, we need 7 wavelet frame generators for ϕ_{222}. The explicit Leurent polynomials Q^ℓ are following. We note that the number of framelets in [CH2] for ϕ_{222} is also seven. ϕ_{222}

$Q^1(\xi,\eta) = \sum_{j=-4}^{4}\sum_{k=-4}^{4} c^1_{jk} e^{-\sqrt{-1}j\xi} e^{-\sqrt{-1}k\eta}$ *with*

$$
(c^1_{jk})_{\substack{-4\le j\le 4\\ -4\le k\le 4}} = \frac{1}{2048}
\begin{bmatrix}
-1 & -2 & -2 & -2 & -1 & 0 & 0 & 0 & 0\\
-2 & -6 & -8 & -8 & -6 & -2 & 0 & 0 & 0\\
-2 & -8 & -22 & -32 & -22 & -8 & -2 & 0 & 0\\
-2 & -8 & -32 & -70 & -70 & -32 & -8 & -2 & 0\\
-1 & -6 & -22 & -70 & 918 & -70 & -22 & -6 & -1\\
0 & -2 & -8 & -32 & -70 & -70 & -32 & -8 & -2\\
0 & 0 & -2 & -8 & -22 & -32 & -22 & -8 & -2\\
0 & 0 & 0 & -2 & -6 & -8 & -8 & -6 & -2\\
0 & 0 & 0 & 0 & -1 & -2 & -2 & -2 & -1
\end{bmatrix}
$$

$$Q^2(\xi,\eta) = \sum_{j=-2}^{4}\sum_{k=-4}^{4} c^2_{jk} e^{-\sqrt{-1}j\xi} e^{-\sqrt{-1}k\eta} \ \ with$$

$$(c^2_{jk})_{\substack{-2\le j\le 4\\ -4\le k\le 4}} = \frac{1}{2048}\begin{bmatrix} -1 & -2 & -4 & -6 & -3 & 0 & 0 & 0 & 0 \\ -2 & -6 & -12 & -20 & -18 & -6 & 0 & 0 & 0 \\ -1 & -6 & -16 & -30 & -35 & -20 & -4 & 0 & 0 \\ 0 & -2 & -12 & -30 & 472 & -30 & -12 & -2 & 0 \\ 0 & 0 & -4 & -20 & -35 & -30 & -16 & -6 & -1 \\ 0 & 0 & 0 & -6 & -18 & -20 & -12 & -6 & -2 \\ 0 & 0 & 0 & 0 & -3 & -6 & -4 & -2 & -1 \end{bmatrix}$$

$$Q^3(\xi,\eta) = \sum_{j=-4}^{4}\sum_{k=-2}^{4} c^3_{jk} e^{-\sqrt{-1}j\xi} e^{-\sqrt{-1}k\eta} \ \ with$$

$$(c^3_{jk})_{\substack{-4\le j\le 4\\ -2\le k\le 4}} = \frac{1}{2048}\begin{bmatrix} -1 & -2 & -1 & 0 & 0 & 0 & 0 \\ -2 & -6 & -6 & -2 & 0 & 0 & 0 \\ -4 & -12 & -16 & -12 & -4 & 0 & 0 \\ -6 & -20 & -30 & -30 & -20 & -6 & 0 \\ -3 & -18 & -35 & 472 & -35 & -18 & -3 \\ 0 & -6 & -20 & -30 & -30 & -20 & -6 \\ 0 & 0 & -4 & -12 & -16 & -12 & -4 \\ 0 & 0 & 0 & -2 & -6 & -6 & -2 \\ 0 & 0 & 0 & 0 & -1 & -2 & -1 \end{bmatrix}$$

$$Q^4(\xi,\eta) = \sum_{j=-2}^{4}\sum_{k=-2}^{4} c^4_{jk} e^{-\sqrt{-1}j\xi} e^{-\sqrt{-1}k\eta} \ \textit{with}$$

$$(c^4_{jk})_{\substack{-2\le j\le 4\\ -2\le k\le 4}} = \frac{1}{2048}\begin{bmatrix} -3 & -6 & -4 & -2 & -1 & 0 & 0 \\ -6 & -18 & -20 & -12 & -6 & -2 & 0 \\ -4 & -20 & -35 & -30 & -16 & -6 & -1 \\ -2 & -12 & -30 & 472 & -30 & -12 & -2 \\ -1 & -6 & -16 & -30 & -35 & -20 & -4 \\ 0 & -2 & -6 & -12 & -20 & -18 & -6 \\ 0 & 0 & -1 & -2 & -4 & -6 & -3 \end{bmatrix}$$

We provide decimal expression of Q^5 and Q^6 because of its complicated expression. (We are willing to provide its exact values upon request.)

$$Q^5(\xi,\eta) = \sum_{j=0}^{8}\sum_{k=0}^{6} c^5_{jk} e^{-\sqrt{-1}j\xi} e^{-\sqrt{-1}k\eta} \ \textit{with}$$

$$(c^5_{jk})_{\substack{0\le j\le 8\\ 0\le k\le 6}} =$$

$$\begin{bmatrix} -0.000061 & -0.000122 & -0.000061 & 0.0 & 0.0 & 0.0 & 0.0 \\ -0.000122 & -0.00036 & -0.00036 & -0.000122 & 0.0 & 0.0 & 0.0 \\ -0.000061 & -0.00036 & -0.004456 & -0.008058 & -0.003906 & 0.0 & 0.0 \\ 0.0 & -0.000122 & -0.008058 & -0.02343 & -0.02319 & -0.007692 & 0.0 \\ 0.003906 & 0.007814 & 0.0 & -0.02319 & -0.03851 & -0.02307 & -0.003845 \\ 0.007814 & 0.02343 & 0.02343 & 0.000122 & -0.02307 & -0.02307 & -0.007692 \\ 0.003906 & 0.02343 & 0.03906 & 0.02343 & 0.000061 & -0.007692 & -0.003845 \\ 0.0 & 0.007814 & 0.02343 & 0.02343 & 0.007814 & 0.0 & 0.0 \\ 0.0 & 0.0 & 0.003906 & 0.007814 & 0.003906 & 0.0 & 0.0 \end{bmatrix}$$

$$Q^6(\xi,\eta) = \sum_{j=0}^{6}\sum_{k=0}^{8} c^6_{jk} e^{-\sqrt{-1}j\xi} e^{-\sqrt{-1}k\eta} \ \textit{with}$$

$$(c^6_{jk})_{\substack{0\le j\le 6\\ 0\le k\le 8}} =$$

$$10^{-3}\begin{bmatrix} -4.909 & -9.820 & -4.909 & 0.0 & 0.048 & 0.096 & 0.048 & 0.0 & 0.0 \\ -9.820 & -29.46 & -29.46 & -9.820 & 0.096 & 0.29 & 0.29 & 0.096 & 0.0 \\ -4.909 & -029.46 & -44.24 & -19.74 & 0.0 & 0.29 & 0.48 & 0.29 & 0.048 \\ 0.0 & -9.820 & -19.74 & -0.29 & 19.36 & 9.820 & 0.29 & 0.29 & 0.096 \\ 0.0 & 0.0 & -0.048 & 0.19.36 & 43.71 & 29.17 & 4.909 & 0.096 & 0.048 \\ 0.0 & 0.0 & 0.0 & 9.725 & 29.17 & 29.17 & 9.725 & 0.0 & 0.0 \\ 0.0 & 0.0 & 0.0 & 0.0 & 4.861 & 9.725 & 4.861 & 0.0 & 0.0 \end{bmatrix}$$

$$Q^7(\xi,\eta) = \sum_{j=0}^{8}\sum_{k=0}^{8} c^7_{jk} e^{-\sqrt{-1}j\xi} e^{-\sqrt{-1}k\eta} \ \textit{with}$$

$$(c^7_{jk})_{\substack{0\le j\le 8\\ 0\le k\le 8}} = \frac{\sqrt{14}}{86016}\begin{bmatrix} -14 & -28 & -98 & -168 & -84 & 0 & 0 & 0 & 0 \\ -28 & -84 & -252 & -532 & -504 & -168 & 0 & 0 & 0 \\ -98 & -252 & -135 & -242 & -681 & -504 & -84 & 0 & 0 \\ -168 & -532 & -242 & 618 & 506 & -158 & -168 & 0 & 0 \\ -84 & -504 & -681 & 506 & 1557 & 888 & 98 & 0 & 0 \\ 0 & -168 & -504 & -158 & 888 & 1092 & 400 & 18 & 0 \\ 0 & 0 & -84 & -168 & 98 & 400 & 263 & 54 & 9 \\ 0 & 0 & 0 & 0 & 0 & 18 & 54 & 54 & 18 \\ 0 & 0 & 0 & 0 & 0 & 0 & 9 & 18 & 9 \end{bmatrix}$$

Then our box spline tight wavelet framelets $\psi^1_{222}, \cdots, \psi^7_{222}$ *on 3-direction mesh are defined as follows :*

$$\psi^1_{222}(x,y) = 4\sum_{j=4}^{4}\sum_{k=-4}^{4} c^1_{j,k}\phi^1_{222}(2x-j, 2y-k),$$

$$\psi^2_{222}(x,y) = 4\sum_{j=-2}^{4}\sum_{k=-4}^{4} c^2_{j,k}\phi^2_{222}(2x-j, 2y-k),$$

$$\psi^3_{222}(x,y) = 4\sum_{j=-4}^{4}\sum_{k=-2}^{4} c^3_{j,k}\phi^3_{222}(2x-j,2y-k),$$

$$\psi^4_{222}(x,y) = 4\sum_{j=-2}^{4}\sum_{k=-2}^{4} c^4_{j,k}\phi^4_{222}(2x-j,2y-k),$$

$$\psi^5_{222}(x,y) = 4\sum_{j=0}^{8}\sum_{k=0}^{6} c^5_{j,k}\phi^5_{222}(2x-j,2y-k),$$

$$\psi^6_{222}(x,y) = 4\sum_{j=0}^{6}\sum_{k=0}^{8} c^6_{j,k}\phi^6_{222}(2x-j,2y-k).$$

$$\psi^7_{222}(x,y) = 4\sum_{j=0}^{8}\sum_{k=0}^{8} c^7_{j,k}\phi^7_{222}(2x-j,2y-k).$$

□

Example 3.5.4 *For box spline ϕ_{1111}, the Laurent polynomial associated with ϕ_{1111} is*

$$P_{1111}(\xi,\eta) = \left(\frac{1+e^{i\xi}}{2}\right)\left(\frac{1+e^{i\eta}}{2}\right)\left(\frac{1+e^{i(\xi+\eta)}}{2}\right)\left(\frac{1+e^{i(\xi-\eta)}}{2}\right),\ i=\sqrt{-1}.$$

Then we have

$$\begin{aligned}
&1-\sum_{\nu\in\{0,\pi\}^2}|P_{1111}(\omega+\nu)|^2 \\
&= \frac{5}{8}-\frac{1}{8}\cos(\xi)-\frac{1}{8}\cos(\eta)-\frac{1}{32}\cos(\xi+\eta)-\frac{1}{32}\cos(\xi-\eta) \\
&= \sum_{j=1}^{2}|\widetilde{P}_j(2\omega)|^2,\ \omega=(\xi,\eta).
\end{aligned}$$

where

$$\begin{aligned}
\widetilde{P}_1(\xi,\eta) &= \frac{\sqrt{6}}{8}(1-e^{i(\xi-\eta)}), \\
\widetilde{P}_2(\xi,\eta) &= -\frac{1}{4}+\frac{\sqrt{6}}{8}+\frac{1}{4}e^{i\xi}+\frac{1}{4}e^{i\eta}-\frac{2+\sqrt{6}}{8}e^{i(\xi+\eta)},\ i=\sqrt{-1}.
\end{aligned}$$

Hence, the constructive steps (3.25) - (3.28) yields 6 tight frame filters and hence, 6 tight frame generators which is less than a half of the number of tight framelets in [CH2].

$$Q^1(\xi,\eta) = \sum_{j=-2}^{3}\sum_{k=-3}^{2} c^1_{jk} e^{-\sqrt{-1}j\xi} e^{-\sqrt{-1}k\eta} \ \ with$$

$$(c^1_{jk})_{\substack{-2\le j\le 3\\ -3\le k\le 2}} = \frac{1}{128}\begin{bmatrix} 0 & -1 & -1 & -2 & -2 & 0 \\ -1 & -2 & -4 & -5 & -4 & -2 \\ -1 & -2 & -4 & 58 & -5 & -2 \\ 0 & -1 & -2 & -4 & -4 & -1 \\ 0 & 0 & -1 & -2 & -2 & -1 \\ 0 & 0 & 0 & -1 & -1 & 0 \end{bmatrix}$$

$$Q^2(\xi,\eta) = \sum_{j=-2}^{3}\sum_{k=-3}^{2} c^2_{jk} e^{-\sqrt{-1}j\xi} e^{-\sqrt{-1}k\eta} \ \ with$$

$$(c^2_{jk})_{\substack{-2\le j\le 3\\ -3\le k\le 2}} = \frac{1}{128}\begin{bmatrix} 0 & 0 & 0 & -1 & -1 & 0 \\ 0 & 0 & -1 & -2 & -2 & -1 \\ 0 & -1 & -2 & -4 & -4 & -1 \\ -1 & -2 & -4 & 58 & -5 & -2 \\ -1 & -2 & -4 & -5 & -4 & -2 \\ 0 & -1 & -1 & -2 & -2 & 0 \end{bmatrix}$$

$$Q^3(\xi,\eta) = \sum_{j=-2}^{3}\sum_{k=-1}^{4} c^3_{jk} e^{-\sqrt{-1}j\xi} e^{-\sqrt{-1}k\eta} \ \ with$$

$$(c^3_{jk})_{\substack{-2\le j\le 3\\ -1\le k\le 4}} = \frac{1}{128}\begin{bmatrix} 0 & -2 & -2 & -1 & -1 & 0 \\ -2 & -4 & -5 & -4 & -2 & -1 \\ -2 & -5 & 58 & -4 & -2 & -1 \\ -1 & -4 & -4 & -2 & -1 & 0 \\ -1 & -2 & -2 & -1 & 0 & 0 \\ 0 & -1 & -1 & 0 & 0 & 0 \end{bmatrix}$$

$$Q^4(\xi,\eta) = \sum_{j=-2}^{3}\sum_{k=-1}^{4} c^4_{jk} e^{-\sqrt{-1}j\xi} e^{-\sqrt{-1}k\eta} \ \ \textit{with}$$

$$(c^4_{jk})_{\substack{-2\le j\le 3\\ -1\le k\le 4}} = \frac{1}{128}\begin{bmatrix} 0 & -1 & -1 & 0 & 0 & 0 \\ -1 & -2 & -2 & -1 & 0 & 0 \\ -1 & -4 & -4 & -2 & -1 & 0 \\ -2 & -5 & 58 & -4 & -2 & -1 \\ -2 & -4 & -5 & -4 & -2 & -1 \\ 0 & -2 & -2 & -1 & -1 & 0 \end{bmatrix}$$

$$Q^5(\xi,\eta) = \sum_{j=0}^{5}\sum_{k=-1}^{4} c^5_{jk} e^{-\sqrt{-1}j\xi} e^{-\sqrt{-1}k\eta} \ \ \textit{with}$$

$$(c^5_{jk})_{\substack{0\le j\le 5\\ -1\le k\le 4}} = \frac{1}{128}\begin{bmatrix} 0 & 2-\sqrt{6} & 2-\sqrt{6} & -2 & -2 & 0 \\ 2-\sqrt{6} & 4-2\sqrt{6} & 2-2\sqrt{6} & -2-\sqrt{6} & -4 & -2 \\ 2-\sqrt{6} & 2-2\sqrt{6} & -2\sqrt{6} & 0 & \sqrt{6}-2 & -2 \\ -2 & -2-\sqrt{6} & 0 & 2\sqrt{6} & 2+2\sqrt{6} & 2+\sqrt{6} \\ -2 & -4 & \sqrt{6}-2 & 2+2\sqrt{6} & 2\sqrt{6}+4 & 2+\sqrt{6} \\ 0 & -2 & -2 & 2+\sqrt{6} & 2+\sqrt{6} & 0 \end{bmatrix}$$

$$Q^6(\xi,\eta) = \sum_{j=0}^{5}\sum_{k=-3}^{2} c^6_{jk} e^{-\sqrt{-1}j\omega} e^{-\sqrt{-1}k\xi} \ \ \textit{with}$$

$$(c^6_{jk})_{\substack{0\le j\le 5\\ -3\le k\le 2}} = \frac{\sqrt{6}}{128}\begin{bmatrix} 0 & 0 & 0 & -1 & -1 & 0 \\ 0 & 0 & -1 & -2 & -2 & -1 \\ 0 & 1 & 0 & -2 & -2 & -1 \\ 1 & 2 & 2 & 0 & -1 & 0 \\ 1 & 2 & 2 & 1 & 0 & 0 \\ 0 & 1 & 1 & 0 & 0 & 0 \end{bmatrix}$$

Then our box spline tight wavelet framelets $\psi^1_{1111}, \cdots, \psi^6_{1111}$ on 4-direction mesh are defined as follows :

$$\psi^1_{1111}(x,y) = 4\sum_{j=-2}^{3}\sum_{k=-3}^{2} c^1_{j,k}\phi^1_{1111}(2x-j, 2y-k),$$

$$\psi^2_{1111}(x,y) = 4\sum_{j=-2}^{3}\sum_{k=-3}^{2} c^2_{j,k}\phi^2_{1111}(2x-j, 2y-k),$$

$$\psi^3_{1111}(x,y) = 4\sum_{j=-2}^{3}\sum_{k=-1}^{4} c^3_{j,k}\phi^3_{1111}(2x-j, 2y-k),$$

$$\psi^4_{1111}(x,y) = 4\sum_{j=-2}^{3}\sum_{k=-1}^{4} c^4_{j,k}\phi^4_{1111}(2x-j, 2y-k),$$

$$\psi^5_{1111}(x,y) = 4\sum_{j=0}^{5}\sum_{k=-1}^{4} c^5_{j,k}\phi^5_{1111}(2x-j, 2y-k),$$

$$\psi^6_{1111}(x,y) = 4\sum_{j=0}^{5}\sum_{k=-3}^{2} c^6_{j,k}\phi^6_{1111}(2x-j, 2y-k).$$

□

Example 3.5.5 *For box spline ϕ_{2211}, the Laurent polynomial associated with ϕ_{2211} is*

$$P_{2211}(\xi,\eta) = \left(\frac{1+e^{i\xi}}{2}\right)^2\left(\frac{1+e^{i\eta}}{2}\right)^2\left(\frac{1+e^{i(\xi+\eta)}}{2}\right)\left(\frac{1+e^{i(\xi-\eta)}}{2}\right),\ i=\sqrt{-1}.$$

Then we have

$$1 - \sum_{\nu\in\{0,\pi\}^2} |P_{2211}(\omega+\nu)|^2 = \sum_{j=1}^{4} |\widetilde{P}_j(2\omega)|^2, \quad \textit{where } \omega\in\mathbb{R}^2$$

where

$$\widetilde{P}_1(\xi,\eta) = \frac{\sqrt{1886}}{224}(1-e^{2i\xi}),$$
$$\widetilde{P}_2(\xi,\eta) = -\frac{3\sqrt{14}}{64} + \frac{\sqrt{40531922}}{25472} + \frac{3\sqrt{14}}{32}e^{i\eta} - \left(\frac{3\sqrt{14}}{64} + \frac{\sqrt{40531922}}{25472}\right)e^{2i\eta},$$
$$\widetilde{P}_3(\xi,\eta) = \frac{7\sqrt{2}}{64} + \frac{7\sqrt{2}}{64}e^{2i\eta} - \frac{\sqrt{2}}{224}e^{i(2\xi+\eta)} - \frac{3\sqrt{2}}{14}e^{i(\xi+\eta)},$$
$$\widetilde{P}_4(\xi,\eta) = \frac{\sqrt{398}}{112} + \frac{\sqrt{398}}{112}e^{2i\xi} - \frac{3135\sqrt{398}}{178304}e^{i\xi} - \frac{7\sqrt{398}}{25472}e^{i(\xi+2\eta)},\ i=\sqrt{-1}.$$

Hence, we will have 8 tight frame generators using the constructive steps (3.25) - (3.28). These 8 tight frames ψ_m which can be expressed in terms of Fourier transform by

$$\widehat{\psi}^{\ell}(\xi,\eta) = Q^{\ell}(\xi/2,\eta/2)\widehat{\phi}_{2211}(\xi/2,\eta/2),\ \ell=1,\cdots,8$$

are given in terms of coefficient matrix as follows:

$$Q^1(\xi,\eta) = \sum_{j=-4}^{4}\sum_{k=-3}^{3} c^1_{jk} e^{-\sqrt{-1}j\omega} e^{-\sqrt{-1}k\xi} \text{ with}$$

$$(c^1_{jk})_{\substack{-4\le j\le 4\\ -3\le k\le 3}} = -\frac{1}{2048}\begin{bmatrix} 0 & 1 & 2 & 2 & 2 & 1 & 0\\ 1 & 4 & 7 & 8 & 7 & 4 & 1\\ 2 & 12 & 22 & 24 & 22 & 12 & 2\\ 7 & 28 & 49 & 56 & 49 & 28 & 7\\ 12 & 38 & 64 & -948 & 64 & 38 & 12\\ 7 & 28 & 49 & 56 & 49 & 28 & 7\\ 2 & 12 & 22 & 24 & 22 & 12 & 2\\ 1 & 4 & 7 & 8 & 7 & 4 & 1\\ 0 & 1 & 2 & 2 & 2 & 1 & 0 \end{bmatrix},$$

$$Q^2(\xi,\eta) = \sum_{j=-2}^{4}\sum_{k=-3}^{3} c^2_{jk} e^{-\sqrt{-1}j\xi} e^{-\sqrt{-1}k\eta} \text{ with}$$

$$(c^2_{jk})_{\substack{-2\le j\le 4\\ -3\le k\le 3}} = -\frac{1}{512}\begin{bmatrix} 0 & 1 & 2 & 2 & 2 & 1 & 0\\ 1 & 4 & 7 & 8 & 7 & 4 & 1\\ 2 & 7 & 12 & 14 & 12 & 7 & 2\\ 2 & 8 & 14 & -240 & 14 & 8 & 2\\ 2 & 7 & 12 & 14 & 12 & 7 & 2\\ 1 & 4 & 7 & 8 & 7 & 4 & 1\\ 0 & 1 & 2 & 2 & 2 & 1 & 0 \end{bmatrix},$$

$$Q^3(\xi,\eta)=\sum_{j=-4}^{4}\sum_{k=-3}^{5}c^3_{jk}e^{-\sqrt{-1}j\xi}e^{-\sqrt{-1}k\eta}\ \ with$$

$$(c^3_{jk})_{\substack{-4\le j\le 4\\ -3\le k\le 5}}=-\frac{1}{1024}\begin{bmatrix}0&0&0&1&2&1&0&0&0\\0&0&1&4&6&4&1&0&0\\0&1&4&11&16&11&4&1&0\\1&4&11&24&32&24&11&4&1\\2&6&16&32&-472&32&16&6&2\\1&4&11&24&32&24&11&4&1\\0&1&4&11&16&11&4&1&0\\0&0&1&4&6&4&1&0&0\\0&0&0&1&2&1&0&0&0\end{bmatrix},$$

$$Q^4(\xi,\eta)=\sum_{j=-2}^{4}\sum_{k=-3}^{5}c^4_{jk}e^{-\sqrt{-1}j\xi}e^{-\sqrt{-1}k\eta}\ \ with$$

$$(c^4_{jk})_{\substack{-2\le j\le 4\\ -3\le k\le 5}}=-\frac{1}{2048}\begin{bmatrix}0&1&2&7&12&7&2&1&0\\1&4&12&28&38&28&12&4&1\\2&7&22&49&64&49&22&7&2\\2&8&24&56&-948&56&24&8&2\\2&7&22&49&64&49&22&7&2\\1&4&12&28&38&28&12&4&1\\0&1&2&7&12&7&2&1&0\end{bmatrix},$$

$$Q^5(\xi,\eta)=\sum_{j=0}^{8}\sum_{k=-1}^{7}c^5_{jk}e^{-\sqrt{-1}j\xi}e^{-\sqrt{-1}k\eta}\ \textit{with}$$

$$(c^5_{jk})_{\substack{0\le j\le 8\\ -1\le k\le 7}}=-\frac{\sqrt{2}}{28672}\begin{bmatrix} 0 & 49 & 98 & 49 & 0 & 49 & 98 & 49 & 0\\ 49 & 196 & 294 & 196 & 98 & 196 & 294 & 196 & 49\\ 98 & 294 & 392 & 198 & 4 & 198 & 392 & 294 & 98\\ 49 & 196 & 198 & -188 & -478 & -188 & 198 & 196 & 49\\ 0 & 49 & -94 & -529 & -772 & -529 & -94 & 49 & 0\\ 0 & 0 & -98 & -392 & -588 & -392 & -98 & 0 & 0\\ 0 & 0 & -4 & -108 & -208 & -108 & -4 & 0 & 0\\ 0 & 0 & -2 & -8 & -12 & -8 & -2 & 0 & 0\\ 0 & 0 & 0 & -2 & -4 & -2 & 0 & 0 & 0 \end{bmatrix},$$

$$\textit{and}\ Q^6(\xi,\eta)=\sum_{j=0}^{8}\sum_{k=-1}^{7}c^6_{jk}e^{-\sqrt{-1}j\xi}e^{-\sqrt{-1}k\eta}\ \textit{with}$$

$$(c^6_{jk})_{\substack{0\le j\le 8\\ -1\le k\le 7}}=$$

$$-\frac{\sqrt{398}}{11411456}\begin{bmatrix} 0 & 1592 & 3184 & 1592 & 0 & 0 & 0 & 0 & 0\\ 1592 & 6368 & 9552 & 6368 & 1592 & 0 & 0 & 0 & 0\\ 3184 & 6417 & 6466 & 6417 & 3184 & -49 & -98 & -49 & 0\\ -1543 & -6172 & -9258 & -6172 & -1592 & -196 & -294 & -196 & -49\\ -6270 & -15626 & -18712 & -15626 & -6368 & -294 & -392 & -294 & -98\\ -1543 & -6172 & -9258 & -6172 & -1592 & -196 & -294 & -196 & -49\\ 3184 & 6417 & 6466 & 6417 & 3184 & -49 & -98 & -49 & 0\\ 1592 & 6368 & 9552 & 6368 & 1592 & 0 & 0 & 0 & 0\\ 0 & 1592 & 3184 & 1592 & 0 & 0 & 0 & 0 & 0 \end{bmatrix}.$$

$$Q^7(\xi,\eta) = \sum_{j=0}^{4}\sum_{k=-1}^{7} c^7_{jk} e^{-\sqrt{-1}j\xi} e^{-\sqrt{-1}k\eta} \text{ with}$$

$$(c^7_{jk})_{\substack{0\le j\le 4\\ -1\le k\le 7}} =$$

$$10^{-3}\begin{bmatrix} 0.0 & -1.165 & -2.330 & -6.645 & -10.96 & 1.165 & 13.29 & 6.645 & 0.0 \\ -1.165 & -4.66 & -12.47 & -26.58 & -27.40 & 4.66 & 34.39 & 26.58 & 6.645 \\ -2.330 & -6.99 & -20.28 & -39.87 & -32.88 & 6.99 & 42.20 & 39.87 & 13.29 \\ -1.165 & -4.66 & -12.47 & -26.58 & -27.40 & 4.66 & 34.39 & 26.58 & 6.645 \\ 0.0 & -1.165 & -2.330 & -6.645 & -10.96 & 1.165 & 13.29 & 6.645 & 0.0 \end{bmatrix}$$

We provide decimal expression of Q^7 because of its complicated expression. (We are willing to provide its exact values upon request.) Finally, we have

$$Q^8(\xi,\eta) = \sum_{j=0}^{8}\sum_{k=-1}^{3} c^8_{jk} e^{-\sqrt{-1}j\xi} e^{-\sqrt{-1}k\eta} \text{ with}$$

$$(c^8_{jk})_{\substack{0\le j\le 8\\ -1\le k\le 3}} = -\frac{\sqrt{1886}}{14336}\begin{bmatrix} 0 & 1 & 2 & 1 & 0 \\ 1 & 4 & 6 & 4 & 1 \\ 2 & 6 & 8 & 6 & 2 \\ 1 & 4 & 6 & 4 & 1 \\ 0 & 0 & 0 & 0 & 0 \\ -1 & -4 & -6 & -4 & -1 \\ -2 & -6 & -8 & -6 & -2 \\ -1 & -4 & -6 & -4 & -1 \\ 0 & -1 & -2 & -1 & 0 \end{bmatrix}.$$

These coefficient matrices are high-pass filters associated with low-pass filter P_{2211}. Then our box spline tight wavelet framelets $\psi^1_{2211}, \cdots, \psi^8_{2211}$ on 4-direction mesh are defined as follows :

$$\psi^1_{2211}(x,y) = 4\sum_{j=-4}^{4}\sum_{k=-3}^{3} c^1_{j,k}\phi^1_{2211}(2x-j, 2y-k),$$

$$\psi^2_{2211}(x,y) = 4\sum_{j=-2}^{4}\sum_{k=-3}^{3} c^2_{j,k}\phi^2_{2211}(2x-j, 2y-k),$$

$$\psi^3_{2211}(x,y) = 4\sum_{j=-4}^{4}\sum_{k=-3}^{5} c^3_{j,k}\phi^3_{2211}(2x-j,2y-k),$$

$$\psi^4_{2211}(x,y) = 4\sum_{j=-2}^{4}\sum_{k=-3}^{5} c^4_{j,k}\phi^4_{2211}(2x-j,2y-k),$$

$$\psi^5_{2211}(x,y) = 4\sum_{j=0}^{8}\sum_{k=-1}^{7} c^5_{j,k}\phi^5_{2211}(2x-j,2y-k),$$

$$\psi^6_{2211}(x,y) = 4\sum_{j=0}^{8}\sum_{k=-1}^{7} c^6_{j,k}\phi^6_{2211}(2x-j,2y-k).$$

$$\psi^7_{2211}(x,y) = 4\sum_{j=0}^{4}\sum_{k=-1}^{7} c^7_{j,k}\phi^7_{2211}(2x-j,2y-k),$$

$$\psi^8_{2211}(x,y) = 4\sum_{j=0}^{8}\sum_{k=-1}^{3} c^8_{j,k}\phi^8_{2211}(2x-j,2y-k).$$

We note that we have 15 tight wavelet frame generators by using method in [CH2] . □

Example 3.5.6 *For box spline ${}_8\phi$, the Laurent polynomial associated with ${}_8\phi$ is*

$$\begin{aligned} {}_8P(\xi,\eta) = &\left(\frac{1+e^{i\xi}}{2}\right)\left(\frac{1+e^{i\eta}}{2}\right)\left(\frac{1+e^{i(\xi+\eta)}}{2}\right)\left(\frac{1+e^{i(\xi-\eta)}}{2}\right) \\ &\left(\frac{1+e^{i(\xi+2\eta)}}{2}\right)\left(\frac{1+e^{i(2\xi+\eta)}}{2}\right)\left(\frac{1+e^{i(\xi-2\eta)}}{2}\right)\left(\frac{1+e^{i(-2\xi+\eta)}}{2}\right),\ i=\sqrt{-1}. \end{aligned} \tag{3.29}$$

Then we have

$$1 - \sum_{\nu\in\{0,\pi\}^2} |{}_8P(\omega+\nu)|^2 = \sum_{j=1}^{10} |\widetilde{P}_j(2\omega)|^2, \ \textit{where } \omega = (\xi,\eta)$$

where

$$\widetilde{P}_1(\xi,\eta) = 0.002884417323 - 0.1269618424\, e^{i(\xi+4\eta)} + 0.002884417323\, e^{2i\xi} + 0.1211930077\, e^{i\xi},$$

$$\widetilde{P}_2(\xi,\eta) = 0.1903794360 - 0.001923584528\, e^{i(4\xi+\eta)} + 0.1903794360\, e^{2i\eta} - 0.3788352874\, e^{i(\xi+\eta)},$$

$$\widetilde{P}_3(\xi,\eta) = 0.005208333333 - 0.2812500000\, e^{i(2\xi+3\eta)} + 0.005208333333\, e^{4i\xi}$$

$$+ 0.2456597222\, e^{2i(\xi+\eta)} + 0.02517361111\, e^{2i\xi},$$

$$\widetilde{P}_4(\xi,\eta) = 0.1220598471 - 0.01200102887\, e^{i(3\xi+2\eta)} + 0.1220598471\, e^{4i\eta} - 0.2321186655\, e^{2i\eta},$$

$$\widetilde{P}_5(\xi,\eta) = 0.04878904686 - 0.09757809372\, e^{i(\xi+3\eta)} + 0.04878904686\, e^{2i\xi},$$

$$\widetilde{P}_6(\xi,\eta) = 0.01811679804 - 0.2627805518\, e^{i(3\xi+\eta)} 0.01811679804\, e^{2i\eta} + 0.2265469557\, e^{i(\xi+\eta)},$$

$$\widetilde{P}_7(\xi,\eta) = 0.1467758481 - 0.1546921950\, e^{i(\xi+2\eta)} + 0.1467758481\, e^{2i\xi}$$

$$- 0.06942975059\, e^{2i(\xi+\eta)} - 0.06942975059\, e^{2i\eta},$$

$$\widetilde{P}_8(\xi,\eta) = 0.06141408852 - 0.3697047155\, e^{2i(\xi+\eta)} 0.06141408852\, e^{2i\eta} + 0.2468765383\, e^{i(\xi+\eta)},$$

$$\widetilde{P}_9(\xi,\eta) = 0.00119995051 - 0.1017294555\, e^{3i(\xi+\eta)} - 0.00119995051\, e^{3i\xi} + 0.1017294555\, e^{3i\eta},$$

$$\widetilde{P}_{10}(\xi,\eta) = 0.02270259867 - 0.02270259867\, e^{3i\xi}.$$

Hence, we will have 14 tight wavelet frame generators using the constructive steps (3.25)-(3.28). These 14 tight frames ψ^ℓ *in terms of Fourier transform can be expressed by*

$$\widehat{{}_8\psi^\ell}(\xi,\eta) = Q^\ell(\xi/2,\eta/2)\ \widehat{{}_8\phi}(\xi/2,\eta/2),\ \ \ell = 1,\cdots,14.$$

where $Q^\ell(\xi,\eta) = \sum_j \sum_k c^\ell_{jk} e^{-\sqrt{-1}j\xi} e^{-\sqrt{-1}k\eta}$. *We do not show* c^ℓ_{jk}*'s for each* $\ell = 1,\cdots,14$ *because of limited space in this dissertation. Each tight wavelet frame generator is the following form*

$${}_8\psi^\ell(\xi,\eta) = 4\sum_j \sum_k c^\ell_{jk}\ {}_8\phi(2\xi,2\eta),\ \ \ell = 1,\cdots,14.$$

We note that if we use the Kronecker product method in [CH2], we have 2^8-1 *tight wavelet framelets.* $\square$

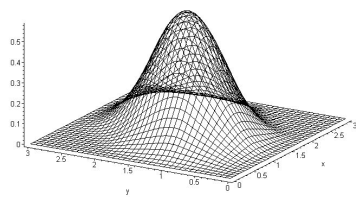

Box Spline ϕ_{221}

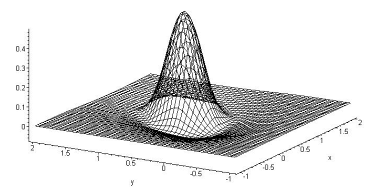

Box Spline Framelet ψ^1_{221}

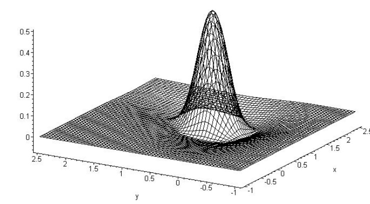

Box Spline Framelet ψ^2_{221}

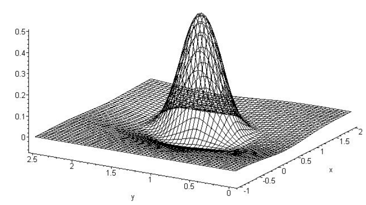

Box Spline Framelet ψ^3_{221}

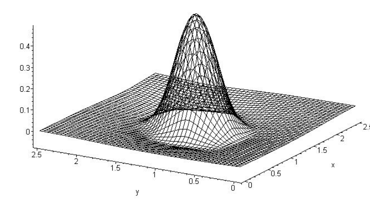

Box Spline Framelet ψ^4_{221}

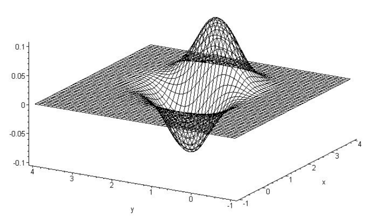

Box Spline Framelet ψ^5_{221}

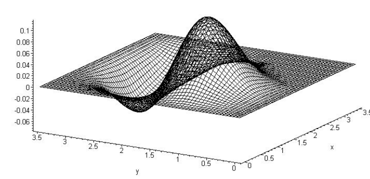

Box Spline Framelet ψ^6_{221}

Figure 3.4: Box Spline $\phi_2 21$ and its Tight Framelets

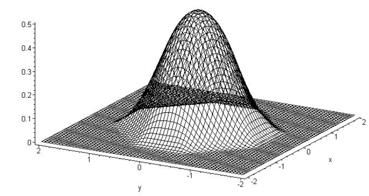

Box Spline ϕ_{1111} ϕ_{1111}

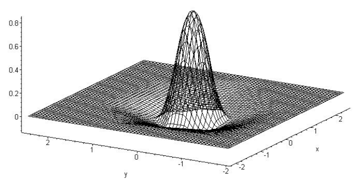

Box Spline Framelet ψ^1_{1111}

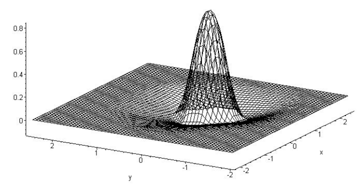

Box Spline Framelet ψ^2_{1111}

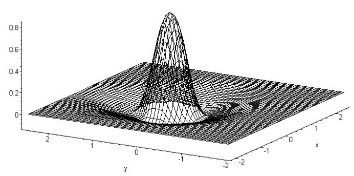

Box Spline Framelet ψ^3_{1111}

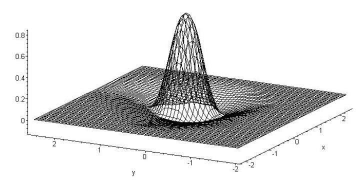

Box Spline Framelet ψ^4_{1111}

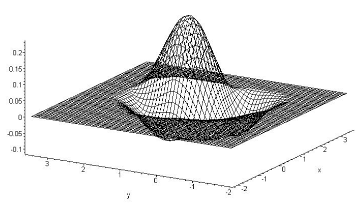

Box Spline Framelet ψ^5_{1111}

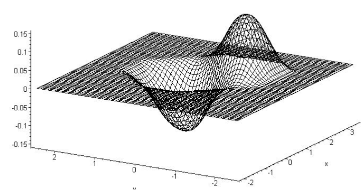

Box Spline Framelet ψ^6_{1111}

Figure 3.5: Box Spline ϕ_{1111} and its Tight Framelets

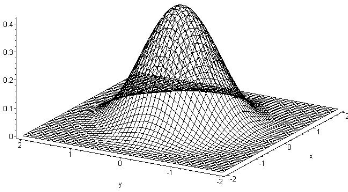

Box Spline ϕ_{2211}

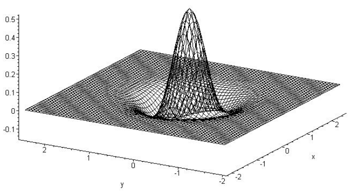

Box Spline Framelet ψ^1_{2211}

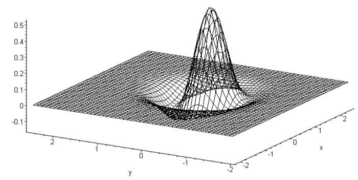

Box Spline Framelet ψ^2_{2211}

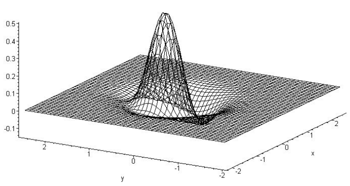

Box Spline Framelet ψ^3_{2211}

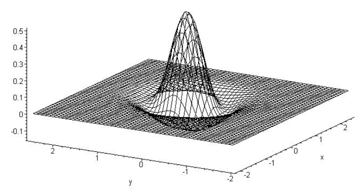

Box Spline Framelet ψ^4_{2211}

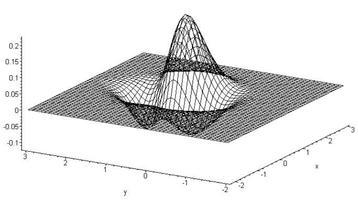

Box Spline Framelet ψ^5_{2211}

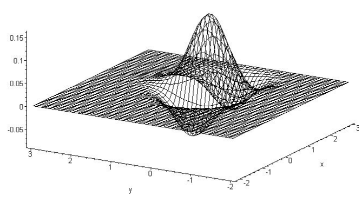

Box Spline Framelet ψ^6_{2211}

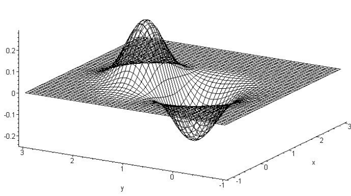

Box Spline Framelet ψ^7_{2211}

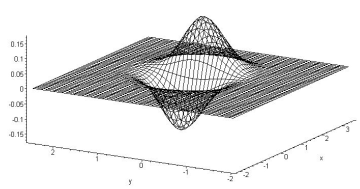

Box Spline Framelet ψ^8_{2211}

Figure 3.6: Box Spline ϕ_{2211} and its Tight Framelets

Chapter 4

Image Processing

Wavelet Transforms have played an important role in analyzing digital images. Wavelet methods have some advantages for edge detection and de-noising (or noise removing) compared to other traditional methods. This is because wavelets decomposition separates the high frequency (detail) parts from the low frequency (smooth) parts of images effectively. All the edges and noise are related to the high frequency parts of images. Usually the high frequency (detail) parts of images consists of a lot of small values. Thus ignoring many of the small numbers by thresholding does not effect much for the visual quality of images. In this aspect, wavelet methods can be used for data compression. For example, the biorthogonal 9/7 wavelet is famous for its application in FBI finger print compression. In this chapter we report numerical experiments for edge detection and denosing using non-separable(non tensor product structure) box spline tight wavelet frames constructed in the previous chapter. For comparison, we also include edge detection and de-noising by tensor products of Haar, Daubechies, biorthgonal 9/7 wavelets and six different edge detection methods from MATLAB Image Processing Toolbox. Numerical evidence provided by edge detection and de-noising on several images shows that box spline tight wavelet frames have definite advantages for image processing.

Before we go further into the numerical experiments, we briefly describe the algorithm of tight wavelet frame decomposition and reconstruction for images in the following section.

4.1 Tight Wavelet Frame Decompositions and Reconstructions

Suppose we have the multivariate tight wavelet frame $\Lambda(\Psi) := \{\psi^1, \cdots, \psi^N\}$ based on MRA generated by a refinable function ϕ. For $f \in L^2(\mathbb{R}^d)$, let $c_{j,\mathbf{k}}$ be the inner product of f with the refinable function $\phi_{j,\mathbf{k}}(\cdot) := 2^{\frac{j}{2}}\phi(2^j \cdot -\mathbf{k})$ and let $d^\ell_{j,\mathbf{k}}$ be the inner product of f with wavelet frames $\psi^\ell_{j,\mathbf{k}}(\cdot) := \psi^\ell(2^j \cdot -\mathbf{k})$'s, i.e., for all $j \in \mathbb{Z}, \mathbf{k} \in \mathbb{Z}^d$ and $\ell = 1, \cdots, N$,

$$c_{j,\mathbf{k}} = \langle f, \phi_{j,\mathbf{k}}(\cdot)\rangle \quad \text{and} \quad d^\ell_{j,\mathbf{k}} = \langle f, \psi^\ell_{j,\mathbf{k}}(\cdot)\rangle.$$

For all $j \in \mathbb{Z}, \mathbf{m} \in \mathbb{Z}^d$ and $\ell = 1, \cdots, N$, we have

$$\phi_{j,\mathbf{m}}(\cdot) = 2^{-d/2}\sum_{\mathbf{k}\in\mathbb{Z}^d} p_{\mathbf{k}-2\mathbf{m}}\phi_{j+1,\mathbf{k}}(\cdot) \quad \text{and} \quad \psi^\ell_{j,\mathbf{m}}(\cdot) = 2^{-d/2}\sum_{\mathbf{k}\in\mathbb{Z}^d} q^\ell_{\mathbf{k}-2\mathbf{m}}\phi_{j+1,\mathbf{k}}(\cdot),$$

by (2.1) and (2.4). Then we have the following tight wavelet frame decomposition algorithm by taking the inner products on both sides of the above two equations.

$$c_{j,\mathbf{m}} = 2^{-d/2}\sum_{\mathbf{k}\in\mathbb{Z}^d} p_{\mathbf{k}-2\mathbf{m}}c_{j+1,\mathbf{k}} \quad \text{and} \quad d^\ell_{j,\mathbf{m}} = 2^{-d/2}\sum_{\mathbf{k}\in\mathbb{Z}^d} q^\ell_{\mathbf{k}-2\mathbf{m}}c_{j+1,\mathbf{k}}, \tag{4.1}$$

for all $j \in \mathbb{Z}, \mathbf{m} \in \mathbb{Z}^d$ and $\ell = 1, \cdots, N$. We also have

$$\phi_{j+1,\mathbf{m}}(\cdot) = 2^{-d/2}\sum_{\mathbf{k}\in\mathbb{Z}^d}\{p_{\mathbf{m}-2\mathbf{k}}\phi_{j,\mathbf{k}}(\cdot) + \sum_{\ell=1}^N q^\ell_{\mathbf{m}-2\mathbf{k}}\psi^\ell_{j,\mathbf{k}}(\cdot)\}. \tag{4.2}$$

By taking inner products on both sides of the above equation we have the tight wavelet frame reconstruction algorithm

$$c_{j+1,\mathbf{m}} = 2^{-d/2}\sum_{\mathbf{k}\in\mathbb{Z}^d}\{p_{\mathbf{m}-2\mathbf{k}}c_{j,\mathbf{k}} + \sum_{\ell=1}^N q^\ell_{\mathbf{m}-2\mathbf{k}}d^\ell_{j,\mathbf{k}}\}. \tag{4.3}$$

See more detail derivation of this algorithm in [CH1] for example. Note that if the refinable function ϕ and tight wavelet frames $\psi^1, \cdots, \psi^N$ are locally supported then $\{p_{\mathbf{k}-2\mathbf{m}}\}$ and $\{q^\ell_{\mathbf{k}-2\mathbf{m}}\}$ are finite sequences for all $\ell = 1, \cdots, N$.

The digital image with a gray level intensity can be considered as a matrix whose each component varies from 0 to 255 and where 0 is black 255 is white. Let $X_j := [x^j_{k_1,x_2}]$ be a sub image of size $I/2^j \times J/2^j$, where I and J are usually some power of 2 and $j \in \mathbb{Z}_+$. We consider X_0 as the original image and X_j as the image at the jth level decomposition. We call each value $x^j_{k_1,x_2}$ a pixel value at each jth level. Let P be the matrix whose components are obtained by the finite sequence $\{p_{k_1,k_2}\}$ satisfying scaling relation of the locally supported refinable function $\phi(x, y)$.

$$\phi(x,y) = \sum_{k_1,k_2} p_{k_1,k_2}\phi(2x - k_1, 2y - k_2).$$

We call the matrix P a low-pass filter which extracts the smooth parts of the image. Similarly, let Q^ℓ be the high-pass filter for $\ell = 1, \cdots, N$ which contains the detail parts of the image. Each component of the matrix Q^ℓ is from the scaling relation of the tight wavelet frame ψ^ℓ such that

$$\psi^\ell(x,y) = \sum_{k_1,k_2} d^\ell_{k_1,k_2}\phi(2x - k_1, 2y - k_2), \quad \ell = 1, \cdots, N.$$

Then the image decomposition is that the the matrix convolution of each P and Q^ℓ with the matrix X_j and deleting all the even number of rows and columns. We call the procedure deleting even number of rows and columns down sampling. Let X_{j+1} be the down sampled matrix after we take convolution of P with X_j. and Y^ℓ_{j+1} be the down sampled matrix after the convolution of Q^ℓ with X_j. Then the size of matrices $X_{j+1}, Y^1_{j+1}, \cdots$, and Y^N_{j+1} is half of the size of the matrix X_j for each $j \in \mathbb{Z}$. We call X_{j+1} a low-pass sub-image and the Y^ℓ_{j+1}'s high-pass sub-images . The low-pass sub-image has low-pass(smooth) parts of the image and the high-pass sub-images have high frequency(detail) parts of the image. We summarize and illustrate this in the Figure 4.1. We can repeat the decomposition process several times by convoluting low-pass filter P and high-pass filters Q^ℓ's with the low-pass sub-image X_{j+1}. The reconstruction process is the reverse process of decomposition. We insert zero rows and columns to the even number of rows and columns of matrices $X_{j+1}, Y^1_{j+1}, \cdots$, and Y^N_{j+1} before we take convolutions of P and Q^ℓ's to the matrices $X_{j+1}, Y^1_{j+1}, \cdots$, and Y^N_{j+1} respectively.

$$
\begin{array}{ccccccccccccc}
 & & *P & \longrightarrow & 2\downarrow & \longrightarrow & X_{j+1} & \longrightarrow & 2\uparrow & \longrightarrow & P* & & \\
 & \nearrow & & & & & & & & & & \searrow & \\
X_j & \longrightarrow & *Q^1 & \longrightarrow & 2\downarrow & \longrightarrow & Y^1_{j+1} & \longrightarrow & 2\uparrow & \longrightarrow & Q^1* & \longrightarrow & \oplus X_j \\
 & \searrow & \vdots & & \vdots & & \vdots & & \vdots & & \vdots & \nearrow & \\
 & & *Q^N & \longrightarrow & 2\downarrow & \longrightarrow & Y^N_{j+1} & \longrightarrow & 2\uparrow & \longrightarrow & Q^N* & &
\end{array}
$$

Tight wavelet frame decomposition $\Leftarrow$ | $\Rightarrow$ Tight wavelet frame reconstruction

Figure 4.1: Tight Wavelet Frame Reconstruction and Decomposition ; $2\downarrow$ is the symbol of deleting odd number of rows and columns from the matrix. $2\uparrow$ is the symbol of adding 0's to the odd number of rows and columns in the matrix. $\oplus$ is the symbol of adding all matrices

4.2 Numerical Experiments : Edge Detection

The wavelet method for edge detection can be described as follows. We first use a wavelet or wavelet frame to decompose an image into one low-pass sub image and several high-pass sub images and then reconstruct the image without the low-pass component. Like we mentioned at the beginning of this chapter, since the abrupt changes and detail parts of the images are located in high-pass components, the reconstructed image without low-pass component shows edges with noise. This is the noise contained in the original image. We need to remove this noise after we reconstruct the image to have clear edges. We normalize the reconstructed image into the standard grey level between 0 to 255 and use one threshold to divide the pixel values into two major groups. That is, if a pixel value is bigger than the threshold, it is set to be 255. If a pixel value is less than the threshold, it is set to be zero. Finally we remove any isolated pixel values.

We use the tight wavelet frames based on the box spline ϕ_{2211} in Example 3.5.5 for edge detection in the following experiments. Many other box spline tight wavelet frames have similar effectiveness. The box spline ϕ_{2211} is defined on 4-direction vectors $\{e_1, e_1, e_2, e_2, e_3, e_4\}$. It has one lowpass filter and 8 highpass filters.

To compare the visual effectiveness of edge detection, we also use wavelet method edge detection by using tensor products of Haar wavelet, Daubechies wavelet, and biorthogonal 9/7 wavelet. In addition, we use commercial edge detection methods from MATLAB Image processing toolbox. There are six different edge detection methods in this toolbox, namely Sobel, Prewitt, Roberts, Laplacian, Zero-crossing and Canny methods. The basic idea of these edge detection methods is that edges can be defined as the pixel where the color intensity changes rapidly, thus one uses the difference operators to approximate the intensity changes. The gradient operator and Laplacian operator are the most commonly used operators. The first three methods detect edges by using gradient operators. Laplacian and Zero-crossing methods detect edges by looking at zero-crossing numbers of the Laplacian operator after smoothing noise by a Gaussian operator. The Canny method is based on several ideas to improve current methods of edge detection. It is known that the Canny method is the optimal method for the step edges of the image corrupted by white noise. The first step is to smooth the image by a Gaussian operator. Next one calculates the gradient to find the regions with high spatial derivatives. Then suppresses any pixel that is not at the maximum in these region. By using two thresholds either remove or make more edges.

The experiments consist of nine different images. The results are shown in Figures. For each image, we use 3 standard wavelets, one box spline tight wavelet frame, and edge detection methods from the MATLAB Image Processing Toolbox. For box spline tight wavelet frame, we only do one level of decomposition. For other standard wavelets (Haar, Daubechies, biorthogonal 9/7 wavelets), we do 1, 2, 3 levels of decomposition dependent on the images. For some images, e.g. the finger image, we must do 3 levels of decomposition while for many other images, two levels of decomposition are enough. We choose the best edge representation among three levels of decompositions to present here. Tensor products of Haar, Daubechies , and biorthogonal 9/7 wavelets have three high-pass filters each of which detect edges of horizontal, vertical, and diagonal direction respectively. Thus they have already had a disadvantage of detecting curvy edges. Among the images, box spline tight wavelet frame detects edge more effectively in all images. Especially, it detects edge better than the MATLAB commercial edge detection methods in many images.

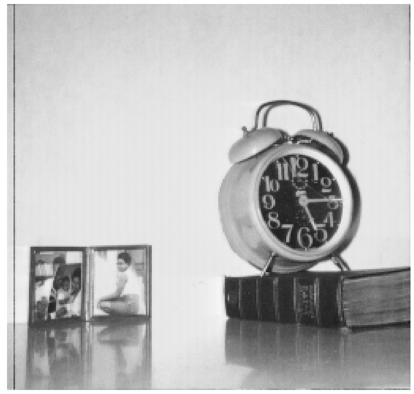

Clock

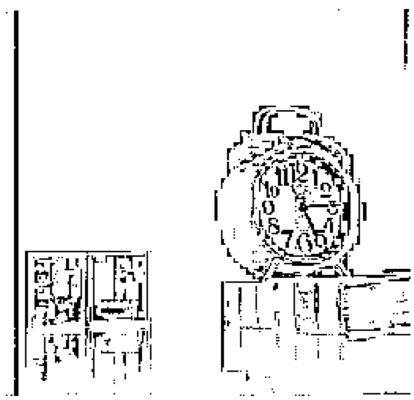

Haar Wavelet

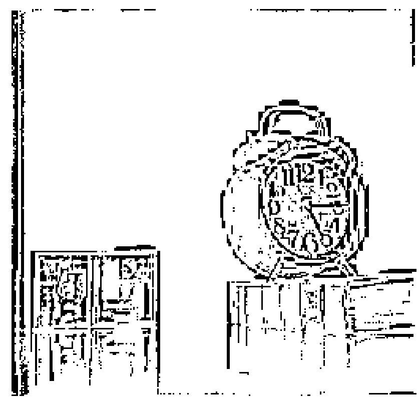

Daubechies Length 6

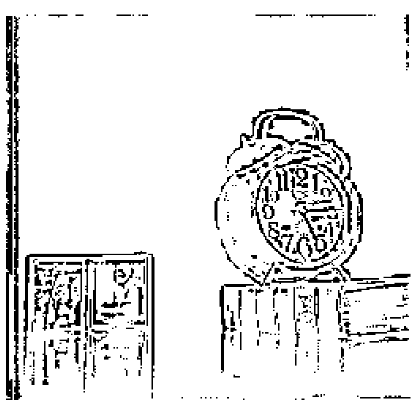

Biorthogonal Wavelet

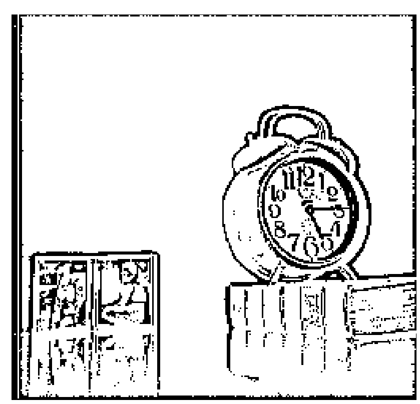

Tight Wavelet Frame

Figure 4.2: Edge detections for Image Clock by wavelets and a tight wavelet frame

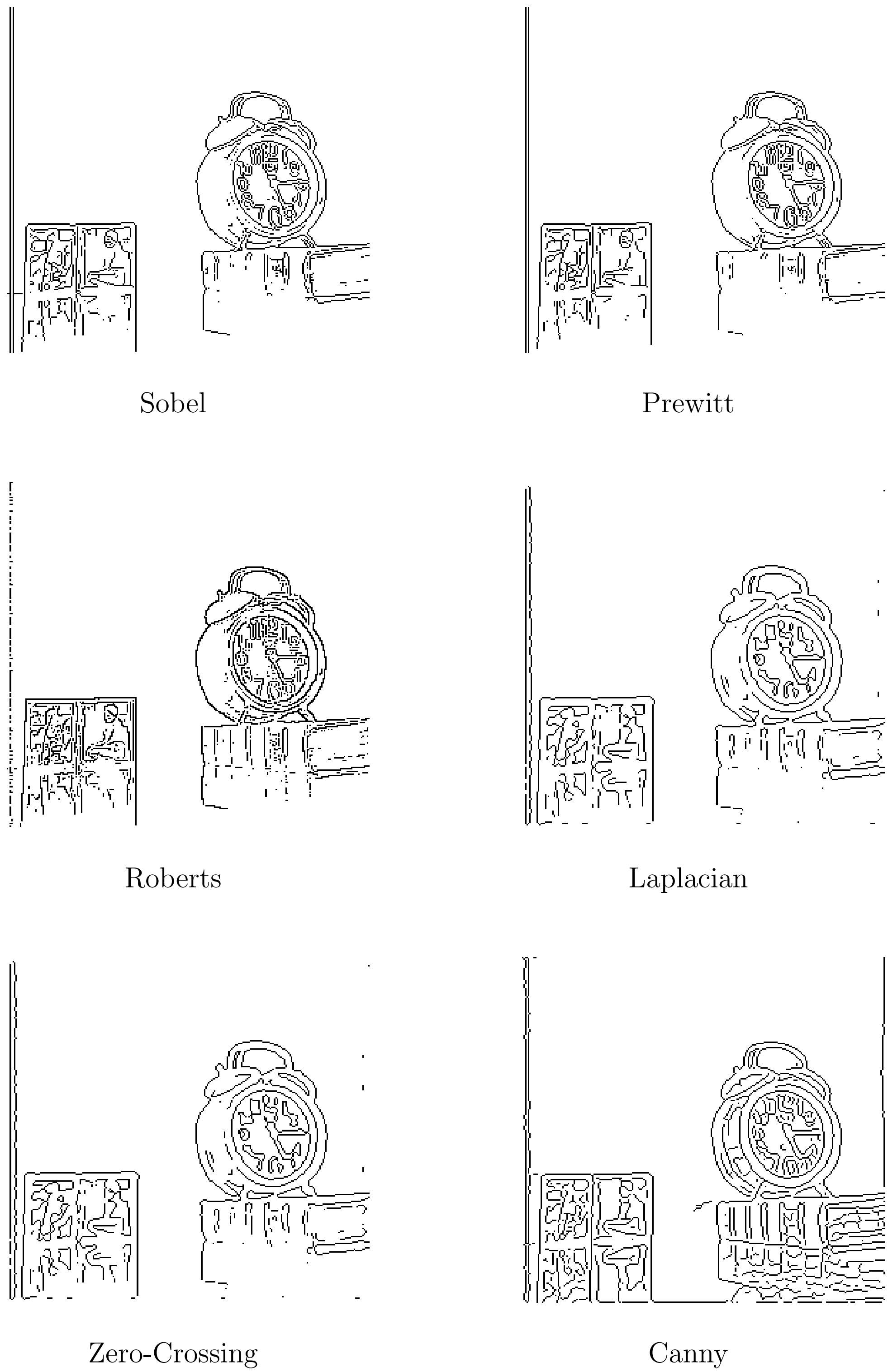

Figure 4.3: Edge detections for Image Clock by the methods from MATLAB Image processing toolbox

F16

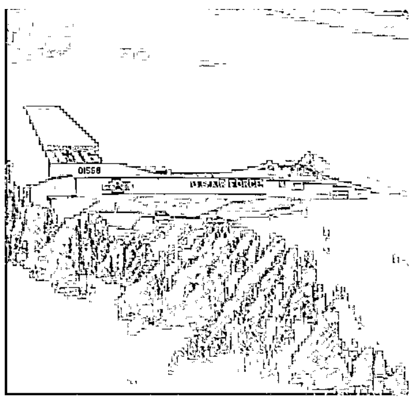

Haar Wavelet

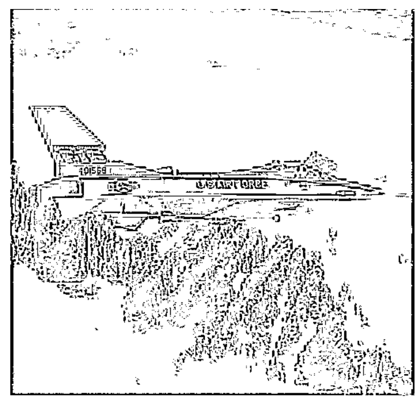

Daubechies Length 6

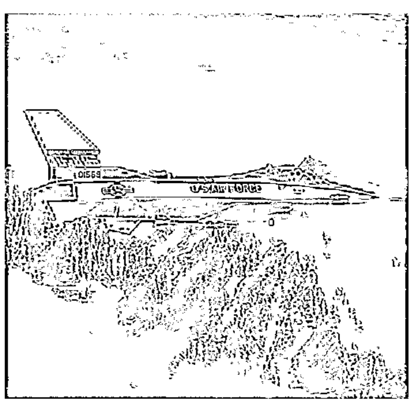

Biorthogonal Wavelet

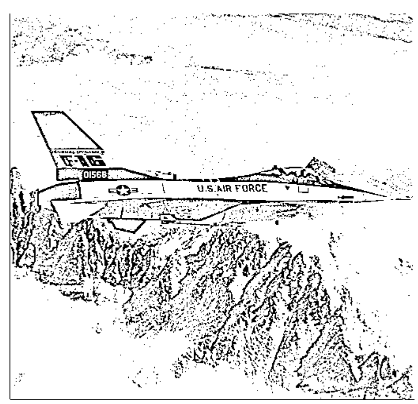

Tight Wavelet Frame

Figure 4.4: Edge detections for Image F16 by wavelets and a tight wavelet frame

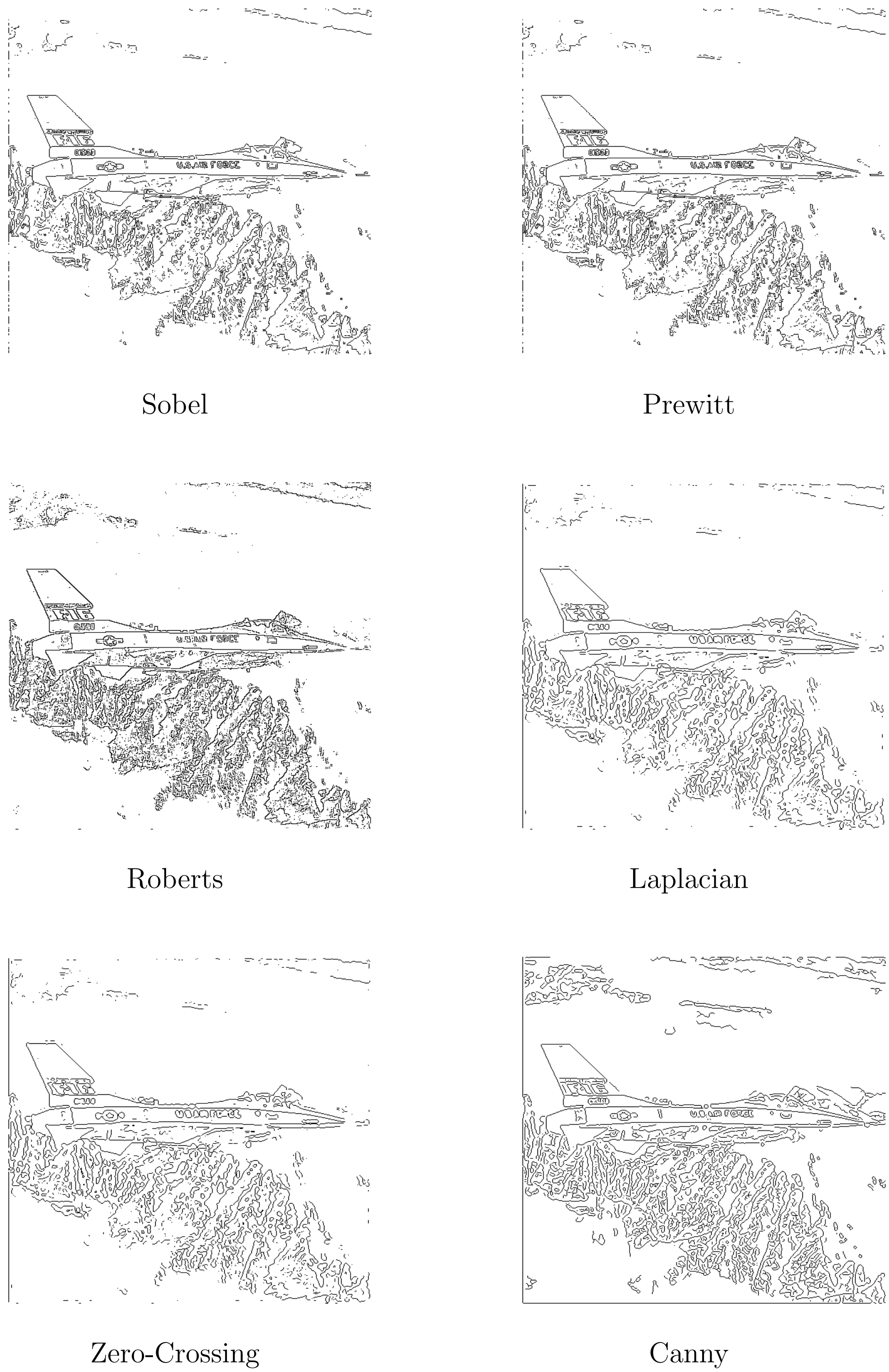

Figure 4.5: Edge detections for Image F16 by the methods from MATLAB Image processing toolbox

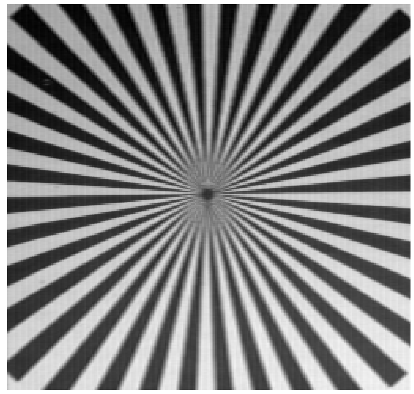

Partition

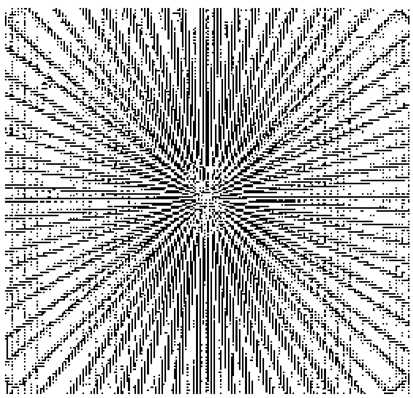

Haar Wavelet

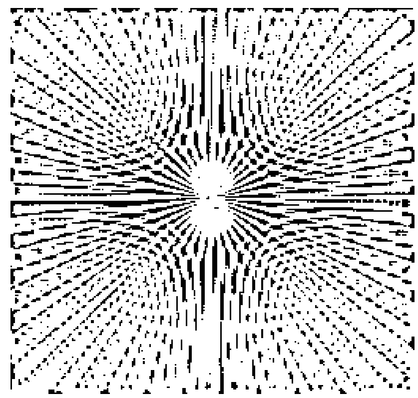

Daubechies Length 6

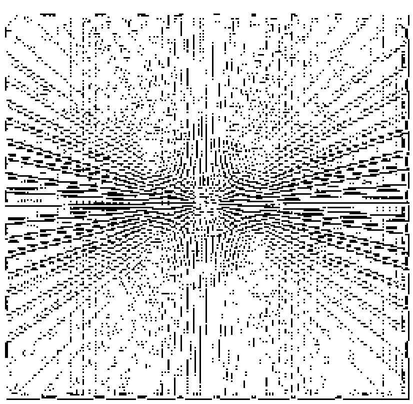

Biorthogonal Wavelet

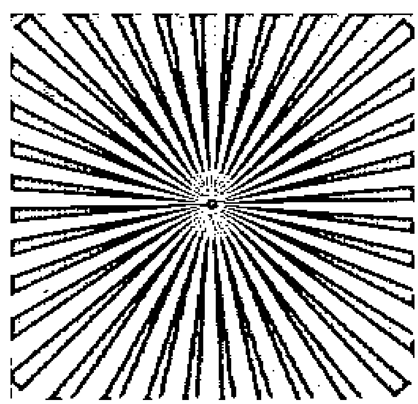

Tight Wavelet Frame

Figure 4.6: Edge detections for Image Partition by wavelets and a tight wavelet frame

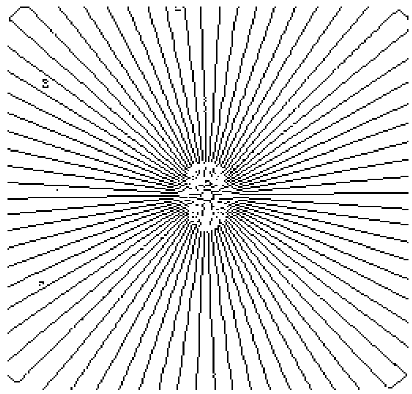

Sobel

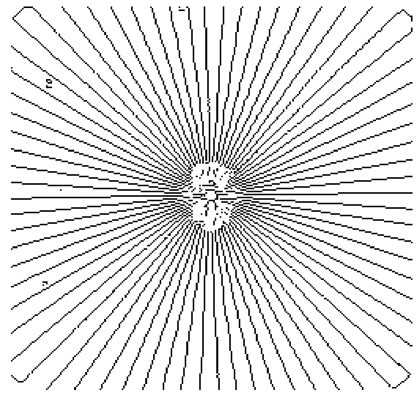

Prewitt

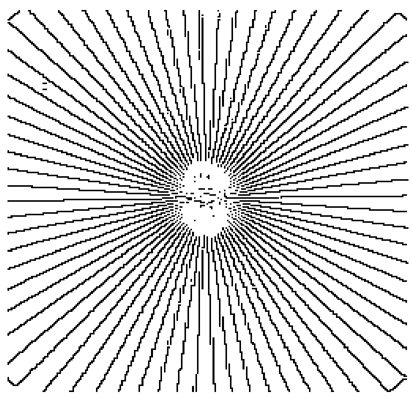

Roberts

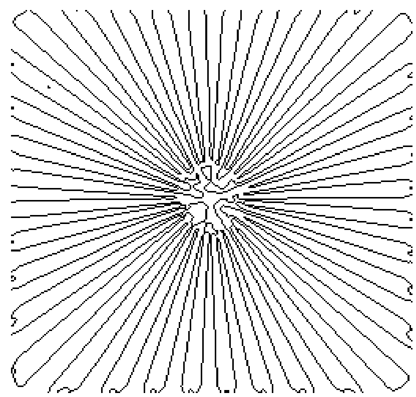

Laplacian

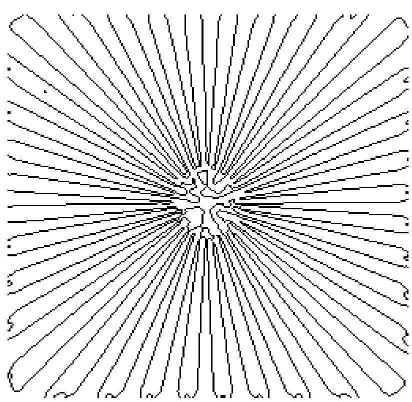

Zero-Crossing

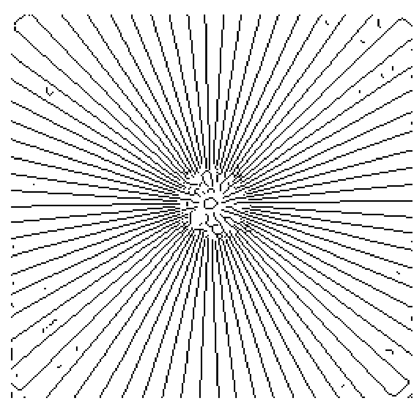

Canny

Figure 4.7: Edge detections for Image Partition by the methods from MATLAB Image processing toolbox

Bank

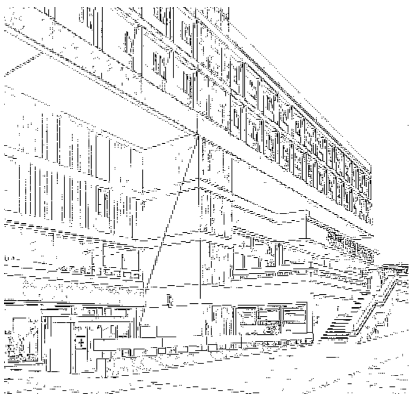

Haar Wavelet

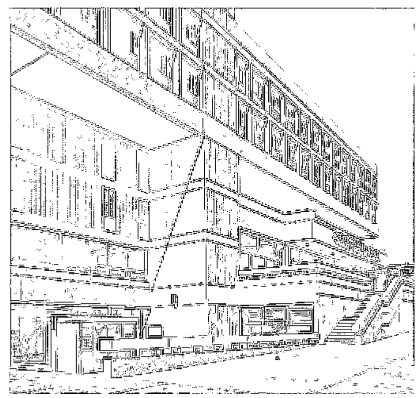

Daubechies Length 6

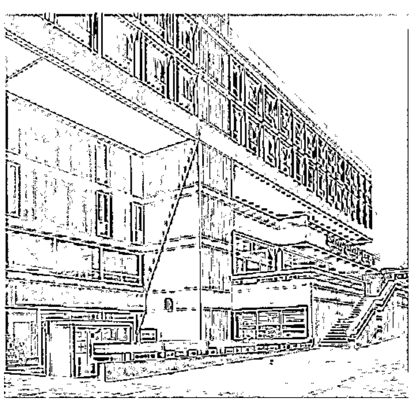

Biorthogonal Wavelet

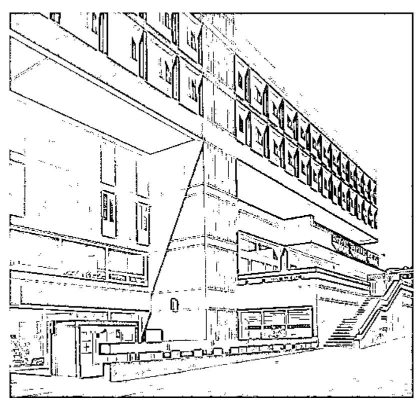

Tight Wavelet Frame

Figure 4.8: Edge detections for Image Bank by wavelets and a tight wavelet frame

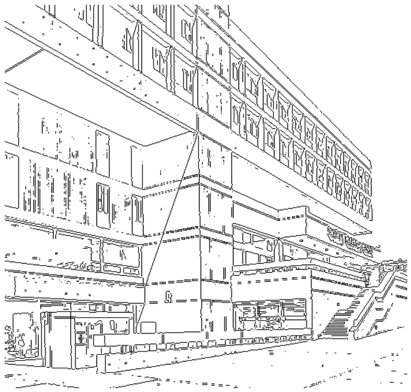

Sobel

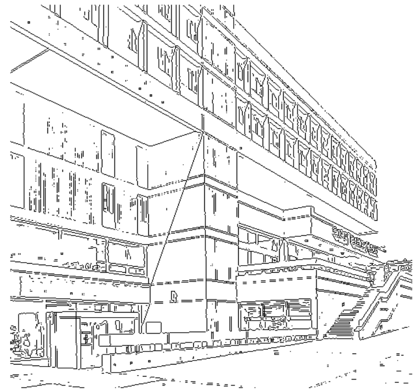

Prewitt

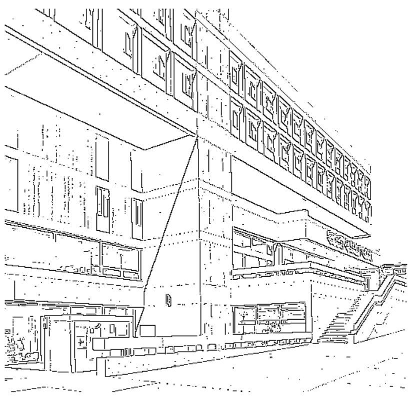

Roberts

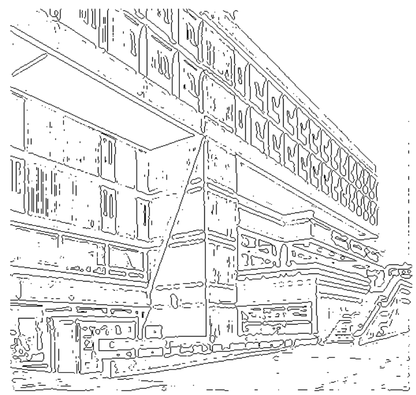

Laplacian

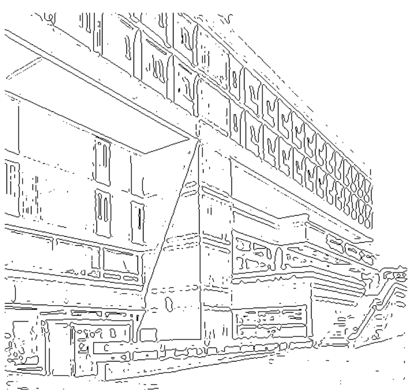

Zero-Crossing

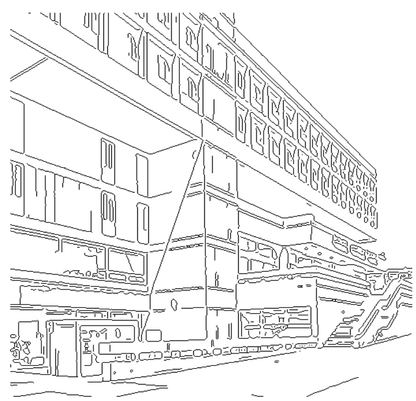

Canny

Figure 4.9: Edge detections for Image Bank by the methods from MATLAB Image processing toolbox

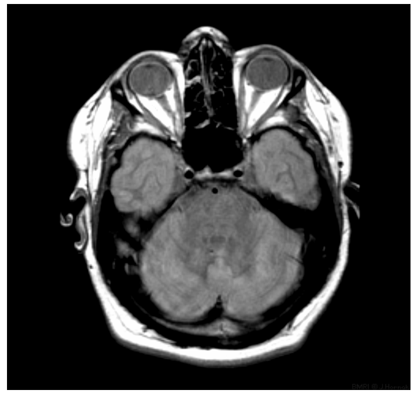

Brain MRI

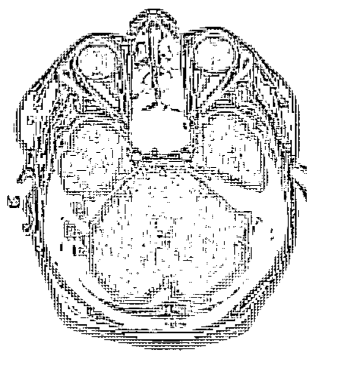

Haar Wavelet

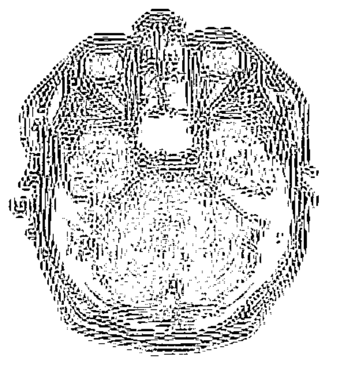

Daubechies Length 6

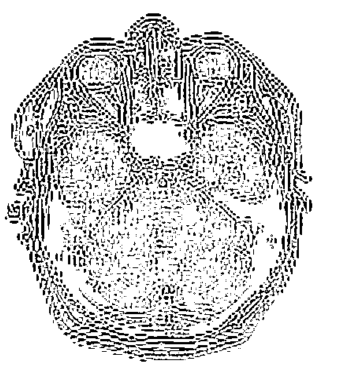

Biorthogonal Wavelet

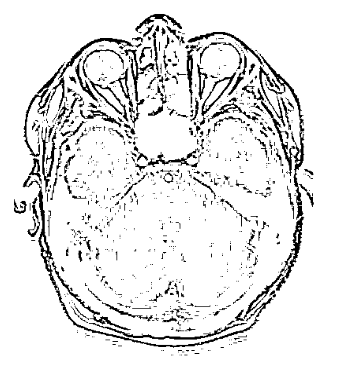

Tight Wavelet Frame

Figure 4.10: Edge detections for Image Brain MRI by wavelets and a tight wavelet frame

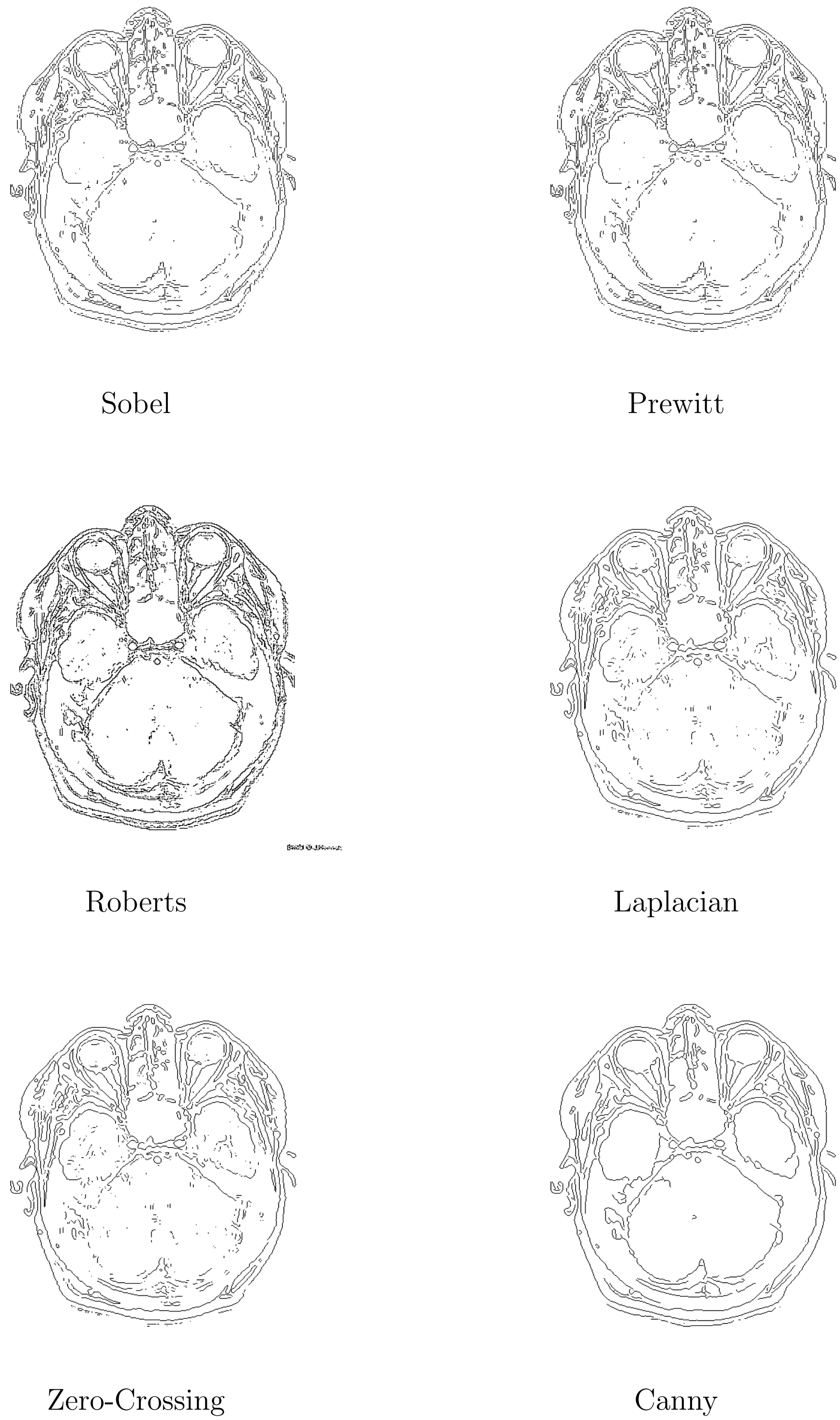

Figure 4.11: Edge detections for Image Brain MRI by the methods from MATLAB Image processing toolbox

Head MRI

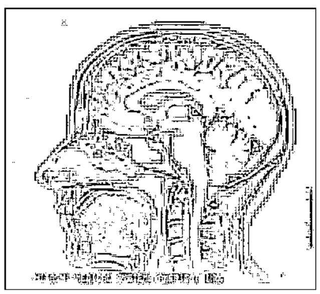

Haar Wavelet

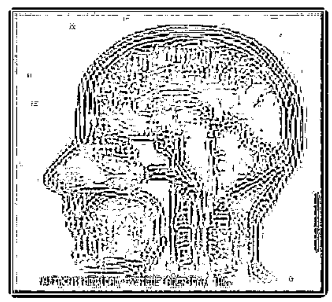

Daubechies Length 6

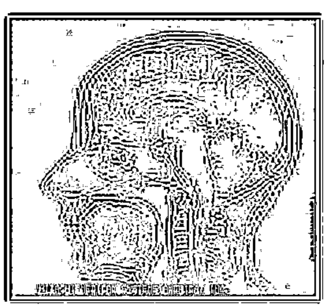

Biorthogonal Wavelet

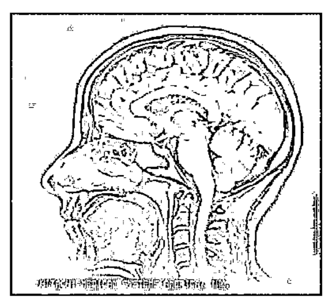

Tight Wavelet Frame

Figure 4.12: Edge detections for Image Head MRI by wavelets and a tight wavelet frame

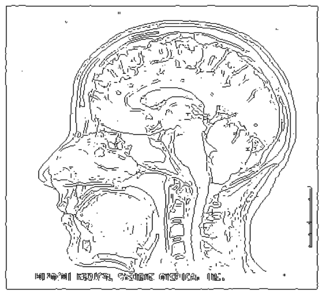

Sobel

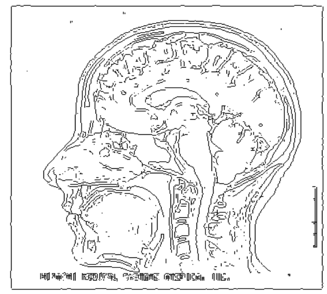

Prewitt

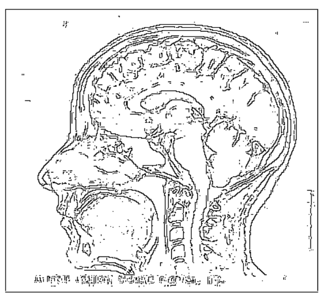

Roberts

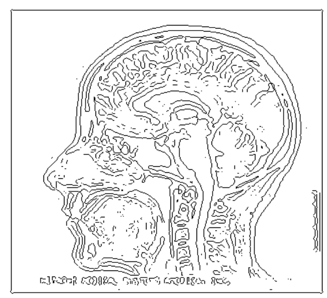

Laplacian

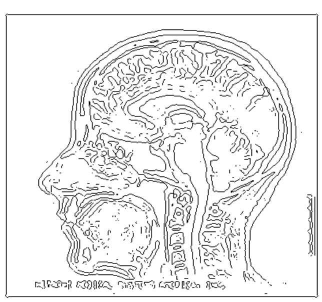

Zero-Crossing

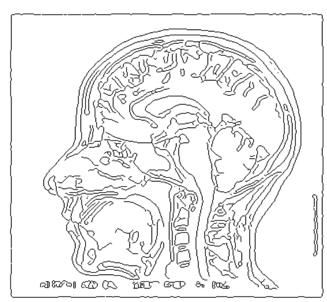

Canny

Figure 4.13: Edge detections for Image Head MRI by the methods from MATLAB Image processing toolbox

Finger Print

Haar Wavelet

Daubechies Length 6

Biorthogonal Wavelet

Tight Wavelet Frame

Figure 4.14: Edge detections for Image Finger Print by wavelets and a tight wavelet frame

Sobel

Prewitt

Roberts

Laplacian

Zero-Crossing

Canny

Figure 4.15: Edge detections for Image Finger Print by the methods from MATLAB Image processing toolbox

Lena

Haar Wavelet

Daubechies Length 6

Biorthogonal Wavelet

Tight Wavelet Frame

Figure 4.16: Edge detections for Image Lena by wavelets and a tight wavelet frame

Sobel

Prewitt

Roberts

Laplacian

Zero-Crossing

Canny

Figure 4.17: Edge detections for Image Lena by the methods from MATLAB Image processing toolbox

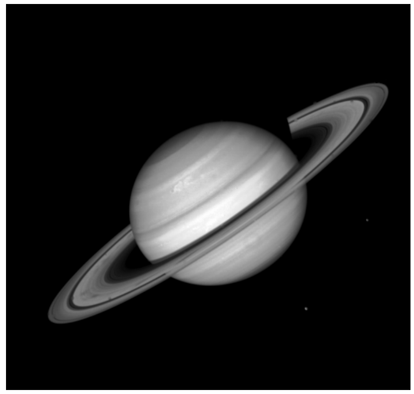

Saturn

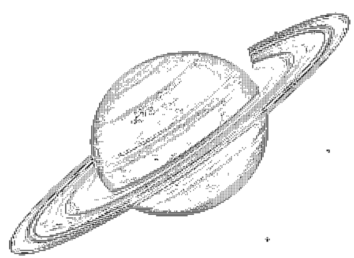

Haar Wavelet

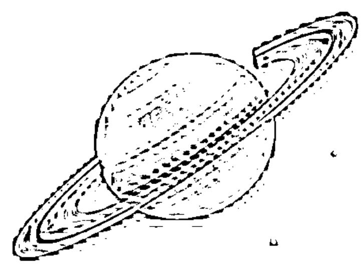

Daubechies Length 6

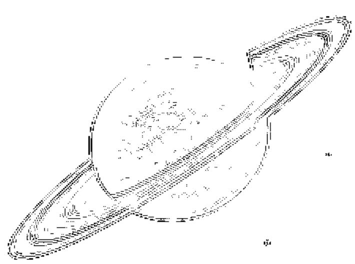

Biorthogonal Wavelet

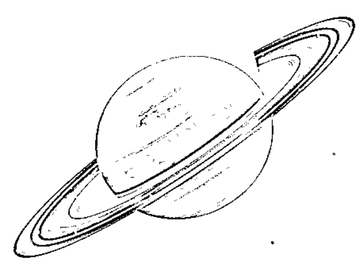

Tight Wavelet Frame

Figure 4.18: Edge detections for Image Saturn by wavelets and a tight wavelet frame

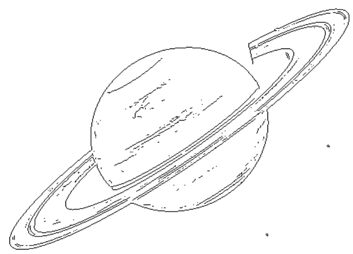

Sobel

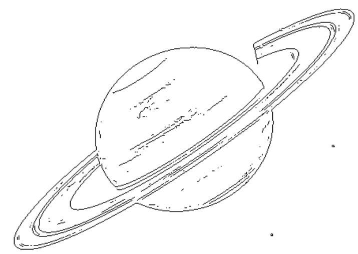

Prewitt

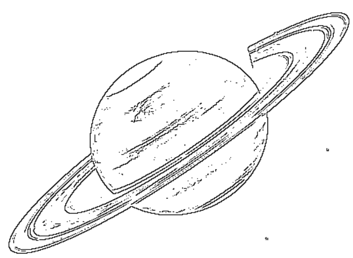

Roberts

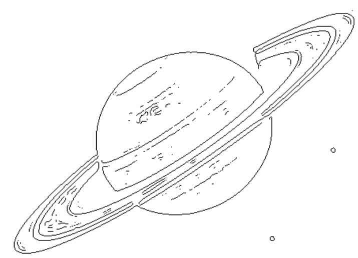

Laplacian

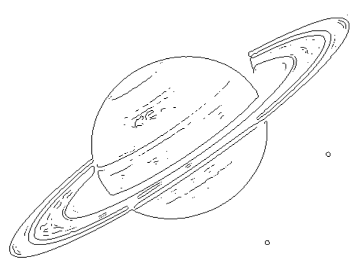

Zero-Crossing

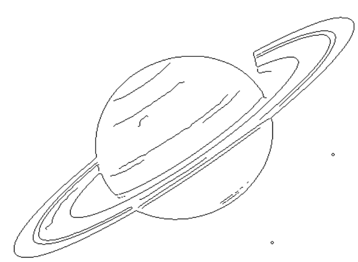

Canny

Figure 4.19: Edge detections for Image Saturn by the methods from MATLAB Image processing toolbox

4.3 Numerical Experiments : De-noising

In our numerical experiment, to make noisy image we first add a white noise to the pixel values $x_{i,j}$ of the image. The white noise has a Gaussian distribution $\delta_{i,j}$ with mean zero and variance σ. Then the pixel values $y_{i,j}$ of noisy image can be presented following

$$y_{i,j} = x_{i,j} + \sigma\delta_{i,j}$$

with $\delta_{i,j} \sim N(0,1)$ where σ is chosen from values $5, 10, 15$ and 20. We then decompose the image into a low-pass part and several high-pass parts of the image by using wavelets or tight wavelet frames.

Next, we apply the soft-thresholding to each high-pass part of the image. Finally, we reconstruct the image after we use noise softening. In 1993, Donoho in [Do] proved theoretically the superiority of using wavelet for image de-noising. He showed that the soft-thresholding provide smoothness and better edge preservation for image de-noising. The soft-thresholding method is to set each pixel value $z_{i,j}$ of image to a new pixel value $z'_{i,j}$ according to the following.

$$z'_{i,j} = \begin{cases} 0 & \text{if } |z_{i,j}| \le \epsilon \\ \text{sign}(z_{i,j})\ (|z_{i,j}| - \epsilon) & \text{if } |z_{i,j}| > \epsilon \end{cases} \tag{4.4}$$

where ϵ is a thresholding value. The main idea of the soft-thresholding method is to reduce the high frequency contents which has the noise of the image by ϵ value.

To measure the quality of the reconstructed image after noise is removed, we use peak signal to noise ratio (PSNR). PSNR in decibels(dB) is computed by the following formula. For given an image $x_{i,j}$ of N by N pixels and a reconstructed image $x'_{i,j}$, where $0 \le x_{i,j} \le 255$,

$$\text{PSNR} = 10\log_{10}\frac{255N^2}{\sum_{i,j=1}^{N}(x'_{i,j} - x_{i,j})^2}$$

The PSNR value itself is not meaningful but the relative comparison among the values from the reconstructed images using different methods gives a quality measurement. Informally, 0.5 dB PSNR improvement is considered to be visible.

We use the box spline ϕ_{1111} constructed in Example 3.5.4 for image de-noising. The other box spline tight wavelet frames that we constructed give similar results. Comparing wavelets for de-noising, tight wavelet frames give better results in the set of pictures we tested.

Since the most of the noise appears in the high-pass parts of the first level of decomposition, we consider only the first level of decomposition. In this case, for each given image and fixed noise we are able to find the optimal threshold values of soft-thresholding for the sub-images decomposed by Haar, Daubechies, or biorthogonal 9/7 wavelets and box spline tight frame ϕ_{1111}.

We present four tables of PSNR values according to different σ values. Each table contains PSNR values of noisy images called Bank, Brain MRI, F-16, Finger, Head MRI, Lena, and Saturn and their denosied images reconstructed by tensor products of Haar, Daubechies, biorthogonal 9/7 wavelets and box spline ϕ_{1111} tight wavelet frame. We also show a set of figures of noisy Clock image and its de-noised images by a Haar wavelet, a biorthogonal wavelet and the tight wavelet frame associated with box spline ϕ_{1111}.

Image	Noise(dB)	Haar	Daubechies	Biorthogonal	Tight wavelet frame
Bank	34.27	36.12	36.06	36.06	35.97
Brain MRI	35.80	37.77	38.52	40.19	39.07
F-16	34.16	36.09	36.45	36.49	36.50
Finger	34.16	35.30	36.20	36.39	35.32
Head MRI	35.29	37.89	38.47	38.78	38.45
Lena	34.16	36.06	36.55	36.63	36.67
Saturn	36.33	40.00	41.40	31.40	43.14

The PSNR comparison with σ =5

Image	Noise(dB)	Haar	Daubechies	Biorthogonal	Tight wavelet frame
Bank	28.31	31.16	31.15	31.16	31.32
Brain MRI	29.81	32.70	33.7	35.15	34.98
F-16	28.16	31.20	31.69	31.76	32.05
Finger	28.16	30.72	32.01	32.27	31.47
Head MRI	29.31	32.91	33.56	33.84	34.17
Lena	28.15	31.43	32.07	32.18	32.78
Saturn	30.33	35.02	35.92	36.01	39.31

The PSNR comparison with σ =10

Image	Noise(dB)	Haar	Daubechies	Biorthogonal	Tight wavelet frame
Bank	24.64	28.26	28.32	28.33	28.80
Brain MRI	26.32	29.85	30.90	31.96	32.85
F-16	24.66	28.35	28.89	28.96	29.74
Finger	24.69	28.34	29.45	29.62	29.93
Head MRI	25.82	30.03	30.56	30.77	31.84
Lena	24.63	28.75	29.33	29.41	30.82
Saturn	26.82	32.03	32.62	32.66	37.16

The PSNR comparison with σ =15

Image	Noise(dB)	Haar	Daubechies	Biorthogonal	Tight wavelet frame
Bank	22.38	26.20	26.31	26.31	27.18
Brain MRI	23.85	27.88	28.87	29.61	31.47
F-16	22.24	26.32	26.87	26.90	28.23
Finger	22.25	26.62	27.43	27.53	28.93
Head MRI	23.36	27.96	28.35	28.50	30.15
Lena	22.14	26.80	27.27	27.34	29.55
Saturn	24.35	29.82	30.22	30.22	35.54

The PSNR comparison with σ =20

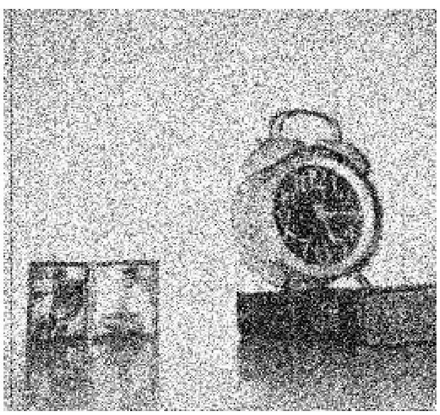

Noisy image-Clock, PSNR=14.84(dB)

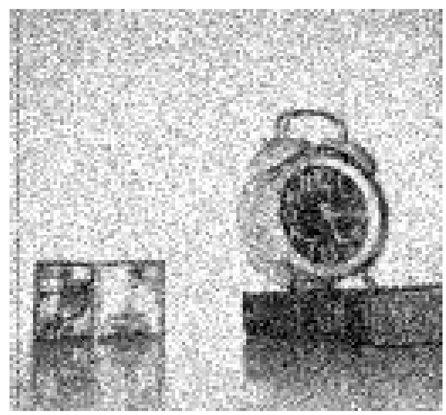

Haar wavelet, PSNR=19.28(dB)

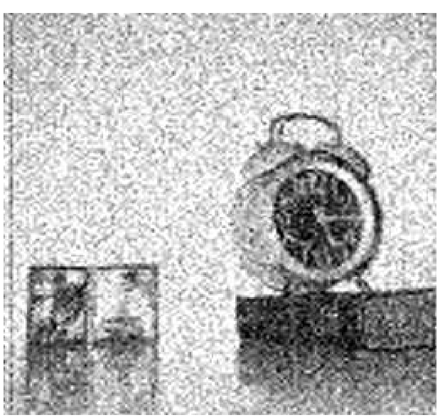

Biorthogonal wavelet, PSNR=19.46(dB)

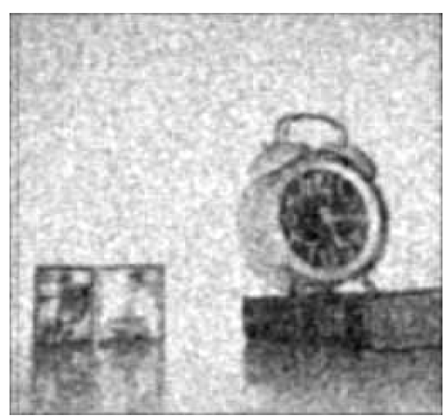

Tight wavelet frame, PSNR=22.85(dB)

Chapter 5

Tight Wavelet Frames over Bounded Domain

5.1 Construction Idea

The tight wavelet frame construction in this paper is based on a half infinite sequence of nested subspaces over a bounded domain Ω in L^2. That is, a sequence of nested subspaces $\{V_k\}_{k\in\mathbb{Z}_+}$ in $L^2(\Omega)$ satisfies

$$V_1 \subset V_2 \subset \cdots \subset V_k \subset \cdots \to L^2(\Omega)$$
$$and \ \overline{\bigcup_{k=1} V_k} = L^2(\Omega).$$

Let $\Phi_k := (\phi_{k,1}, \cdots, \phi_{k,m_k})^T$ be a column vector of locally supported functions in V_k which generate V_k, i.e., $V_k = \mathrm{span}\{\phi_{k,1}, \cdots, \phi_{k,m_k}\}$. Though this sequence of subspaces $\{V_k\}_{k\in\mathbb{Z}_+}$ does not have both translation and dilation invariant properties, we say $\{\Phi_k\}_{k\in\mathbb{Z}_+}$ generates a multiresolution analysis(MRA) over bounded domains.

We work with the vector Φ_k in $V_k \subset L^2(\Omega)$. Because V_k is a subspacce of V_{k+1}, there exists a matrix of size $m_k \times m_{k+1}$ $(m_k \le m_{k+1})$, namely P_k, such that

$$\Phi_k = P_k \Phi_{k+1}. \tag{5.1}$$

We call the matrix P_k a refinement matrix.

We want to find a matrix Q_k of size $n_k \times m_{k+1}$ satisfying

$$\Psi_k := Q_k \Phi_{k+1}. \tag{5.2}$$

Let each component of the vector Ψ_k be $\psi_{k,1}, \cdots, \psi_{k,n_k}$. Based on the above notation, we give the definition of a tight wavelet frame over bounded domains.

Definition 5.1.1 *We say the family of vectors* $\{\Psi_k\}_{k\in\mathbb{Z}_+}$ *defined in (5.2) is* **a (MRA) tight wavelet frame** *associated with* $\{\Phi_k\}_{k\in\mathbb{Z}_+}$ *in* $L^2(\Omega)$ *if*

$$\|f\|^2 = \sum_{j=1}^{m_\ell} |\langle f, \phi_{\ell,j}\rangle|^2 + \sum_{k=\ell}^{\infty}\sum_{j=1}^{n_k} |\langle f, \psi_{k,j}\rangle|^2, \qquad \forall f \in L^2(\Omega),$$

for each component $\phi_{k,1}, \cdots, \phi_{k,m_k}$ *of the column vector* Φ_k *and* $\psi_{k,1}, \cdots, \psi_{k,n_k}$ *of* Ψ_k*. We call each function* $\psi_{k,j}$ *for* $j = 1, \cdots, n_k$ *and* $k \in \mathbb{Z}_+$ **a tight framelet** *(or a tight wavelet frame generator).*

For any $f \in L^2(\Omega)$, let $c_{k,i} := \langle f, \phi_{k,i}\rangle$ for all $i = 1, \cdots, m_k$ and $C_k := (c_{k,1}, \cdots, c_{k,m_k})^T$ be a column vector of size m_k for any $k \in \mathbb{Z}_+$. In this way, let $d_{k,j} := \langle f, \psi_{k,j}\rangle$ for all $j = 1, \cdots, n_k$ and $D_k := (d_{k,1}, \cdots, d_{k,n_k})^T$. Then we know

$$C_k = \langle f, \Phi_k\rangle = \langle f, P_k\Phi_{k+1}\rangle = P_kC_{k+1},$$

$$D_k = \langle f, \Psi_k\rangle = \langle f, Q_k\Phi_{k+1}\rangle = Q_kC_{k+1}.$$

For a given vector of functions Φ_k suppose we can find a vector of functions Ψ_k satisfying

$$< f, \Phi_{k+1} >^T \Phi_{k+1} = < f, \Phi_k >^T \Phi_k + < f, \Psi_k >^T \Psi_k, \qquad \forall f \in L^2(\Omega). \tag{5.3}$$

The condition in (5.3) can be expressed the following form according to our notations,

$$C_{k+1}^T\Phi_{k+1} = C_k^TP_k\Phi_{k+1} + D_k^TQ_k\Phi_{k+1}.$$

Furthermore we have

$$C_{k+1}^TC_{k+1} = C_{k+1}^T(P_k^TP_k + Q_k^TQ_k)C_{k+1}.$$

Thus if we find Q^k for all $k \in \mathbb{Z}_+$ satisfying

$$I_{m_{k+1}} = P_k^TP_k + Q_k^TQ_k, \tag{5.4}$$

then we have

$$C_{k+1}^TC_{k+1} = C_k^TC_k + D_k^TD_k. \tag{5.5}$$

Furthermore by the recursive condition in (5.5), for any $\ell \in \mathbb{Z}_+$,

$$C_{k+1}^TC_{k+1} = C_\ell^TC_\ell + \sum_{j=\ell}^{k} D_j^TD_j$$

and

$$C_{k+1}^T \Phi_{k+1} = C_\ell^T \Phi_\ell + \sum_{j=\ell}^{k} D_j^T \Psi_j.$$

If $C_{k+1}^T \Phi_{k+1}$ converges to f in $L^2(\Omega)$, for any $\ell \in \mathbb{Z}_+$, we have

$$\begin{aligned}
\|f\|^2 =& \langle f, \lim_{k\to+\infty} C_{k+1}^T \Phi_{k+1} \rangle \\
=& \lim_{k\to+\infty} \langle f, C_{k+1}^T \Phi_{k+1} \rangle \\
=& \lim_{k\to+\infty} \langle f, C_\ell^T \Phi_\ell + \sum_{j=\ell}^{k} D_j^T \Psi_j \rangle \\
=& C_\ell^T C_\ell + \sum_{j=\ell}^{\infty} D_j^T D_j \\
=& \sum_{j=1}^{m_\ell} |\langle f, \phi_{\ell,j} \rangle|^2 + \sum_{k=\ell}^{\infty} \sum_{j=1}^{n_k} |\langle f, \psi_{k,j} \rangle|^2
\end{aligned} \tag{5.6}$$

If we apply (5.6) for a fixed f and for all g in $L^2(\Omega)$, then

$$\|f+g\|^2 = \sum_{j=1}^{m_\ell} |\langle f+g, \phi_{\ell,j} \rangle|^2 + \sum_{k=\ell}^{\infty} \sum_{j=1}^{n_k} |\langle f+g, \psi_{k,j} \rangle|^2, \tag{5.7}$$

$$\|f-g\|^2 = \sum_{j=1}^{m_\ell} |\langle f-g, \phi_{\ell,j} \rangle|^2 + \sum_{k=\ell}^{\infty} \sum_{j=1}^{n_k} |\langle f-g, \psi_{k,j} \rangle|^2. \tag{5.8}$$

If we subtract the equation (5.8) from (5.7), we have

$$4\langle f, g \rangle = 4(\langle \sum_{j=1}^{m_\ell} \langle f, \phi_{\ell,j} \rangle \phi_{\ell,j} + \sum_{k=\ell}^{\infty} \sum_{j=1}^{n_k} \langle f, \psi_{k,j} \rangle \psi_{k,j}\ ,\ g \rangle)$$

Thus for all $f \in L^2(\Omega)$ and for all $\ell \in \mathbb{Z}_+$,

$$f = \sum_{j=1}^{m_\ell} \langle f, \phi_{\ell,j} \rangle \phi_{\ell,j} + \sum_{k=\ell}^{\infty} \sum_{j=1}^{n_k} \langle f, \psi_{k,j} \rangle \psi_{k,j}, \quad weakly.$$

Therefore any function in $L^2(\Omega)$ can be analyzed by any level of refinable functions and of tight framelets associated with these refinable functions.

5.2 Construction Method

According to the construction idea from the the previous section, once we have the matrix Q_k associated with the refinement matrix P_k satisfying the condition in (5.4) for all $k \in \mathbb{Z}_+$, we have a tight wavelet frame $\{\Psi_k\}_{k\in\mathbb{Z}_+}$ associated with $\{\Phi_k\}_{k\in\mathbb{Z}_+}$. Thus the condition in (5.4) will be the key identity to construct a tight wavelet frame over bounded domains. We summarize this as follows.

Theorem 5.2.1 *Let $\{V_k\}$ be a MRA generated by a family of functions $\Phi_k = P_k\Phi_{k+1}$, where P_k is a banded matrix for each $k \in \mathbb{Z}_+$. If $I_{m_k} - P_k \cdot P_k^T$ is positive semi-definite for the identity matrix I_{m_k} of size $m_k \times m_k$, then there exists a tight wavelet frame $\{\Psi_k\}_{k\in\mathbb{Z}_+}$ of $L^2(\Omega)$ defined such a way in (5.2). Moreover, if each component function $\phi_{k,j}$ of a vector Φ_k is locally supported then each component function $\psi_{k,j}$ of a vector Ψ_k is locally supported.*

Proof Since the symmetric matrix $I_{m_k} - P_k \cdot P_k^T$ is positive semi-definite, there exists a unique lower triangular matrix L_k such that

$$I_{m_k} = P_k \cdot P_k^T + L_k \cdot L_k^T. \tag{5.9}$$

Using this lower triangular matrix L_k we let

$$R_k = I_{m_{k+1}+m_k} - \begin{bmatrix} {P_k}^T \\ L_k^T \end{bmatrix} \begin{bmatrix} P_k & L_k \end{bmatrix}. \tag{5.10}$$

Note that the matrix R_k is symmetric and $R_k^T R_k = R_k$. Writing $R_k = \begin{bmatrix} \widetilde{Q}_k & W_c \end{bmatrix}$ with matrix $\widetilde{Q}_k$ of size $(m_{k+1} + m_k) \times m_{k+1}$ and W_c being the term who cares, we observe

$$\widetilde{Q}_k^T \widetilde{Q}_k = I_{m_{k+1}} - P_k^T P_k.$$

It is clear that the rank of $\widetilde{Q}_k$ is less than or equal to m_{k+1}. Write

$$\widetilde{Q}_k = \begin{bmatrix} J_k \\ \widehat{J}_k \end{bmatrix}$$

with J_k being of size $m_{k+1} \times m_{k+1}$ and $\widehat{J}_k$ of size $m_k \times m_{k+1}$. Then we multiply m_{k+1} Householder transformations $H_{m_k} H_{m_k-1} \cdots H_2 H_1$ of size $(m_k + m_{k+1}) \times (m_k + m_{k+1})$ on the left side of matrix $\widetilde{Q}_k$. That is,

$$H_{m_k} H_{m_k-1} \cdots H_2 H_1 \widetilde{Q}_k = \begin{bmatrix} Q_k \\ 0 \end{bmatrix}, \tag{5.11}$$

where Q_k is a upper triangular matrix of size $m_{k+1} \times m_{k+1}$. Let us denote $U_k := H_{m_k} H_{m_k-1} \cdots H_2 H_1$. Then U_k is a unitary matrix and we have

$$Q_k^T Q_k = (U_k \widetilde{Q}_k)^T (U_k \widetilde{Q}_k) = \widetilde{Q}_k^T \widetilde{Q}_k = I_{m_{k+1}} - P_k^T P_k,$$

The matrix Q_k in (5.11) is the matrix we want to have with full rank m_k. If P_k is a banded matrix, so is $P_k \cdot P_k^T$. It follows that L_k is banded. Thus, it is easy to see from the definition of Q_k that Q_k is banded. Thus, $\psi_{k,j}$ are locally supported for each $k \in \mathbb{Z}_+$ and $j = 1, \cdots, m_{k+1}$.

□

5.3 B-spline Tight Wavelet Frames

In this section, we apply the construction method from the proof in Theorem 5.2.1 to construct tight wavelet frames over a bounded domain associated with B-spline functions defined in equally spaced simple knots. Because of the efficiency and simplicity of computation, B-splines often have been used for constructing wavelet functions.

Let us recall the scaling relation of B-spline ϕ^m for $m \geq 2$ from the Section 3.1.

$$\phi^m(x) = \sum_{j \in \mathbb{Z}} c_j^m \phi^m(2x - j),$$

where

$$c_j^m = \begin{cases} 2^{-m+1} \binom{m}{j} & \text{for } 0 \leq j \leq m \\ 0 & \text{otherwise} \end{cases} \tag{5.12}$$

Consider B-spline function ϕ^m of order m whose dyadic translations are restricted into domain $[0, b]$, i.e., $\phi^m(2^k \cdot -i)|_{[0,b]}$. Let us denote $\phi_{k,j}^m(\cdot)$ be all translations of $2^{k-1}\phi^m(2^{k-1}\cdot)$ restricted over domain $[0, b]$ and

$$V_k^m := \{\phi_{k,j}^m : 1 \leq j \leq m_k\}.$$

Then the family of nested sequence of subspaces $\{V_k^m : k \in Z_+\}$ is a MRA generated by $\{\phi_{k,1}^m, \cdots, \phi_{k,m_k}^m\}$. Thus if we denote

$$\Phi_k^m := (\phi_{k,1}^m, \cdots, \phi_{k,m_k}^m)^T,$$

we can find a refinement matrix P_k^m of size $m_k \times m_{k+1}$ of a vector satisfying $\Phi_k^m = P_k^m \Phi_{k+1}^m$ for each $k \in \mathbb{Z}_+$. First, we check the positive semi-definite property of the matrix $I_{m_k} - P_k^m \cdot P_k^{mT}$ for the identity matrix I_{m_k}.

Lemma 5.3.1 *The symmetric matrix $I_{m_k} - P_k^m \cdot P_k^{mT}$ of size $m_k \times m_k$ for the refinement matrix P_k^m of Φ_k^m is positive semi-definite for each $k \in \mathbb{Z}$ and $m \geq 2$.*

Proof Let us denote $(p_{i,j}^{m,k}) := P_k^m$. Then for each $i = 1, \cdots, m_k$

$$0 \leq \sum_{j=1}^{m_{k+1}} p_{i,j}^{m,k} \leq \frac{1}{2} \sum_{j=0}^{m} c_j^m = 1, \tag{5.13}$$

where c_j^m is in (5.12) . Let us denote $G_k^m := (g_{i,j}^{m,k}) = P_k^m \cdot P_k^{mT}$. To show that matrix $I_{m_k} - G_k^m$ is positive semi-definite, we use diagonal dominance of matrix $I_{m_k} - G_k^m$. Since matrix G_k^m is symmetry, it is sufficient to check $|1 - g_{i,i}^{m,k}| \geq \sum_{i \neq j} | g_{i,j}^{m,k} |$ for $i \leq \lfloor \frac{m_k}{2} \rfloor + 1$. Notice that

$$g_{i,j}^{m,k} = \sum_{\ell=1}^{m_{k+1}} p_{i,\ell}^{m,k} p_{\ell,j}^{m,k}.$$

Then for each $k \in \mathbb{Z}_+$,

$$\begin{aligned} 1 - |g_{i,i}^{m,k}| - \sum_{j \neq i} | g_{i,j}^{m,k} | &= 1 - \sum_{j=1}^{m_{k+1}} \sum_{\ell=1}^{m_{k+1}} p_{i,\ell}^{m,k} p_{j,\ell}^{m,k} \\ &= 1 - \left(\sum_{\ell=1}^{m_{k+1}} p_{i,\ell}^{m,k} \right) \left(\sum_{\ell=1}^{m_{k+1}} p_{j,\ell}^{m,k} \right). \end{aligned}$$

Since (5.13), $1 - |g_{i,i}^{m,k}| \geq \sum_{j \neq i} | g_{i,j}^{m,k} |$ for all $i = 1, \cdots, m_k$. Therefore the symmetry matrix $I_{m_k} - P_k^m \cdot P_k^{mT}$ is positive semi-definite. $\square$

By the above lemma, we know that for the refinement matrix P_k^m of a vector Φ_k^m whose component B-spline functions generate subspace V_k^m in $L^2([0, b])$ is satisfying the sufficient condition in Theorem 5.2.1. That is, we can construct B-spline tight wavelet frame over a bounded domain by using the constructive scheme in the proof of Theorem 5.2.1.

We now follow the construction steps in the proof of Theorem 5.2.1. We find the lower triangular matrix L_k such that $I_{m_k} - P_k^m \cdot P_k^{mT} = L_k \cdot L_k$ by using cholesky factorization. Set

$$R_k = I_{m_{k+1}+m_k} - \begin{bmatrix} P_k^{mT} \\ L_k^T \end{bmatrix} \begin{bmatrix} P_k^m & L_k \end{bmatrix}$$

Let $\widetilde{Q}_k$ be the first left side block matrix of the size $(m_{k+1}+m_k)\times m_{k+1}$ of the matrix R_k. Since $R_k^T R_k = R_k$, we observe that

$$\widetilde{Q}_k^T \widetilde{Q}_k = I_{m_{k+1}} - P_k^{mT} P_k^m.$$

Write

$$\widetilde{Q}_k = \begin{bmatrix} J_k \\ \widehat{J}_k \end{bmatrix}$$

with J_k being of size $m_{k+1}\times m_{k+1}$ and $\widehat{J}_k$ of size $m_k \times m_{k+1}$. We decompose the matrix $\widetilde{Q}_k$ by using QR-decomposition. Then we have the upper triangular matrix of size m_{k+1} on the top and $\mathbf{0}$-block on the bottom such as

$$U_k\widetilde{Q}_k = \begin{bmatrix} Q_k^m \\ \mathbf{0} \end{bmatrix}, \quad \text{for some unitary matrix } U_k.$$

Then

$$Q_k^{mT} Q_k^m = (U_k\widetilde{Q}_k)^T (U_k\widetilde{Q}_k) = \widetilde{Q}_k\widetilde{Q}_k = I_{m_{k+1}} - P_k^{mT} P_k^m,$$

the matrix Q_k^m is the matrix we want to have. Therefore, by setting $\Psi_k^m = Q_k^m \Phi_{k+1}^m$ for $\Phi_{k+1}^m = \{\phi_{k+1,1}^m, \cdots, \phi_{k+1,m_{k+1}}^m\}$, we have the collection of tight framelets $\Psi_k^m = \{\psi_{k,1}^m, \cdots, \psi_{k,m_{k+1}}^m\}$ for $k \in \mathbb{Z}_+$.

In the following examples, we give the explicit form of matrix Q_1^m associated with B-spline tight framelets Ψ_1^m of order $m = 2, 3, 4$ for the given matrix P_1^m associated with Φ_1^m. We can compute P_k^m and Q_k^m for any $k \in \mathbb{Z}_+$ and for arbitrary integer order $m \geq 2$ of B-spline functions.

Example 5.3.1 *For the linear B-spline ϕ^m over the interval $[0,2]$, where $m = 2$, we have the column vectors $\Phi_1^2 = [\ \phi^2(x+1)|_{[0,2]}\ \phi^2(x)|_{[0,2]}\ \phi^2(x-1)|_{[0,2]}\ ]^T := [\phi_{1,1}^2\ \phi_{1,2}^2\ \phi_{1,3}^2]^T$ and $\Phi_2^2 = [\ 2\phi^2(2x+2)|_{[0,2]}\ 2\phi^2(2x+1)|_{[0,2]}\ 2\phi^2(2x)|_{[0,2]}\ 2\phi^2(2x-1)|_{[0,2]}\ 2\phi^2(2x-2)|_{[0,2]}\ ]^T$. Then* *from the relation* $\Phi_1^2 = P_1^2 \cdot \Phi_2^2$*, we have the refinement matrix* P_1^2 *as follows*

$$P_1^2 = \sqrt{2}\begin{bmatrix} \frac{1}{2} & \frac{1}{4} & 0 & 0 & 0 \\ 0 & \frac{1}{4} & \frac{1}{2} & \frac{1}{4} & 0 \\ 0 & 0 & 0 & \frac{1}{4} & \frac{1}{2} \end{bmatrix}.$$

Then the vector of tight wavelet frame generators is $\Psi_1^2 = Q_1^2 \cdot \Phi_2^2 := [\psi_{1,1}^2 \ \psi_{1,2}^2 \ \psi_{1,3}^2 \ \psi_{1,4}^2 \ \psi_{1,5}^2]^T$ *, where*

$$Q_1^2 = \begin{bmatrix} \frac{\sqrt{2}}{2} & -\frac{\sqrt{10}}{4} & 0 & 0 & 0 \\ 0 & \frac{\sqrt{10}}{4} & -\frac{\sqrt{10}}{10} & -\frac{\sqrt{10}}{20} & 0 \\ 0 & 0 & \frac{\sqrt{10}}{5} & -\frac{3\sqrt{10}}{20} & 0 \\ 0 & 0 & 0 & \frac{\sqrt{2}}{2} & -\frac{\sqrt{2}}{4} \\ 0 & 0 & 0 & 0 & \frac{\sqrt{6}}{4} \end{bmatrix}.$$

We illustrate the linear B-spine and its tight wavelet frame generators of the level 1 in the Figure 5.1. □

Example 5.3.2 *For the quadratic B-spline* ϕ^m *over the interval* $[0, 3]$*, where* $m = 3$*, we have the column vectors*

$$\Phi_1^3 = [\ \phi^3(x+2)|_{[0,3]}\ \phi^3(x+1)|_{[0,3]}\ \phi^3(x)|_{[0,3]}\ \phi^3(x-1)|_{[0,3]}\ \phi^3(x-2)|_{[0,3]}\ ]^T := [\phi_{1,1}^3\ \cdots\ \phi_{1,5}^3]^T$$

and $\Phi_2^3 = [\ 2\phi^3(2x+4)|_{[0,3]}\ \cdots\ 2\phi^3(2x-4)|_{[0,3]}\ ]^T$*. Then from the relation* $\Phi_1^3 = P_1^3 \cdot \Phi_2^3$*, we have the refinement matrix* P_1^3 *as follows*

$$P_1^3 = \sqrt{2}\begin{bmatrix} \frac{3}{8} & \frac{1}{8} & 0 & 0 & 0 & 0 & 0 & 0 \\ \frac{1}{8} & \frac{3}{8} & \frac{3}{8} & \frac{1}{8} & 0 & 0 & 0 & 0 \\ 0 & 0 & \frac{1}{8} & \frac{3}{8} & \frac{3}{8} & \frac{1}{8} & 0 & 0 \\ 0 & 0 & 0 & 0 & \frac{1}{8} & \frac{3}{8} & \frac{3}{8} & \frac{1}{8} \\ 0 & 0 & 0 & 0 & 0 & 0 & \frac{1}{8} & \frac{3}{8} \end{bmatrix}.$$

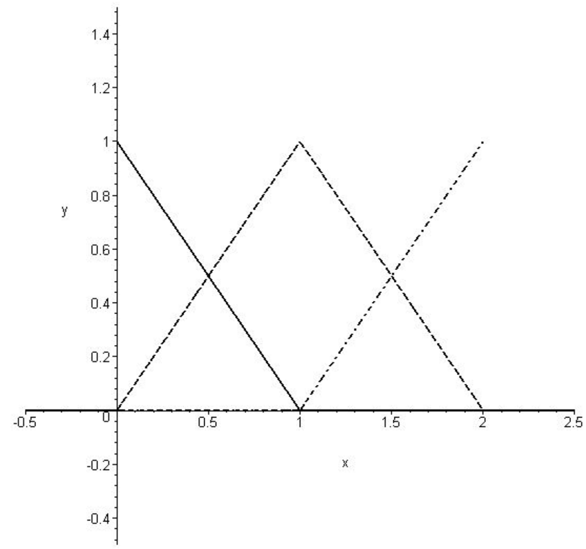

Linear B-spline $\{\phi_{1,1}^2, \phi_{1,2}^2, \phi_{1,3}^2\}$

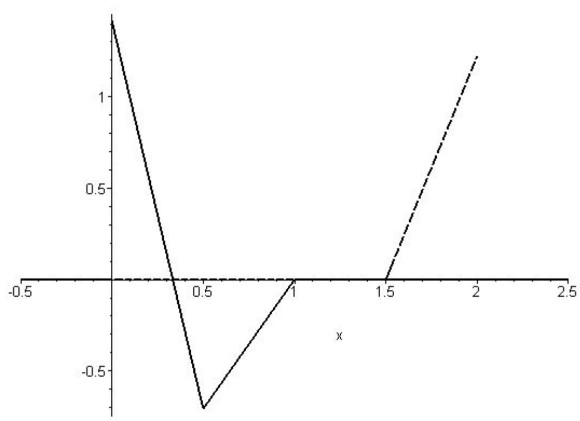

Linear Framelets $\psi_{1,1}^2$ and $\psi_{1,5}^2$

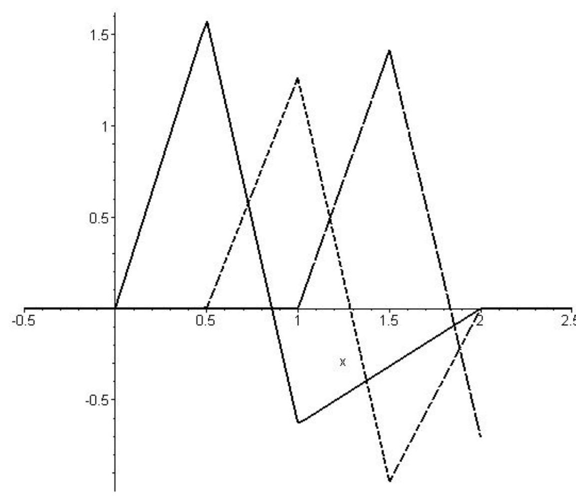

Linear Framelets $\psi_{1,2}^2$, $\psi_{1,3}^2$, $\psi_{1,4}^2$

Figure 5.1: Linear B-splines $\{\phi_{1,1}^2, \phi_{1,2}^2, \phi_{1,3}^2\}$ and its tight framelets $\{\psi_{1,1}^2, \cdots, \psi_{1,5}^2\}$ of the ground level over a bounded domain in Example 5.3.1.

Then the vector of tight wavelet frame generators is $\Psi_1^3 = Q_1^3 \cdot \Phi_2^3 := [\psi_{1,1}^3 \ \cdots \ \psi_{1,8}^3]^T$ *, where*

$$Q_1^3 = \begin{bmatrix} \frac{\sqrt{11}}{4} & -\frac{3\sqrt{11}}{44} & -\frac{3\sqrt{11}}{88} & -\frac{\sqrt{11}}{88} & 0 & 0 & 0 & 0 \\ 0 & \frac{\sqrt{77}}{11} & -\frac{27\sqrt{77}}{616} & -\frac{9\sqrt{77}}{616} & 0 & 0 & 0 & 0 \\ 0 & 0 & \frac{\sqrt{413}}{28} & -\frac{27\sqrt{413}}{1652} & -\frac{3\sqrt{413}}{472} & -\frac{\sqrt{413}}{472} & 0 & 0 \\ 0 & 0 & 0 & \frac{\sqrt{1947}}{59} & -\frac{51\sqrt{1947}}{5192} & -\frac{17\sqrt{1947}}{5192} & 0 & 0 \\ 0 & 0 & 0 & 0 & \frac{\sqrt{935}}{44} & -\frac{9\sqrt{935}}{748} & -\frac{3\sqrt{935}}{680} & -\frac{\sqrt{935}}{680} \\ 0 & 0 & 0 & 0 & 0 & \frac{3\sqrt{17}}{17} & -\frac{15\sqrt{17}}{136} & -\frac{5\sqrt{17}}{136} \\ 0 & 0 & 0 & 0 & 0 & 0 & \frac{\sqrt{185}}{20} & -\frac{21\sqrt{185}}{740} \\ 0 & 0 & 0 & 0 & 0 & 0 & 0 & \frac{\sqrt{703}}{37} \end{bmatrix}.$$

We illustrate the quadratic B-spine and its tight wavelet frame generators of the level 1 in the Figure 5.2. □

Example 5.3.3 *For the cubic B-spline* ϕ^m *over the interval* $[0,4]$*, where* $m = 4$*, we have the column vectors*

$$\Phi_1^4 = [\ \phi^4(x+3)|_{[0,4]} \ \cdots \ \phi^4(x)|_{[0,4]} \ \cdots \ \phi^4(x-3)|_{[0,4]}\ ]^T := [\phi_{1,1}^4 \ \cdots \ \phi_{1,4}^4 \ \cdots \ \phi_{1,7}^4]^T$$

and $\Phi_2^4 = [\ 2\phi^4(2x+5)|_{[0,4]} \ \cdots \ 2\phi^4(2x-5)|_{[0,4]}\ ]^T$*. Then from the relation* $\Phi_1^4 = P_1^4 \cdot \Phi_2^4$*, we have the refinement matrix* P_1^4 *as follows*

$$P_1^4 = \sqrt{2} \begin{bmatrix} \frac{1}{4} & \frac{1}{16} & 0 & 0 & 0 & 0 & 0 & 0 & 0 & 0 & 0 \\ \frac{1}{4} & \frac{3}{8} & \frac{1}{4} & \frac{1}{16} & 0 & 0 & 0 & 0 & 0 & 0 & 0 \\ 0 & \frac{1}{16} & \frac{1}{4} & \frac{3}{8} & \frac{1}{4} & \frac{1}{16} & 0 & 0 & 0 & 0 & 0 \\ 0 & 0 & 0 & \frac{1}{16} & \frac{1}{4} & \frac{3}{8} & \frac{1}{4} & \frac{1}{16} & 0 & 0 & 0 \\ 0 & 0 & 0 & 0 & 0 & \frac{1}{16} & \frac{1}{4} & \frac{3}{8} & \frac{1}{4} & \frac{1}{16} & 0 \\ 0 & 0 & 0 & 0 & 0 & 0 & 0 & \frac{1}{16} & \frac{1}{4} & \frac{3}{8} & \frac{1}{4} \\ 0 & 0 & 0 & 0 & 0 & 0 & 0 & 0 & 0 & \frac{1}{16} & \frac{1}{4} \end{bmatrix}.$$

Then the vector of tight wavelet frame generators is $\Psi_1^4 = Q_1^4 \cdot \Phi_2^4 := [\psi_{1,1}^4 \ \cdots \ \psi_{1,11}^4]^T$ *, where*

$$Q_1^4 = [V_1\,;\, V_2], \qquad \textit{where}$$

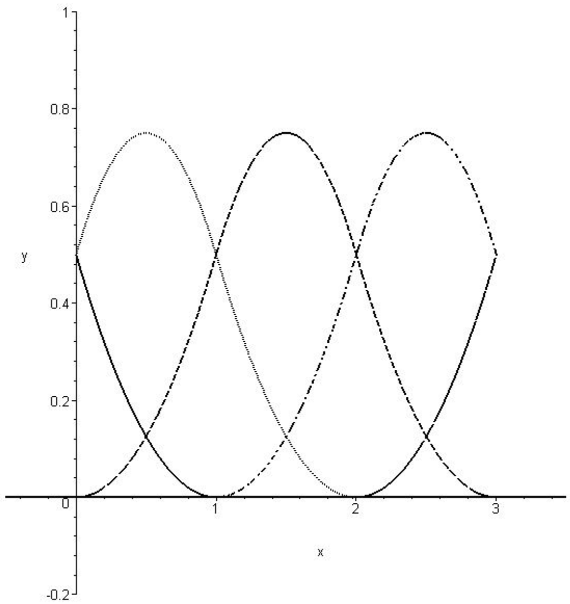

Quadratic B-spline $\{\phi^3_{1,1}, \cdots, \phi^3_{1,5}\}$

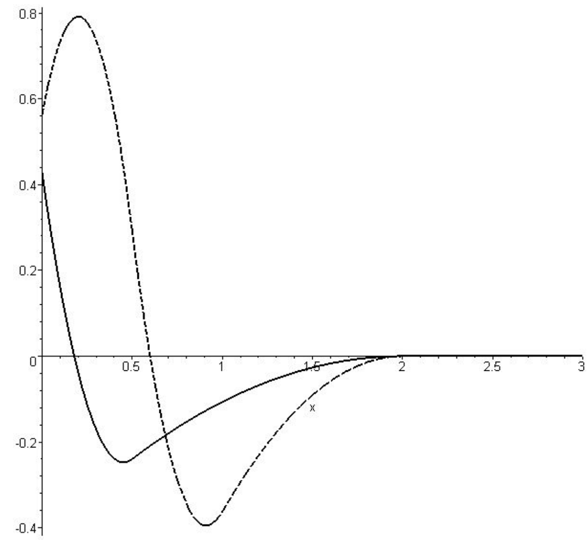

Quadratic Framelets $\psi^3_{1,1}$ and $\psi^3_{1,2}$

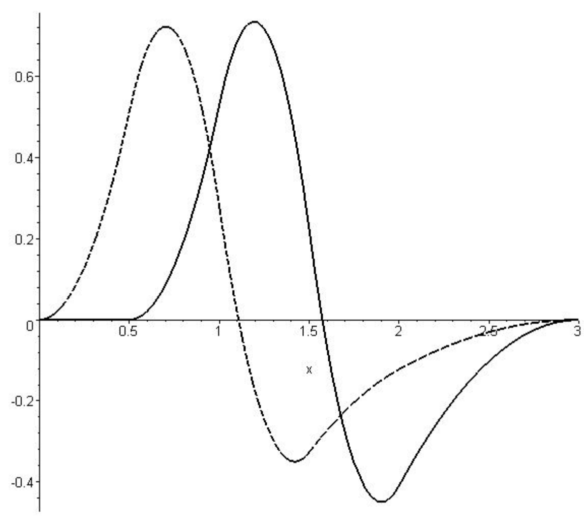

Quadratic Framelets $\psi^3_{1,3}$ and $\psi^3_{1,4}$

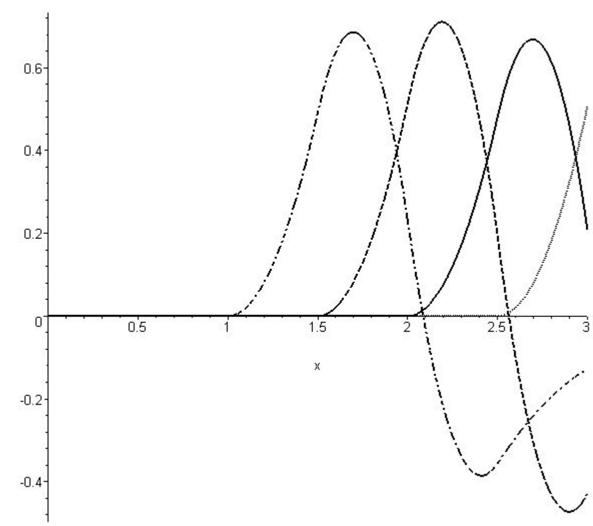

Quadratic Framelets $\psi^3_{1,5}, \psi^3_{1,6}, \psi^3_{1,7}, \psi^3_{1,8}$

Figure 5.2: Quadratic B-splines $\{\phi^3_{1,1}, \cdots, \phi^3_{1,5}\}$ and Quadratic B-spline tight framelets $\{\psi^3_{1,1}, \cdots, \psi^3_{1,8}\}$ of the ground level over a bounded domain in Example 5.3.2.

$$V_1 = \begin{bmatrix} -866.0 & 252.6 & 144.3 & 36.08 & 0.00 \\ 0.0 & -799.6 & -319.2 & 128.6 & 39.08 \\ 0.0 & 0.0 & -792.0 & 334.6 & 173.6 \\ 0.0 & 0.0 & 0.0 & -757.2 & 372.3 \\ 0.0 & 0.0 & 0.0 & 0.0 & -761.4 \\ 0.0 & 0.0 & 0.0 & 0.0 & 0.0 \\ 0.0 & 0.0 & 0.0 & 0.0 & 0.0 \\ 0.0 & 0.0 & 0.0 & 0.0 & 0.0 \\ 0.0 & 0.0 & 0.0 & 0.0 & 0.0 \\ 0.0 & 0.0 & 0.0 & 0.0 & 0.0 \\ 0.0 & 0.0 & 0.0 & 0.0 & 0.0 \end{bmatrix},$$

and

$$V_2 = \begin{bmatrix} 0.008 & 0.00 & 0.00 & 0.00 & 0.00 & 0.00 \\ 9.771 & 0.00 & 0.00 & 0.00 & 0.00 & 0.00 \\ 43.39 & 0.00 & 0.00 & 0.00 & 0.00 & 0.00 \\ 144.7 & 41.27 & 10.32 & 0.00 & 0.00 & 0.00 \\ 368.4 & 184.3 & 46.09 & 0.00 & 0.00 & 0.00 \\ -737.9 & 396.6 & 152.1 & 42.35 & 10.59 & 0.00 \\ 0.0 & -746.4 & 385.9 & 190.0 & 47.50 & 0.00 \\ 0.0 & 0.0 & -727.2 & 410.4 & 156.3 & 42.97 \\ 0.0 & 0.0 & 0.0 & -737.3 & 396.5 & 193.5 \\ 0.0 & 0.0 & 0.0 & 0.0 & -720.5 & 419.4 \\ 0.0 & 0.0 & 0.0 & 0.0 & 0.0 & -731.3 \end{bmatrix}$$

We illustrate the cubic B-spine and its tight wavelet frame generators of the level 1 in the Figure 5.3. □

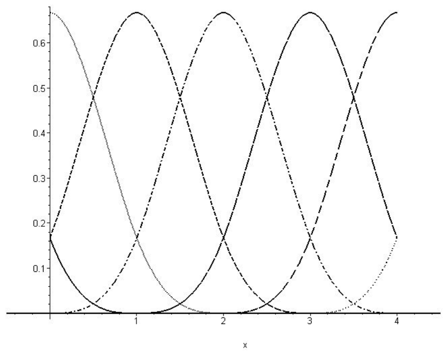

Cubic B-splines $\{\phi^4_{1,1}, \cdots, \phi^4_{1,7}\}$

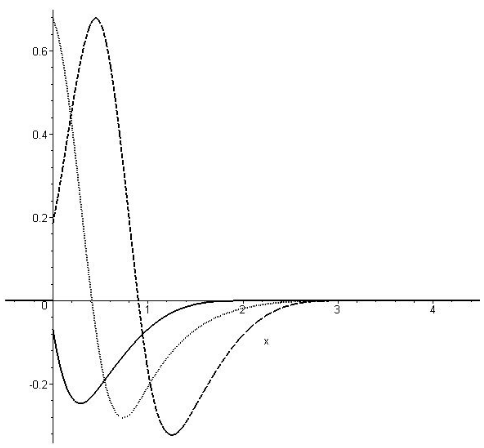

Cubic Framelets $\{\psi^4_{1,1}, \psi^4_{1,2}, \psi^4_{1,3}\}$

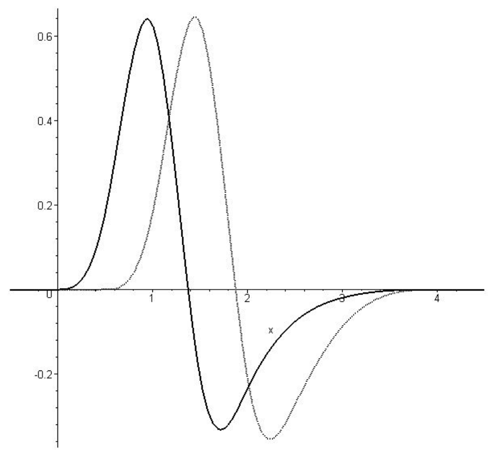

Cubic Framelets $\psi^4_{1,4}$ and $\psi^4_{1,5}$

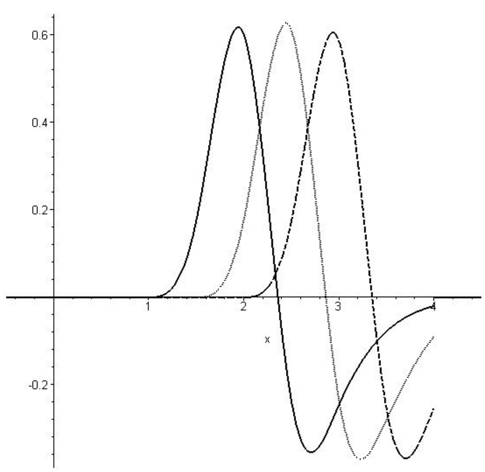

Cubic Framelets $\psi^4_{1,6}$ and $\psi^4_{1,7}$

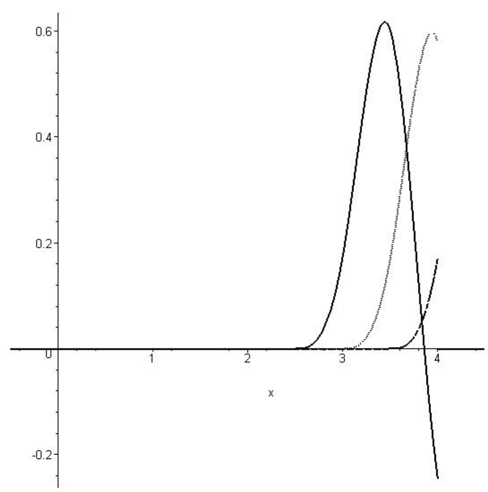

Cubic Framelets $\{\psi^4_{1,8}, \psi^4_{1,9}, \psi^4_{1,10}, \psi^4_{1,11}\}$

Figure 5.3: Cubic B-splines $\{\phi^4_{1,1}, \cdots, \phi^4_{1,7}\}$ and cubic B-spline tight framelets $\{\psi^4_{1,1}, \cdots, \psi^4_{1,11}\}$ of the ground level over bounded domain $[0, 4]$ in Example 5.3.3.

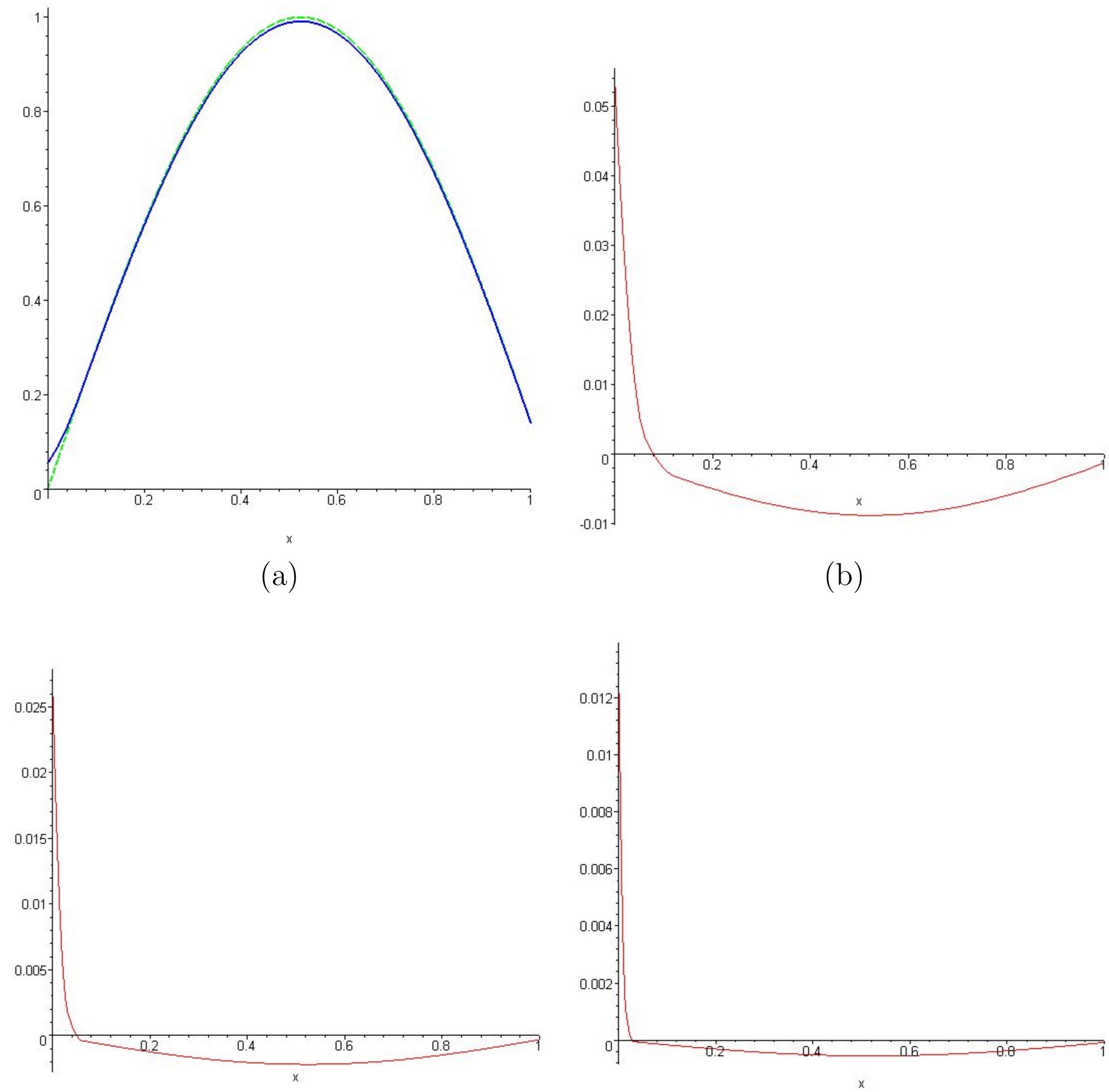

(a) (b)

(c) (d)

Figure 5.4: (1) Approximation of $f(x) = \sin(3x)$ by using Quadratic B-spline tight framelets over bounded domain $[0, 1]$. (2) ,(3) and (4) are the difference of f(x) and the approximation by the 3rd, 4th and 5th level of tight wavelet frame generators respectively.

5.4 Box Spline Tight Wavelet Frames

Our tight wavelet frame construction method can be applied multivariate settings. In this section we apply the tight wavelet frame construction scheme on Theorem 5.2.1 to 3-direction mesh Box spline functions.

Let us recall a 3-direction mesh box spline $\phi^{\ell mn}(x, y)$ whose Fourier transform is defined as follows for $\ell, n, m \in \mathbb{Z}_+$,

$$\widehat{\phi}^{\ell mn}(\xi,\eta) = \left(\frac{1-e^{-\sqrt{-1}\xi}}{\sqrt{-1}\xi}\right)^{\ell}\left(\frac{1-e^{-\sqrt{-1}\eta}}{\sqrt{-1}\eta}\right)^{m}\left(\frac{1-e^{-\sqrt{-1}(\xi+\eta)}}{\sqrt{-1}(\xi+\eta)}\right)^{n}.$$

To make our notations simple, let us denote $\phi^\nu := \phi^{\ell mn}$. The two-scale relation of 3-direction mesh box splines is

$$\phi^\nu(x,y) = \sum_{i,j\in\mathbb{Z}} c_{i,j}\phi^\nu(2x-i, 2y-j),$$

and its Fourier transformation is

$$\begin{aligned} &\widehat{\phi}^\nu(2\xi, 2\eta) = C(\xi,\eta)\,\widehat{\phi}^\nu(\xi,\eta), \\ \text{where} \quad &C(\xi,\eta) = \frac{1}{4}\sum_{i,j\in\mathbb{Z}} c_{i,j}e^{\sqrt{-1}(i\xi+j\eta)} \qquad (5.14)\\ \text{and} \quad &|\,C(0,0)\,| = 4. \end{aligned}$$

Consider a 3-direction mesh box spline ϕ^ν whose dyadic translations are restricted into the domain $[0,a]\times[0,b]$, i.e., $\phi^\nu(2^k x - i, 2^k y - j)|_{[0,a]\times[0,b]}$. Let us denote $\phi^\nu_{k,q}$ be all translations of $2^{2k}\phi^\nu(2^k x, 2^k y)\big|_{[0,a]\times[0,b]}$ and

$$V^\nu_k := \{\phi^\nu_{k,q} : 1 \le q \le m_k\}.$$

Then the family of nested sequence of subspaces $\{V^\nu_k : k \in Z_+\}$ is a MRA generated by $\{\phi^\nu_{k,1}, \cdots, \phi^\nu_{k,m_k}\}$. Thus if we denote

$$\Phi^\nu_k := (\phi^\nu_{k,1}, \cdots, \phi^\nu_{k,m_k})^T,$$

we can find a refinement matrix P^ν_k of size $m_k \times m_{k+1}$ of a vector satisfying $\Phi^\nu_k = P^\nu_k \Phi^\nu_{k+1}$ for each $k \in \mathbb{Z}_+$.

The following lemma says the refinement matrix P_k^ν of a vector Φ_k^ν whose component functions generate subspace V_k^ν in $L^2([0,a]\times[0,b])$ is satisfying the sufficient condition in Theorem 5.2.1.

Lemma 5.4.1 *If P_k^ν is a matrix of size $m_k \times m_{k+1}$ generated by a collection of box spline functions Φ_k^ν over bounded domain, i.e. $\Phi_k^\nu = P_k^\nu \Phi_{k+1}^\nu$, then*

$$I_{m_k} - P_k^\nu \cdot P_k^{\nu T}, \qquad \textit{for each } k \in \mathbb{Z}_+$$

is positive semi-definite.

Proof Let us denote $(p_{i,j}^{\nu,k}) := P_k^\nu$ and $(g_{i,j}^{\nu,k}) := G_k^\nu = P_k^\nu \cdot P_k^{\nu T}$. Because of (5.14) ,

$$0 \le \sum_{j=0}^{m_{k+1}} p_{i,j}^{\nu,k} \le \frac{1}{4} \sum_{\ell=1}^{m_{k+1}} c_{i,\ell} c_{\ell,j} = 1. \tag{5.15}$$

To show that matrix $I_{m_k} - G_k^\nu$ is positive semi-definite, we use diagonal dominance of matrix $I_{m_k} - G_k^\nu$. Since the matrix G_k^ν is symmetry, it is sufficient to check $|1 - g_{i,i}^{\nu,k}| \ge \sum_{i \ne j} |\, g_{i,j}^{\nu,k}\,|$ for $i \le \lfloor \frac{m_k}{2} \rfloor + 1$.

$$0 \le g_{i,j}^{\nu,k} = \sum_{\ell=1}^{m_{k+1}} p_{i,\ell}^{\nu,k} p_{\ell,j}^{\nu,k} = 1.$$

Because of (5.15),

$$\begin{aligned} 1 - |g_{i,i}^{\nu,k}| - \sum_{j \ne i} |\, g_{i,j}^{\nu,k}\,| &= 1 - \sum_{j=1}^{m_{k+1}} \sum_{\ell=1}^{m_{k+1}} p_{i,\ell}^{\nu,k} p_{j,\ell}^{\nu,k} \\ &= 1 - \left(\sum_{\ell=1}^{m_{k+1}} p_{i,\ell}^{\nu,k} \right) \left(\sum_{\ell=1}^{m_{k+1}} p_{j,\ell}^{\nu,k} \right) \ge 0\,. \end{aligned}$$

Therefore the symmetry matrix $I_{m_k} - P_k^\nu \cdot P_k^{\nu T}$ is positive semi-definite. □

Thus we can construct box spline tight wavelet frame over the bounded domain $[0,a] \times [0,b]$. by using the constructive scheme in the proof of Theorem 5.2.1. Each construction steps are the same as we described for the B-spline tight wavelet frame construction over the bounded interval in the previous section. In the following examples we illustrate the refinement matrix P_1^ν associated with the vector Φ_1^ν of refinable functions $\phi_{1,1}^\nu, \cdots, \phi_{1,m_1}^\nu$

over the bounded domain $[0,a] \times [0,b]$ and Q_1^ν associated with the vector Ψ_1^ν of the tight wavelet frame generators obtained by setting $\Psi_1^\nu = Q_1^\nu \Phi_1^\nu$.

Example 5.4.1 *111 Box spline Tight Framelets ψ^{111} over $[0,2]\times[0,2]$. We set the column vector Φ_1^{111} with all the integer translations of ϕ^{111} over the domain $[0,2]\times[0,2]$ as follows*

$$\Phi_1^{111} = [\ \phi^{111}(x+1,y+1)|_{[0,2]\times[0,2]} \ \cdots \ \phi^{111}(x-1,y-1)|_{[0,2]\times[0,2]}\ ]^T := [\phi_{1,1}^{111} \ \cdots \ \phi_{1,9}^{111}]^T.$$

Similarly, set the column vector Φ_2^{111} as follows $\Phi_2^{111} = [\ 2\phi^{111}(2x{+}2,2y{+}2)|_{[0,4]} \ \cdots \ 2\phi^{111}(2x{-}2,2y-2)|_{[0,4]}\ ]^T$. Then from the relation $\Phi_1^{111} = P_1^{111}\cdot\Phi_2^{111}$, we have the refinement matrix P_1^{111} as follows

$$P_1^{111} = \frac{1}{2}\begin{bmatrix}
1 & \frac12 & 0 & 0 & 0 & \frac12 & \frac12 & 0 & 0 & 0 & 0 & 0 & 0 & 0 & 0 & 0 & 0 & 0 & 0 & 0 & 0 & 0 & 0 & 0 & 0\\
0 & \frac12 & 1 & \frac12 & 0 & 0 & 0 & \frac12 & \frac12 & 0 & 0 & 0 & 0 & 0 & 0 & 0 & 0 & 0 & 0 & 0 & 0 & 0 & 0 & 0 & 0\\
0 & 0 & 0 & \frac12 & 1 & 0 & 0 & 0 & 0 & \frac12 & 0 & 0 & 0 & 0 & 0 & 0 & 0 & 0 & 0 & 0 & 0 & 0 & 0 & 0 & 0\\
0 & 0 & 0 & 0 & 0 & \frac12 & 0 & 0 & 0 & 0 & 1 & \frac12 & 0 & 0 & 0 & \frac12 & \frac12 & 0 & 0 & 0 & 0 & 0 & 0 & 0 & 0\\
0 & 0 & 0 & 0 & 0 & 0 & \frac12 & \frac12 & 0 & 0 & 0 & \frac12 & 1 & \frac12 & 0 & 0 & 0 & \frac12 & \frac12 & 0 & 0 & 0 & 0 & 0 & 0\\
0 & 0 & 0 & 0 & 0 & 0 & 0 & 0 & \frac12 & \frac12 & 0 & 0 & 0 & \frac12 & 1 & 0 & 0 & 0 & 0 & \frac12 & 0 & 0 & 0 & 0 & 0\\
0 & 0 & 0 & 0 & 0 & 0 & 0 & 0 & 0 & 0 & 0 & 0 & 0 & 0 & 0 & \frac12 & 0 & 0 & 0 & 0 & 1 & \frac12 & 0 & 0 & 0\\
0 & 0 & 0 & 0 & 0 & 0 & 0 & 0 & 0 & 0 & 0 & 0 & 0 & 0 & 0 & 0 & \frac12 & \frac12 & 0 & 0 & 0 & \frac12 & 1 & \frac12 & 0\\
0 & 0 & 0 & 0 & 0 & 0 & 0 & 0 & 0 & 0 & 0 & 0 & 0 & 0 & 0 & 0 & 0 & 0 & \frac12 & \frac12 & 0 & 0 & 0 & \frac12 & 1
\end{bmatrix}$$

Then the vector of tight wavelet frame generators constructed by our method is $\Psi_1^{111} = Q_1^{111}\cdot\Phi_2^{111} := [\psi_{1,1}^{111} \ \cdots \ \psi_{1,25}^{111}]^T$, where

$$Q_1^{111} = \begin{bmatrix}
V_{11}; & V_{12}; & Z; & Z; & Z\\
Z; & V_{22}; & V_{23}; & V_{24}; & Z\\
Z; & Z; & V_{33}; & V_{34}; & Z\\
Z; & Z; & Z; & V_{44}; & V_{45}\\
Z; & Z; & Z; & Z; & V_{55}
\end{bmatrix} \quad \text{, and where } Z = \begin{bmatrix}
0 & 0 & 0 & 0 & 0\\
0 & 0 & 0 & 0 & 0\\
0 & 0 & 0 & 0 & 0\\
0 & 0 & 0 & 0 & 0\\
0 & 0 & 0 & 0 & 0
\end{bmatrix}$$

We omit the explicit expression of each block matrix $V_{i,j}$.

□

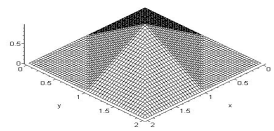

Box Spline ϕ_{111}

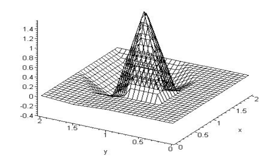

The Box Spline Tight Framelet located on the center of the domain

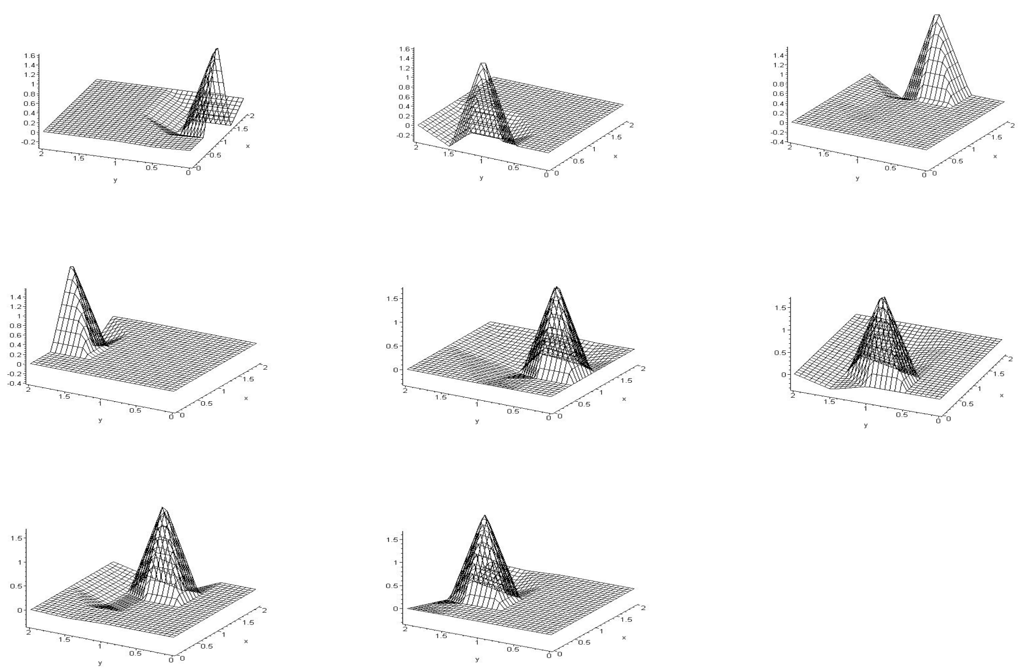

Box Spline Tight Framelets located on the boundary of the domain

Figure 5.5: Box Spline ϕ_{111} and its some of Tight Framelets over the bounded domain

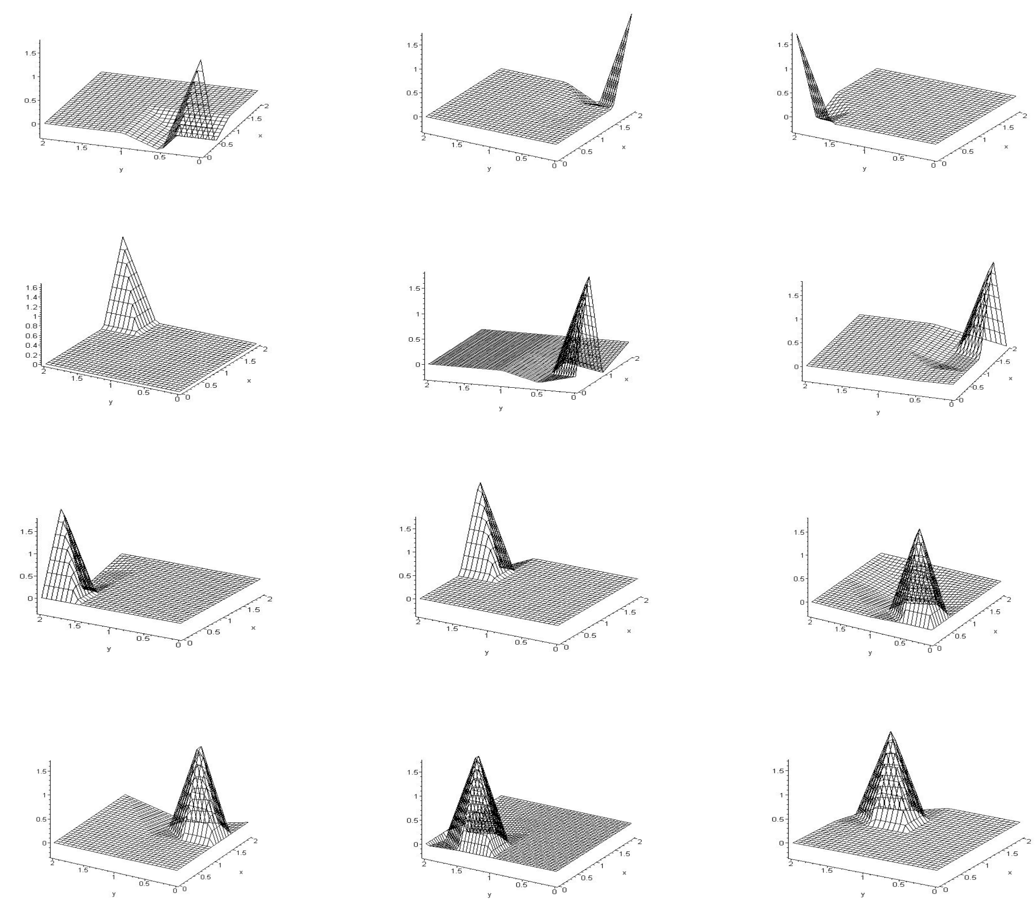

Figure 5.6: Box Spline Tight Framelets located at the four conners of the domain

Bibliography

[BHR] C. de Boor, K. Hölig, S. Riemenschneider, Box Splines, *Springer Verlag*, New York, 1993.

[BL] J. Benedetto, S. Li, The theory of multiresolution analysis frames and applications to filter banks, *Appl. Comput. Harmon. Anal.* **5** (1998), pp. 389–427.

[C1] C. K. Chui, Multivariate Splines, SIAM Publications, Philedalphia, 1988.

[C2] C. K. Chui, An introduction to wavelets, Accademic Press, Boston, 1992.

[C3] C. K. Chui, Wavelets: A mathematical tool for signal analysis , SIAM Publications, Philedalphia, 1997.

[CDF] A. Cohen, I. Daubechies and J. C. Feauveau, Biorthogonal bases of compactly supported wavelets, *Comm. Pure Appl. Math.* **45** (1992), pp. 485–460.

[CH1] C. K. Chui and W. He, Compactly supported tight frames associated with refinable functions, *Appl. Comp. Harmonic Anal.* **8** (2000), 293–319.

[CH2] C. K. Chui and W. He, Construction of multivariate tight frames via Kronecker Products , *Appl. Comp. Harmonic Anal.* **11** (2001), 305–312.

[CHS1] C. K. Chui, W. He and Stöckler, Compactly supported tight and sibling frames with maximum vanishing moments. *Appl. Comput. Harmon. Anal.* **13** (2002), no. 3, 224–262.

[CHS2] C. K. Chui, W. He and Stöckler, Nonstationary tight wavelet frames ,I: Bounded Intervals, *Appl. Comput. Harmon. Anal.* **17** (2004) pp. 141–197.

[CJS] Chui, Jetter, and Stöckler, Wavelets and frames on the four-directional mesh. Wavelets: theory, algorithms, and applications (Taormina, 1993), 213–230,*Wavelet Anal. Appl.*, **5**, Academic Press, San Diego, CA, 1994.

[CS] C. K. Chui, X. Shi, Bessel sequences and affine frames.*Appl. Comput. Harmon. Anal.* **1** (1993), no. 1, 29–49.

[D] I. Daubechies, Ten Lectures on Wavelets, SIAM Publications, Philedalphia, 1992.

[DGM] Painless nonorthogonal expansions, *J. Math. Phys.* **27** (1986), no. 5, 1271–1283.

[DHRS] I. Daubechies, B. Han, A. Ron, Z. W. Shen, Framelets: MRA-based constructions of wavelet frames, *Appl. Comp. Harmonic Anal.*, 2003. no 1,1–46

[Do] D.L. Donoho, De-Noising by Soft Thresholding, *IEEE Trans. Info. Theory 43*, (1993) pp. 933–936.

[DS] R.J. Duffin and A.C.Shaeffer , A class of nonharmonic Fourier Series, *Trans. Amer. Math. Soc.* **72**, (1952), 147-158.

[F] L. Fejér, Über trigonometrische Polynome, J. Reine und Angewandte Mathematik **146** (1915), 53–82.

[GL] J.S. Geronimo, M.J.Lai, Factorization of Multivariate Laurent Polynomials, submitted, 2005.

[GR] K. Gröchenig, A. Ron, Tight compactly supported wavelet frames of arbitrarily high smoothness, *Proc. Amer. Math. Soc.* **126** (1998), no. 4, 1101–1107.

[H] B. Han, On dual wavelet tight frames. *Appl. Comput. Harmon. Anal.* **4** (1997), no. 4, 380–413.

[J] Maarten Jansen, Noise Reduction by Wavelet Thresholding, *Springer-Verlag*, New York Inc. 2001

[L1] M. J. Lai, Fortran subroutines for B-nets of box splines on three and four directional meshes, *Numerical Algorithm*, **2** (1992), 33–38.

[L2] M. J. Lai, Methods for Constructing Nonseparable Compactly Supported Orthonormal Wavelets, Wavelet Analysis: Twenty Year's Development, edited by D. X. Zhou, World Scientific, 2002, pp. 231–251.

[Lim] J. S. Lim, Two-dimension Signal and Image Processing, Prentice Hall, New Jersey, 1990.

[LS] M. J. Lai and J. Stöckler, Construction of Compactly Supported Tight Frames, submitted for publication, 2003. See www.math.uga.edu/∼mjlai/pub.html for a copy.

[Ma] S. Mallat, Multiresolution approximations and wavelet orthonormal basis of $L^2(\mathbb{R})$, *Trans. Amer. Math. Soc.*, **315** (1989), 69-87.

[Me] Y. Meyer, Wavelets and Operators, *Advanced mathematics*, Cambridge University Press, 1992.

[NH] A.N. Netravali and B.G. Haskell, Digital Pictures: Representation, Compression, and Standards (2nd Ed), Plenum Press, New York, NY (1995).

[RS1] A. Ron and Z. Shen, Affine systems in $L^2(\mathbb{R}^d)$: the analysis of the analysis operator, *J. Functional Anal. Appl.* **148** (1997), pp. 408–447.

[RS2] A. Ron and Z. Shen, Affine systems in $L^2(\mathbb{R}^d)$ II: the dual systems, *J. Functional Anal. Appl.* **3** (1997), pp. 617–637.

[RS3] A. Ron and Z. Shen, Construction of compactly supported affine frames in $L^2(\mathbb{R}^d)$, *Math. Comp.* **67** (1998), pp. 191–207

[RS4] A. Ron and Z. Shen, Frames and stable bases for shift-invariant subspaces of $L^2(\mathbb{R}^d)$, *Canad. J. Math.* **47** (1995), 1051–1094.

[Ri] F. Riesz, Über ein Problem des Herr Carathéodory, J. Reine und Angewandte Mathematik **146** (1915), 83–87.

[Ru] W. Rudin, The existence problem for positive definite functions, *Illinois J. Math.*, **7** (1963),pp. 532–539.